B.A.D. #125
Version 7
December 4, 2001

# Measurement of $B^0\overline{B}^0$ Mixing With Fully Reconstructed Hadronic $B$ Decays

Sören Prell, Gerhard Raven,
Shahram Rahatlou, Vivek Sharma and David MacFarlane
**University of California at San Diego**
Ben Brau
**Massachusetts Institute of Technology**
Fernando Martinez-Vidal
**INFN Sezioni Di Pisa**
Jürg Beringer
**University of California at Santa Cruz**
Julian von Wimmersperg, Steve Sekula,
Yibin Pan, Zhitang Yu, Hongbo Hu
**University of Wisconsin**

December 4, 2001

**Abstract**

$B^0\overline{B}^0$ oscillations have been studied in $e^+e^-$ annihilation data collected with the *BABAR* detector at center-of-mass energies near the $\Upsilon(4S)$ resonance. The event sample consists of one neutral $B$ meson reconstructed in a hadronic mode, while the flavor of the recoiling $B$ meson in the event is determined with a tagging algorithm that uses the relation between the flavor of the $b$ quark and the charges of its decay products. By simultaneously fitting the time dependence of the mixed and unmixed final states, the oscillation frequency $\Delta m_d$ is determined to be $0.516 \pm 0.016(stat) \pm 0.010(syst)\,\hbar\,\mathrm{ps}^{-1}$
.

# Contents

# Preamble

## Version 7

Decided to correct $\Delta m_d$ for the extrapolation of the sideband to the signal region. Systematic error due to uncertainty on the boost divided by 3 to be in line with the NIM paper The value of $\Delta m_d$ was unblinded. The toy MC was updated to the full 2K samples. A plot of the dependence on the assumed lifetime was added. Minor text changes

## Version 6

Update fitresults where the $B^0$ lifetime was *not* set at its nominal value. The numbers in version 5 for those tests still refered to results obtained without the $J/\psi\ K^{*0}$ sample. Also, Fig. 4 and 5 were not up to date. A minor typo was found in the configuration of the toy MC, leading to an inconsistency. Fixing this removed the small bias described in Version 5. In addition, the toy results have been updated to include the $J/\psi\ K^{*0}$ sample. Note that sofar only 446 experiments have finished – more experiments will be added in the near future.

## Version 5

The previous version (V4) uploaded to the BAD system covered the analysis of the full run1 data sample (20 $\text{fb}^{-1}$), with a statistical error on $\Delta m_d$ of 0.020, and a systematic error of 0.016. The largest contribution to the systematic error was due to a MC based correction of the value of $\Delta m_d$ by 0.009: the full size of the shift was considered as a systematic error. As mentioned in Sec. 2, it was found that the MC was generated with an inconsistent fraction of mixed events (compared to the values used for $\Delta m_d$ and $\tau_{B^0}$). Correcting this effect increased the observed value of $\Delta m_d$ in the MC, *increasing* the size of the correction. At the same time more MC events became available, decreasing the statistical error on the MC results, ruling out that this bias was just "bad luck" (aka. statistics).

For a period of time, the analysis of the run1 sample was repeated with a vertexing configuration which did *not* use the beam/beamspot constraints, to be consistent with the first sin2$\beta$ publication, which dropped these constraints because of a problem observed in the description of the $\Delta t$ resolution of $J/\psi\ K^0_s$ events. However, after many studies, nothing was found to be wrong with these constraints (nor their implementation), and for the the second sin2$\beta$ publication on the "summer 2001" sample, these constraints were switched back on. As this analysis had no reason to drop the constraints in the first place, as soon as sin2$\beta$ changed back, this analysis also switched back.

Since then, many studies were carried out in order to find the origin of the observed MC bias, and ways to reduce this effect.

To reduce the effect of long-lived charm daughters (and the fact that it was clear that these introduced a tagging-vertexing correlation due to the fact that $D^+$ have a significantly larger mistag rate, and are more likely to cause outliers in the $\Delta t$ measurement), the vertexing

algorithm was slightly modified by removing identified kaons from the input list of the algorithm. In addition, the description of the $\Delta t$ resolution was improved by adding the "scaling of the bias" (see Sec. 6.11 and references therein), which takes better into account the effect of the remaining charm daughters. As the "scaling" does not hold for the entire range of $\sigma_{\Delta t}$ a cut was placed on $\sigma_{\Delta t}$ at 1.4 ps (which rejects $\approx 10\%$ of the events, but the removed events have the least contribution because they have the largest $\sigma_{\Delta t}$). This cut also reduces the fraction of outliers, thus cleaning up $\Delta t$ measurement in addition..

Furthermore, additional studies pointed out the correlation between the $\Delta t$ resolution and the mistag rates. This effect, which is well modeled in the MC (see also Sec. 6.13 and references therein), can be shown to be responsible for part of the remaining bias in the signal MC fit.

In addition to these changes, the analysis was updated to the "summer 2001" sample, for a total of 30 fb$^{-1}$. The resolution model was extended to allow different resolution parameters for run1 and run2. As a result of the increased yields, the statistical error has gone down from 0.020 to 0.016.

The increase in statistics has also made it possible to study some systematics in more detail. For example, the extrapolation of the sideband $\Delta t$ distribution into the signal region is now studied by slicing the sideband into seven individual regions, and seeing how $\Delta m_d$ varies as one picks one of the seven regions.

As of this version, the value of $\Delta m_d$ on data is still blind. The value was re-blinded before adding the new data, and while various vertex options were explored.

Before unblinding, there are a few items remaining:

- we could correct the value of $\Delta m_d$ for the extrapolation of the sideband $\Delta t$ into the signal region. Right now a 0.0025 systematic is quoted for this, but maybe we want to correct down by 0.0020, and quote the shift as systematic

- we could quote the difference due to explicitly using the mistag-$\sigma_{\Delta t}$ correlation in the fit as systematic. It would add 0.002 in quadrature, which does NOT change the sum of 0.010 at all (this might be double counting, on the other hand, it doesn't change the final sum).

- the systematic due to the lifetime is not symmetric. Should we quote it as asymmetric, or (what is done so-far) is to take the largest of the two, and quote it symmetric?

Finally, due to an "administrative" oversight (aka "bug"), several fits on data were done without the $J/\psi\ K^{*0}$ sample. Virtually all of these have been updated to include this sample, however, the toy MC still reflects the sample without the $J/\psi\ K^{*0}$, ie. it was generated from the parameters of the nominal fit when that fit did not contain $J/\psi\ K^{*0}$. The toy MC is being repeated, but due to the amount of CPU hours required, it has not yet finished. It will be updated in the near future.

# 1 Introduction

In the Standard Model, $B^0\overline{B}^0$ mixing occurs through second-order weak diagrams involving the exchange of up-type quarks, with the top quark contributing the dominant amplitude. A measurement of $\Delta m_d$ is therefore sensitive to the value of the Cabibbo-Kobayashi-Maskawa matrix [1] element $V_{td}$. At present the sensitivity to $V_{td}$ is not limited by experimental precision on $\Delta m_d$, but by other uncertainties in the calculation, in particular the quantity $f_B^2 B_B$, where $f_B$ is the $B^0$ decay constant, and $B_B$ is the so-called bag factor, representing the strong interaction matrix elements.

In this analysis, we study the time-dependent probability to observe $B^0\overline{B}^0$, $B^0B^0$ and $\overline{B}^0\overline{B}^0$ pairs produced in $\Upsilon(4S)$ decay. We fully reconstruct one $B$ in a flavor eigenstate, and use the remaining particles from the decay of the other $B$ to identify, or "tag", its flavor. The charges of identified leptons and kaons are the primary indicators of the flavor of the tagging $B$, but other particles also carry flavor information that can be identified with a neural network algorithm. The flavor tagging algorithm used in this analysis is identical to that employed by *BABAR* in *CP* violation studies, in which one $B$ is fully reconstructed in a *CP* eigenstate [2]. There are however small differences in the $\Delta t$ reconstruction: although the same code is used, it is configured such that charged kaons are rejected from the vertex determination, and to improve the modelling of the resolution function, the per-event error on $\Delta t$ is required to be less than 1.4 ps.

# 2 Data and Monte Carlo Samples

The data sample used in this analysis is the $29.7\,\text{fb}^{-1}$ taken in 1999, 2000 and 2001 at the $\Upsilon(4S)$ resonance. Our fully-simulated signal Monte Carlo sample consists of $B^0\overline{B}^0$ events, generated in a mixture of all of the decay modes under study, in amounts proportional to the product of the $B$ branching fractions and the $B$'s daughter's branching fractions. This so called "signal MC Cocktail" contains 2.9 million $B^0$ events and corresponds to a luminosity of 574 $\text{fb}^{-1}$ at the $\Upsilon(4S)$. A comparable $B^+$ MC cocktail sample of about 1 million events corresponding to 355 $\text{fb}^{-1}$ is also used. All samples were processed from skimmed `micro` Objectivity collections with the physics `analysis-11` release and some small number of additional tags [3]. The additional tags implement the possibility to remove identified charged kaons from the tag side prior to the start of the process of finding the tag vertex. Details of the collections and `ascii` files used are available in [4].

We have corrected a defect in the generation of our MC samples as follows: The $B^0$ cocktail was generated with a value of $\Delta m_d = 0.472\ \hbar\,\text{ps}^{-1}$ and a $B^0$ lifetime of 1.548 ps (PDG 2000 values). The corresponding value of $\chi_d$ (the fraction of mixed events) should have been 0.17402, but by mistake it was fixed to 0.17206 in version 1.1 of `ProdDecayFiles/B0B0bar_Breco_DX+DstarX_cocktail.dec` (the value which corresponds to the *1998* PDG value of $\Delta m_d$). This version was used in tags of `ProdDecayFiles` upto (but not including) V00-03-29. To compensate for this difference, 1.36% of the unmixed MC events (selected based on MC truth) was removed from the sample. This problem only affects MC events

with a run number between 300000 and 480000 (which represent approximately half the available sample). In addition, 40K of $J/\psi\ K^{*0}$ MC has been used. This MC was generated with PDG 2000 values of $\Delta m_d$ and the $B^0$ lifetime, but again with an incorrect $\chi_d$ of 0.170. The $\chi_d$ of this sample was also corrected by removing 2.79% of the unmixed MC events (selected based on MC truth).

# 3 Event Selection

We reconstruct neutral $B$ mesons in the hadronic decay modes $D^{(*)+}\pi^-$, $D^{(*)+}\rho^-$, $D^{(*)+}a_1^-$ and $J/\psi K^{*0}(K^{*0} \to K^+\pi^-)$.[1] A detailed description of the event reconstruction and selection criteria is available in [5]. In the case of multiple candidates per event, if there is more than one candidate made of the same $D^{(*)}$ and B mode (e.g. $D^+\pi^-$ with $D^+ \to K\pi\pi$) wich differ for the D meson candidate, then the best D candidates is picked up. The D candidate quality criteria are:

- the D candidate reconstructed mass divided by its errors as computed from the tracks and neutral deposits covariance matrices in the case of $D^+$ or $D^0$ mesons.
- $\chi^2 = (\frac{\Delta M - \Delta M^{PDG}}{\sigma_{\Delta M}})^2 + (\frac{M_{D0} - M_{D0}^{PDG}}{\sigma_{M_{D0}}})^2$ in the case of $D^{*+}$ or $D^{*0}$ mesons. $\Delta M$ is the difference between the exited D meson and the $D^0$ candidates (we reconstruct $D^{*+} \to D^0\pi^+$ and $D^{*0} \to D^0\pi^0$ or $D^0\gamma$) and errors are all computed from the tracks and neutral deposits covariance matrices.

All other ambiguities among multiple candidates are resolved choosing the candidate with the smallest $|\Delta E|$.

In total, 34 out of 14754 events in run1 and 24 out of 7734 events in run2 have candidates in more than one mode (in the range $5.2 < m_{\rm ES} < 5.3\,{\rm GeV}$). The distribution of beam-energy substituted mass for the selected $B$ candidates with a tag vertex but no tagging category requirement is shown in Fig. 1. Superimposed is the result of a fit using a Gaussian distribution for the signal and an ARGUS background parameterization [8] given by:

$$B(m_{\rm ES}|m_0,\xi) = \frac{\theta(m_{\rm ES} < m_0)}{N} \times m_{\rm ES}\sqrt{1-(m_{\rm ES}/m_0)^2} \times \exp\Big[\xi(1-(m_{\rm ES}/m_0)^2)\Big], \qquad (1)$$

where $m_0 = 5.2909\,{\rm GeV}/c^2$ is taken as the kinematic upper limit to insure a finite probability for all candidates. The peak corresponds to a signal of $9323 \pm 110$ signal events with a purity (signal fraction) of $83.4 \pm 0.4\%$ for the candidates with $m_{\rm ES} > 5.27\,{\rm GeV}/c^2$.

The background to the selected hadronic $B$ decays have contributions from the continuum (udsc) events and $B\overline{B}$ events [5]. The relative ratios vary depending on the track multiplicity in the reconstructed decay mode. The fraction of combinatorial (non-peaking) background candidates in the signal sample is determined from a fit to the $m_{\rm ES}$ distribution in which the signal is described by a Gaussian and the background by the ARGUS shape [8]. A small

[1] Unless specifically noted, charge conjugation is implied throughout this paper.

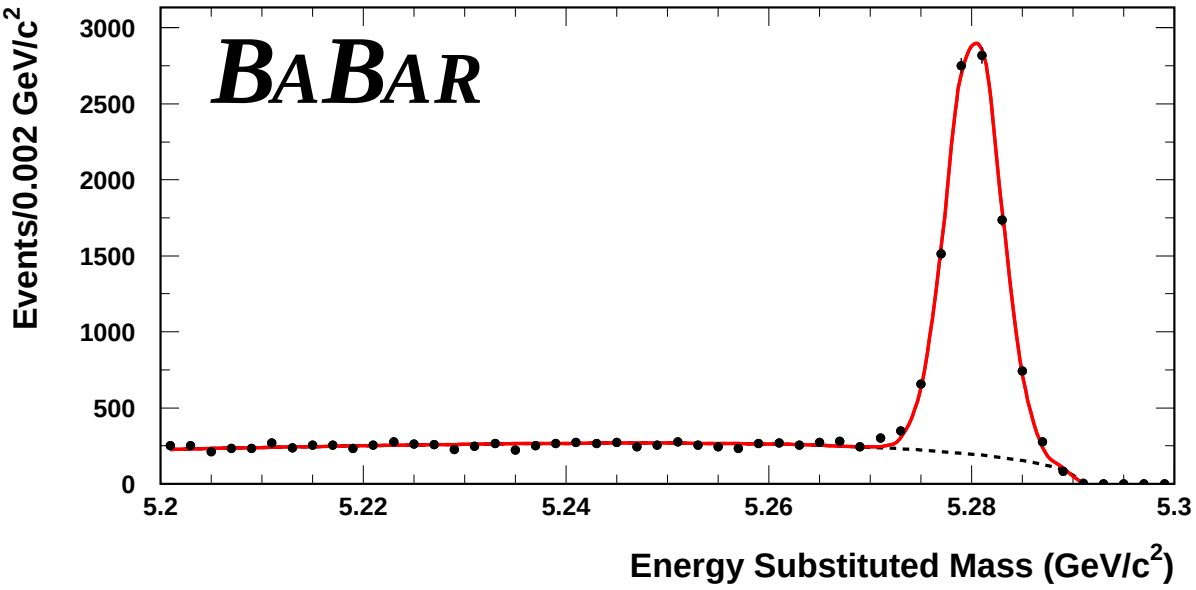


Figure 1: Beam-energy substituted mass, $m_{\rm ES}$, for the selected $B$ candidates in data (with a computed tag vertex, but *without* requiring tagging).

fraction of the signal peak ($\sim 1-2\%$) arises from so-called peaking backgrounds which are caused in the reconstruction when a slow pion from the reco B is swapped with a slow pion from the other $B$ decay. The peaking background from neutral $B$ decays is considered signal, whereas the peaking background from charged $B$ decays will be accounted for explicitly in the fit to the $\Delta t$ distributions because of its different $\Delta t$ dependence.

# 4 Unbinned Likelihood Fit

The likelihood functions that are described below are implemented in the maximum likelihood fitting package for time-dependent fitting `tFit` [9].

## 4.1 Time-Dependence of $B^0\overline{B}^0$ Oscillations

In the absence of detector resolution effects and backgrounds, the log likelihood function describing the time-dependence of $B^0\overline{B}^0$ oscillations is given by

$$\log\mathcal{L} = \sum_{\text{unmixed events}} \log f_+(\Delta t) + \sum_{\text{mixed events}} \log f_-(\Delta t) \tag{2}$$

with

$$f_\pm(\Delta t) = \frac{\Gamma_0}{4}\exp(-\Gamma_0|\Delta t|)\left[1 \pm D\cos(\Delta m_d \Delta t)\right] \tag{3}$$

where the tagging dilution $D = 1-2w$ is related to the flavor mistag rate $w$. The input variable to the likelihood fit is the measured $\Delta t = t_{reco} - t_{tag}$, calculated using the average $\tau_B$ approximation technique in [7] for the unmixed and mixed samples. The potential fit parameters are the $B^0$ lifetime $\tau_0 = 1/\Gamma_0$, the tagging dilution $D$ and the mixing frequency $\Delta m_d$.

The time-dependent mixing asymmetry $A_{\text{mixing}}(\Delta t)$ between unmixed and mixed events is proportional to the tagging dilution $D$:

$$A_{\text{mixing}} = \frac{N_{\text{unmix}} - N_{\text{mix}}}{N_{\text{unmix}} + N_{\text{mix}}} = D\cos(\Delta m_d \Delta t) \tag{4}$$

The four tagging categories (lepton tag, kaon tag, etc) have significantly different mistag rates (and the $\Delta t$ resolution functions could also potentially be different). Averaging over tagging categories with different tagging performance degrades the sensitivity to $\Delta m_d$. Therefore, we fit for the tagging dilutions of the four tagging categories separately. In addition, to account for a possible difference in the tagging dilution for $B^0$ tagged events and $\overline{B}^0$ tagged events, rather than fitting for a combined dilution $D$, we fit for an average dilution $\langle D\rangle = 1/2(D_{B^0} + D_{\overline{B}^0})$ and a dilution difference $\Delta D = D_{B^0} - D_{\overline{B}^0}$, where the subscript refers to the true flavor of the tagging $B$.

## 4.2 Detector Resolution Function

Limited detector resolution in the measurement of $\Delta t$ requires a modification of the likelihood function. The detector resolution function $\mathcal{R}$ is approximated by three Gaussians with different RMS and mean

$$\begin{aligned}
&\mathcal{R}_{\rm reso}(\Delta t, \Delta t_{\rm true}, \sigma_{\Delta t} | f_{\rm tail}, f_{\rm outlier}, S_{\rm core}, \delta_{\rm core}, S_{\rm tail}, \delta_{\rm tail}, \sigma_{\rm outlier}, \delta_{\rm outlier}) = \\
&(1 - f_{\rm tail} - f_{\rm outlier}) \frac{\exp -\frac{1}{2}\left(\frac{\Delta t - \delta_{\rm core}\cdot\sigma_{\Delta t} - \Delta t_{\rm true}}{S_{\rm core}\sigma_{\Delta t}}\right)^2}{\sqrt{2\pi} S_{\rm core}\sigma_{\Delta t}} \\
&+ f_{\rm tail} \frac{\exp -\frac{1}{2}\left(\frac{\Delta t - \delta_{\rm tail}\cdot\sigma_{\Delta t} - \Delta t_{\rm true}}{S_{\rm tail}\sigma_{\Delta t}}\right)^2}{\sqrt{2\pi} S_{\rm tail}\sigma_{\Delta t}} \\
&+ f_{\rm outlier} \frac{\exp -\frac{1}{2}\left(\frac{\Delta t - \delta_{\rm outlier}\cdot\sigma_{\Delta t} - \Delta t_{\rm true}}{\sigma_{\rm outlier}}\right)^2}{\sqrt{2\pi} \sigma_{\rm outlier}}
\end{aligned}$$

where $\sigma_{\Delta t}$ is the event-by-event error on $\Delta t$ computed from the vertex fit.

For most of the events (in data, $f_{\rm core} = 1 - f_{\rm tail} - f_{\rm outlier} \approx 97\%$) the decay time difference $\Delta t$ is well reconstructed. The distribution of $(\Delta t - \Delta t_{\rm true})/\sigma_{\Delta t}$ of those events can be described by a single Gaussian with an RMS close to one. To account for a possible deviation from unit RMS, we allow for a global scale factor $S_{\rm core}$ to the error in $\Delta t$. A possible mean bias $\delta_{\rm core}$ in the distribution caused by using tracks from secondary charmed particle decays in the tagging $B$ vertex is taken into account. For a small fraction of the events the $\Delta t$ error, $S_{\rm core}\sigma_{\Delta t}$, underestimates the true $\Delta t$ uncertainty. These events are described by two other Gaussians in the resolution function: a *tail* Gaussian and an *outlier* Gaussian. The parametrization of the tail Gaussian is identical to the parametrization of the core Gaussian. The RMS ($\sigma_{\rm outlier} = 8\,{\rm ps}$) and the mean ($\delta_{\rm outlier} = 0\,{\rm ps}$) of the outlier Gaussian is fixed to be the same for all events and does not use the calculated $\sigma_{\Delta t}$ values. The fractions of the outlier and the tail Gaussians and the means and sigmas of the core and the tail Gaussian for the signal candidates are free fit parameters. For background candidates, in order to reduce the number of parameters, the fractions of events in the tail Gaussian is fixed to zero. In section 7.8 we discuss the (small) systematic error due to this simplification.

In general, the mean bias of the $(\Delta t - \Delta t_{\rm true})$ distribution depends on the fraction of tracks from secondary charm decays (and their momenta) in the reconstruction of the tagging $B$ vertex and can be very different for the four tagging categories. Therefore, we allow a different $\delta_{\rm core}$ for each tagging category. In addition, it was found that the bias is larger for events with larger $\sigma_{\Delta t}$; more details can be found in [6], and in section 6.11.

The time-evolutions for $B^0\overline{B}^0$ oscillations are convolved with the resolution function to take into account the uncertainties in $\Delta t$.

$$F_\pm(\Delta t) \;=\; \int_{-\infty}^{\infty} d(\Delta t')\mathcal{R}(\Delta t - \Delta t') f_\pm(\Delta t') \qquad (5)$$

For a single Gaussian resolution function with RMS $\sigma$, we obtain

$$F_{\pm}(\Delta t) = \int_{-\infty}^{\infty} d(\Delta t') \frac{1}{\sqrt{2\pi}\sigma} e^{-(\Delta t - \Delta t')^2/2\sigma^2} f_{\pm}(\Delta t' | \Gamma, \Delta m_d, D) \quad (6)$$

These integrals can be expressed in terms of the complex (complementary) error function $\mathrm{erfc}(z)$

$$\begin{aligned} F_{\pm}(\Delta t) &= \frac{\Gamma}{8}\left[ e^{-\Gamma\Delta t + (\sigma^2\Gamma^2)/2} \mathrm{erfc}\left( \frac{-\Delta t + \sigma^2\Gamma}{\sqrt{2}\sigma} \right) \right. \\ &\pm \left. \Re\left( D e^{-(\Gamma - i\Delta m_d)\Delta t + \sigma^2(\Gamma - i\Delta m_d)^2} \mathrm{erfc}\left( \frac{-\Delta t + \sigma^2(\Gamma - i\Delta m_d)}{\sqrt{2}\sigma} \right) \right) \right] \end{aligned} \quad (7)$$

To take into account the two-sided exponential shape of the $\Delta t$ distributions, we add the contributions from positive and negative $\Delta t$ values (with the correct sign of the $\Delta t$ bias):

$$\log \mathcal{F}_{\pm}(\Delta t) = \frac{1}{2}(F_{\pm}(\Delta t - \delta) + F_{\pm}(-\Delta t + \delta)) \quad (8)$$

The equations above do not take into account the possibility to fit in a finite $\Delta t$ range. The likelihood implementation in tFit does include this normalization, and for the measurement described here we only include the $\Delta t$ range from $-20$ to $+20$ ps. Fits in different ranges of $\Delta t$ are done as well, and are described in Sec. 6.11.

## 4.3 Backgrounds

We distinguish between two types of background in the sample of the selected $B^0$ candidates. The first background is called combinatorial background (see section 4.3.1) and it arises from random combinations of charged tracks and neutral showers from both $B$ mesons in $B\overline{B}$ events or from continuum events. This background (by definition) does not peak at the $B$ mass in the $m_{\mathrm{ES}}$ distribution. The second background is the so-called peaking background. The peaking background consists of events in which, for example, a slow pion from the reconstructed $B$ is replaced by a slow pion from the tagging $B$ causing an enhancement near the nominal $B$ mass. The peaking background from charged $B$ decays is considered explicitly in the likelihood function (see section 4.3.2), whereas the peaking background from neutral $B$ decays has time-dependent properties very similar to the signal and is treated as such.

### 4.3.1 Combinatorial Background

Combinatorial backgrounds arise from many different sources and the true time-dependence cannot be derived from first principles. We approximate the $\Delta t$ distributions of the backgrounds with analytical functions and measure the parameters with control samples (e.g. $m_{\mathrm{ES}}$ sideband). In the likelihood fit, we describe the backgrounds by separate terms in the likelihood function

$$\log \mathcal{L} = \sum_{\mathrm{unmix}} \log\left(p_{\mathrm{sig}} f_{+,\mathrm{sig}} + (1 - p_{\mathrm{sig}}) f_{+,\mathrm{bgd}}\right) + \sum_{\mathrm{mix}} \log\left(p_{\mathrm{sig}} f_{-,\mathrm{sig}} + (1 - p_{\mathrm{sig}}) f_{-,\mathrm{bgd}}\right) \quad (9)$$

We use an empirical description for the time dependence of the backgrounds in the likelihood fit containing up to three components for each background.

$$f_{\pm,\mathrm{bgd}} = \sum_{j=1}^{3} p_j F_{\pm,j}(\Delta t) \tag{10}$$

where $p_j$ is the fraction of the background component $j$ and $F_{\pm,j}(\Delta t)$ contains the time dependence. The three components with different $\Delta t$ characteristics are listed below:

1. **Zero Lifetime Component:**
   $F_{\pm,1} = (1 \pm D'_1)$
2. **Non-Zero Lifetime Component (non-mixing):**
   $F_{\pm,2} = (1 \pm D'_2)\ \Gamma_2/2 \exp(-\Gamma_2|\Delta t|)$
3. **Non-Zero Lifetime Component (mixing):**
   $F_{\pm,3} = \Gamma_3/2\ \exp(-\Gamma_3|\Delta t|)\ (1 \pm D_3 \cos(\Delta m_3 \Delta t))$

The decay times $1/\Gamma_i$ of the backgrounds are not expected to be the exact lifetimes of decaying particles such as $B$ or $D$ mesons. Due to mis-reconstruction, the background lifetimes can be smaller or larger. Based on the same argument, we do not expect the mixing frequency of the background to be equal to $\Delta m_d$. The dilutions $D'$ are not dilutions in the sense of mistag rates $D = 1 - 2w$. They contain both effects of production asymmetry and flavor mis-assignment. In this sense dilutions are also meaningful for non-$B\overline{B}$ events. This rather general approach allows for more fit parameters then may be absolutely necessary to describe the $\Delta t$ distributions of the backgrounds. Since the background levels in the signal region are low, the background and signal fit parameters are largely uncorrelated, making the final result relatively insensitive to the quality of the fit to the background candidates or the details of the parametrization of their $\Delta t$ dependence. Note that the goal is to provide an empirical description of the $\Delta t$ distribution of the background and not to perform a measurement of "physical" parameters of the background candidates.

#### 4.3.2 peaking $B^+$ Background

The time-dependence of the background from $B^+$ decays (without detector smearing) can be described by

$$F_{\pm,charged} = \frac{\Gamma_+}{4} \exp(-\Gamma_+|\Delta t|)(1 \pm D_+) \tag{11}$$

where $\Gamma_+$ is the $B^+$ width and the dilution $D_+$ is different from the dilution for $B^0$ decays. We fix the $B^+$ lifetime to the PDG value [10] and the corresponding tagging dilutions to values obtained from a study of hadronic $B^+$ decays [2], which have been cross-checked by doing a combined fit on the $B^0$ and $B^+$ samples. In addition, we check on MC the $\Delta t$ distribution of this peaking background (See Sec. 7.9.2).

# 5 Results

We extract $\Delta m_d$ and the mistag rates by fitting the $\Delta t$ distributions of the selected $B$ candidates with the likelihood function described in section 4. We determine the combinatorial background fraction in the signal sample from a fit to the $m_{\rm ES}$ distribution. More precisely, we fit the $m_{\rm ES}$ distribution to a single Gaussian $S(m_{\rm ES})$ for the signal and the Argus function $B(m_{\rm ES})$ (Eq. 1) for the combinatorial background. Based on this fit, we determine an event-by-event signal probability as

$$p_{i,\rm sig}(m_{\rm ES}) = \frac{S_i(m_{\rm ES})}{S_i(m_{\rm ES}) + B_i(m_{\rm ES})} \tag{12}$$

where the index $i$ runs over the tagging categories.

Events contribute to the signal term or the background term in the likelihood function with probabilities $p_{i,\rm sig}(m_{\rm ES})$ and $1-p_{i,\rm sig}(m_{\rm ES})$ respectively. We describe the $\Delta t$ distributions of the combinatorial background with a component that has zero lifetime and a component that has non-zero lifetime (an oscillatory term is added for systematic studies). We fit for separate resolution function parameters for the signal and the background to minimize correlations between the background parameters and the signal parameters.

The measurement sensitivity of $\Delta m_d$ is proportional to the flavor tagging dilutions. Because the mistag rates differ between tagging categories, the population of the signal sample in each tagging category determines the overall tagging dilution. The break-down of the data sample according to tagging category is shown in Table 1. The tagging efficiencies and signal purities for the individual tagging categories in data and simulated signal events are extracted from fits to the $m_{\rm ES}$ distributions shown in Fig. 2 and are listed in Table 1.

Table 1: Tagging efficiencies for hadronic $B$ decays in simulated events and in data and signal purities (in the region $m_{\rm ES} > 5.27\,{\rm GeV}/c^2$) in data separately for the four tagging categories. Note: the signal purity is *not* corrected for possible peaking backgrounds; The MC numbers are obtained *after* requiring truth association.

| Tagging Category | Efficiency [%] | | | $B$ candidates | | | S/(S+B) [%] | |
|---|---|---|---|---|---|---|---|---|
| | MC | Data | | MC | Data | | | |
| | | Run1 | Run2 | | Run1 | Run2 | Run1 | Run2 |
| before tagging | – | – | – | 177262 | 6149 ±89 | 3181±64 | 83.9 ±0.5 | 82.5 ±0.7 |
| All tags | 69.79±0.11 | 67.8 ±0.6 | 68.7 ±0.8 | 123722 | 4167 ±73 | 2186 ±52 | 86.3 ±0.6 | 84.8 ±0.8 |
| Lepton | 13.16±0.08 | 12.0 ±0.4 | 11.3 ±0.6 | 23321 | 738 ±28 | 360 ±20 | 96.6 ±0.7 | 94.9 ±1.2 |
| Kaon | 32.56±0.11 | 33.3 ±0.6 | 34.9 ±0.8 | 57708 | 2050 ±51 | 1110 ±37 | 85.0 ±0.8 | 84.0 ±1.1 |
| NT1 | 8.94 ±0.07 | 8.7 ±0.4 | 8.3 ±0.5 | 15841 | 533 ±25 | 264 ±17 | 87.9 ±1.5 | 90.7 ±1.7 |
| NT2 | 15.15±0.09 | 13.8 ±0.4 | 14.1 ±0.6 | 26852 | 846 ±35 | 450 ±26 | 80.9 ±1.6 | 77.0 ±2.2 |

In the nominal fit to the $\Delta t$ distributions of the selected candidates (unmixed and mixed), we fit all four tagging categories simultaneously with 44 parameters to describe signal and

Figure 2: Beam-energy substituted mass $m_{\rm ES}$ for the selected $B$ candidates in data separated by tagging category and by run1 vs. run2. The per-event signal probability is determined from these fits.

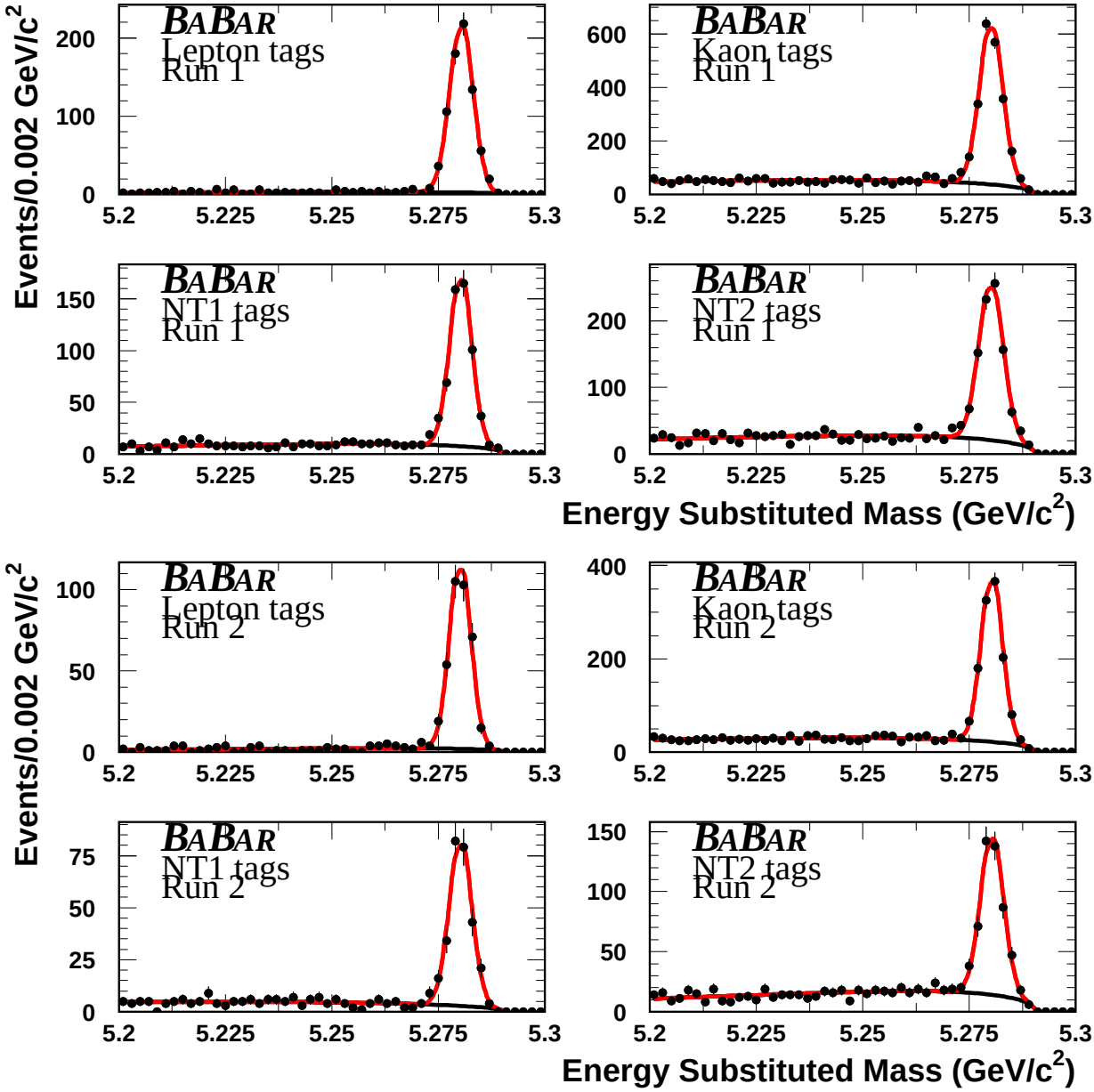

background properties. The fit parameters for the signal events are the $B^0\overline{B}^0$ oscillation frequency $\Delta m_d$ the average dilution $\langle D_i \rangle$ and the dilution difference $\Delta D_i$ for each of the four tagging categories $i$ and the scale factors, biases and fractions of events in the resolution function terms (double Gaussian resolution + outlier: $\mathcal{S}_{core}$, $4\times\delta_{\mathrm{core},i}$, $\delta_{\mathrm{tail}}$, $f_{\mathrm{tail}}$ and $f_{\mathrm{outlier}}$). Note that $\mathcal{S}_{\mathrm{tail}}$ is fixed to 3 for both run 1 and run 2 (see also [11]). The background parameters in the nominal fit are the average dilution for each tagging category for the prompt ($D'_{\tau=0,i}$) and the non-prompt component ($D'_{\tau>0,i}$), the fraction of events in the prompt component $f_{\tau=0,i}$ and the average lifetime of the non-prompt events $\tau_{\tau>0}$. The background $\Delta t$ resolution is described by a scale factor $\mathcal{S}_{\mathrm{Bkg}}$ and an average bias $\delta_{\mathrm{Bkg}}$ of a single Gaussian resolution function and the fraction of $\Delta t$ outliers $f_{\mathrm{Bkg,\ outlier}}$. No time-dependent mixing term is included in background description of the nominal fit, but the impact of such a term is studied as a source of systematic error (see section 7.7). Due to the high signal purity and the large $m_{\mathrm{ES}}$ side band region the correlations between the signal parameters and the background parameters are small. This greatly limits any potential bias in the signal parameters due to an incorrect description of the background. The remaining non-trivial external input parameters into the fit are the $B^0$ lifetime (fixed to the PDG average 1.548 ps); The fraction of $B^+$ peaking background (fixed to 1.3%), the $B^+$ lifetime (fixed to the PDG value of 1.653 ps) and $B^+$ "dilutions" (0.908,0.764,0.574 and 0.256 for the lepton, kaon, NT1 and NT2 tagging categories, taken from [2]. All external parameters are varied within their uncertainties to obtain the corresponding systematic uncertainties.

The results of the likelihood fit to the $\Delta t$ distributions for signal candidates in data and simulated signal events are listed in Table 2. In signal MC, the fitted value of the $B^0\overline{B}^0$ oscillation frequency $\Delta m_d = 0.4786 \pm 0.0032\hbar\,\mathrm{ps}^{-1}$, which should be compared to the value used for Monte Carlo generation of $0.472\hbar\,\mathrm{ps}^{-1}$. As will be described in Section 7.1.2, $\Delta m_d$ will be corrected by this observed difference. The fitted mistag rates are in good agreement with the values obtained from MC truth information, confirming an unbiased measurement of those parameters (see Table 6). The fitted signal parameters in data are largely compatible with the corresponding values in MC.

A goodness-of-fit confidence level that reflects the nature of the unbinned likelihood fit is derived using a toy MC technique. We generate a large number of samples of signal and background events with toy MC using the same pdf's with the parameters as measured from the selected events in data (for a more detailed description, see Section 7.1.1). The fraction of events with a smaller log likelihood than the one obtained from the fit to the data is interpreted as a goodness-of-fit confidence level. By not binning events in $\Delta t$ and tagging category and not averaging over $\sigma_{\Delta t}$ this technique takes correctly into account the individual contribution from each event. The distribution of log likelihoods from the fits to 1981 toy MC samples is shown in Fig. 3 and the derived confidence level for the data fit is 44.4±1.1%.

The $\Delta t$ distributions of the candidates overlaid with the likelihood fit results are shown in Figs. 4 and 6 for all candidates and in Figs. 5 and 7 separated by tagging category for signal Monte Carlo and data, respectively. The $\Delta t$ distributions for the background candidates in data from the $m_{\mathrm{ES}}$ sideband ($m_{\mathrm{ES}} < 5.27\,\mathrm{GeV}$) are shown in Figs. 8 and 9. In Figures 10 and

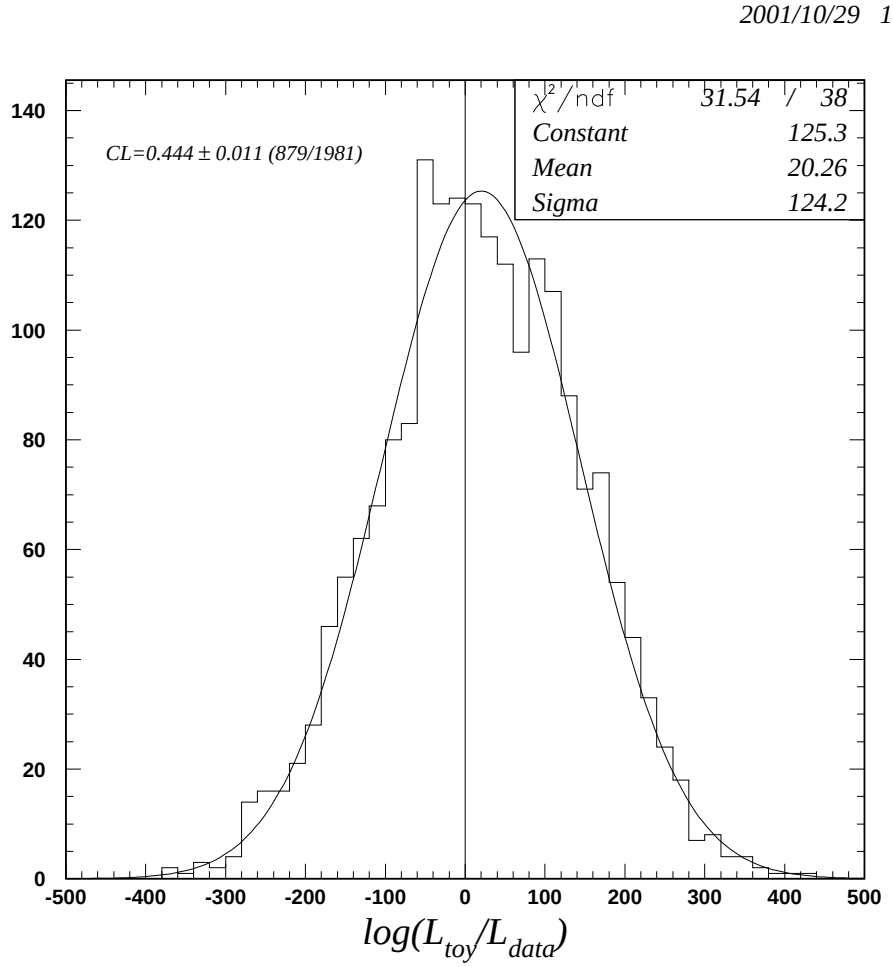


Figure 3: Distribution of the log of the likelihood obtained from fits to toy MC samples relative to the one found for the data. The vertical line represents the value found in data. 44.4% of the toy experiments have likelihoods smaller than the data.

11 the mixing asymmetry $A_{\rm mixing}(\Delta t)$ is shown and the basic cosine dependence is clearly visible.

All fit curves describe the data well. We calculate the Poisson $\chi^2$ (see [10],page 196) for each bin of the $\Delta t$ distributions of unmixed and mixed events. We then take the square root of the $\chi^2$, sign it according to whether the data is above or below the fit, and plot these for the signal region ($m_{\rm ES} > 5.27$) in Figure 6 and in Figure 7. The same distributions for the sideband ($m_{\rm ES} < 5.27$) are shown in Figure 8 and Figure 9.

We calculate the mistag rates $w = (1 - D)/2$ and the tagging separation $Q = \epsilon_{\rm tag} D^2$ from the efficiencies and dilutions listed in Table 1 and 2 for data and simulated events. The results are listed in Table 3. The measured mistag rates in data are on average larger than in signal Monte Carlo. This results in a smaller tagging separation $Q$ for data (27.5 $\pm$1.7

Table 2: Results from the likelihood fit to the $\Delta t$ distributions of the hadronic $B$ decays in simulated signal events and in data. In addition to the fit parameter values, the correlation coefficient $\rho$ of the parameter under study with respect to $\Delta m_d$ is given. In the case of $\Delta m_d$ the correlation reported is the *global* correlation. The measured values for $\Delta m_d$ and the dilutions in data have not been corrected for potential biases determined from the signal MC events. Note that the background parameters for data and signal MC should *not* be compared, since the background levels and sources are very different. The value of $\Delta m_d$ used for event generation in the MC sample is 0.4720 $\hbar\,\mathrm{ps}^{-1}$.

| Parameter | Fit Value (MC) | $\rho$ | Fit Value (Data) | $\rho$ |
|---|---|---|---|---|
| $\Delta m_d$ [$\hbar\,\mathrm{ps}^{-1}$] | 0.4786 ±0.0032 | 0.52 | XXXXX ± 0.016 | 0.51 |
| $D$(lepton) | 0.853 ±0.006 | 0.24 | 0.842 ±0.028 | 0.24 |
| $D$(kaon) | 0.708 ±0.004 | 0.31 | 0.669 ±0.023 | 0.30 |
| $D$(NT1) | 0.625 ±0.009 | 0.12 | 0.563 ±0.044 | 0.11 |
| $D$(NT2) | 0.310 ±0.008 | 0.08 | 0.313 ±0.041 | 0.11 |
| $\Delta D$(lepton) | 0.005 ±0.009 | -0.01 | -0.006 ±0.045 | 0.02 |
| $\Delta D$(kaon) | 0.037 ±0.007 | -0.00 | 0.024 ±0.033 | 0.01 |
| $\Delta D$(NT1) | -0.051 ±0.014 | 0.00 | -0.086 ±0.068 | 0.00 |
| $\Delta D$(NT2) | 0.070 ±0.012 | 0.00 | 0.100 ±0.060 | -0.00 |
| $f_{\tau=0,\mathrm{lepton}}$ | NA | | 0.047 ±0.103 | 0.01 |
| $f_{\tau=0,\mathrm{kaon}}$ | NA | | 0.423 ±0.046 | 0.01 |
| $f_{\tau=0,\mathrm{NT1}}$ | NA | | 0.329 ±0.077 | 0.01 |
| $f_{\tau=0,\mathrm{NT2}}$ | NA | | 0.321 ±0.078 | 0.01 |
| $\tau_{\tau>0}$ [ps] | NA | | 0.853 ±0.036 | -0.01 |
| $D'_{\tau=0,\mathrm{lepton}}$ | NA | | 0.040 ±2.909 | -0.02 |
| $D'_{\tau=0,\mathrm{kaon}}$ | NA | | 0.517 ±0.076 | -0.03 |
| $D'_{\tau=0,\mathrm{NT1}}$ | NA | | 0.669 ±0.273 | -0.01 |
| $D'_{\tau=0,\mathrm{NT2}}$ | NA | | -0.046 ±0.131 | -0.00 |
| $D'_{\tau>0,\mathrm{lepton}}$ | NA | | 0.338 ±0.127 | 0.02 |
| $D'_{\tau>0,\mathrm{kaon}}$ | NA | | 0.258 ±0.056 | 0.04 |
| $D'_{\tau>0,\mathrm{NT1}}$ | NA | | -0.125 ±0.112 | 0.01 |
| $D'_{\tau>0,\mathrm{NT2}}$ | NA | | 0.122 ±0.031 | 0.01 |
| $\mathcal{S}_{\mathrm{core,\ sig}}$ | 1.133 ±0.019 | 0.10 | 1.368 ±0.089 ; 0.25 ; 1.184 ±0.113 | 0.16 |
| $\delta_{\mathrm{core,\ sig,lepton}}$ | -0.059 ±0.022 | 0.04 | 0.057 ±0.125 ; 0.08 ; -0.039 ±0.156 | 0.00 |
| $\delta_{\mathrm{core,\ sig,kaon}}$ | -0.230 ±0.014 | 0.03 | -0.221 ±0.081 ; 0.03 ; -0.253 ±0.091 | 0.00 |
| $\delta_{\mathrm{core,\ sig,NT1}}$ | -0.150 ±0.027 | 0.02 | -0.068 ±0.152 ;-0.00 ; -0.452 ±0.211 | 0.00 |
| $\delta_{\mathrm{core,\ sig,NT2}}$ | -0.202 ±0.020 | 0.02 | -0.461 ±0.119 ; 0.01 ; -0.199 ±0.158 | 0.03 |
| $f_{\mathrm{tail}}$ | 0.036 ±0.008 | -0.02 | 0.014 ±0.020 ; 0.06 ; 0.015 ±0.010 | 0.07 |
| $\mathcal{S}_{\mathrm{tail,\ sig}}$ | 3.672 ±0.283 | 0.16 | NA (fixed at 3) ; NA (fixed at 3) | |
| $\delta_{\mathrm{tail,\ sig}}$ | -2.181 ±0.430 | 0.21 | -5.025 ±4.177 ; 0.04 ; -7.465 ±2.417 | 0.06 |
| $f_{\mathrm{outlier,\ sig}}$ | 0.004 ±0.001 | -0.08 | 0.008 ±0.004 ;-0.09 ; 0.000 ±0.014 | 0.01 |
| $\mathcal{S}_{\mathrm{core,\ bgd}}$ | NA | | 1.211 ±0.043 ;-0.00 ; 1.131 ±0.046 | 0.00 |
| $\delta_{\mathrm{core,\ bgd}}$ | NA | | -0.135 ±0.031 ;-0.00 ; -0.015 ±0.038 | -0.00 |
| $f_{\mathrm{outlier,\ bgd}}$ | NA | | 0.022 ±0.004 ;-0.01 ; 0.036 ±0.007 | 0.02 |

% and 27.7 ±1.7 % for run1 and run2 resp.) compared to simulated events (30.1 ±0.2 % ). Note that the efficiency used in the computation of $Q$ is relative to the sample of events which have a reconstruced value of $\Delta t$, and that the dilutions for both run1 and run2 are assumed to be the same (see also [2]).

Table 3: Mistag rate $w$ and tagging separation $Q$ for hadronic $B$ decays for the four tagging categories in data and simulated signal events. The measured mistag rates in data have not been corrected for potential biases determined from MC events.

| Tagging Category | Mistag Rate $w$ [%] | | Tagging Separation $Q$ [%] | | |
|---|---|---|---|---|---|
| | MC | Data (run 1 and 2 combined) | MC | Data run1 | Data run 2 |
| Lepton | 7.0 ±0.2 | 8.5 ± 1.5 | 9.73 ±0.14 | 8.4 ± 0.7 | 7.9 ± 0.7 |
| Kaon | 15.4 ±0.2 | 16.7 ± 1.2 | 15.58 ±0.15 | 14.8 ± 1.1 | 15.3 ± 1.2 |
| NT1 | 19.3 ±0.3 | 21.4 ± 2.3 | 3.37 ±0.07 | 2.9 ± 0.5 | 2.7 ± 0.5 |
| NT2 | 34.7 ±0.3 | 34.0 ± 2.2 | 1.42 ±0.05 | 1.4 ± 0.4 | 1.4 ± 0.4 |
| All | — | — | 30.1 ±0.2 | 27.5 ± 1.5 | 27.3 ±1.5 |

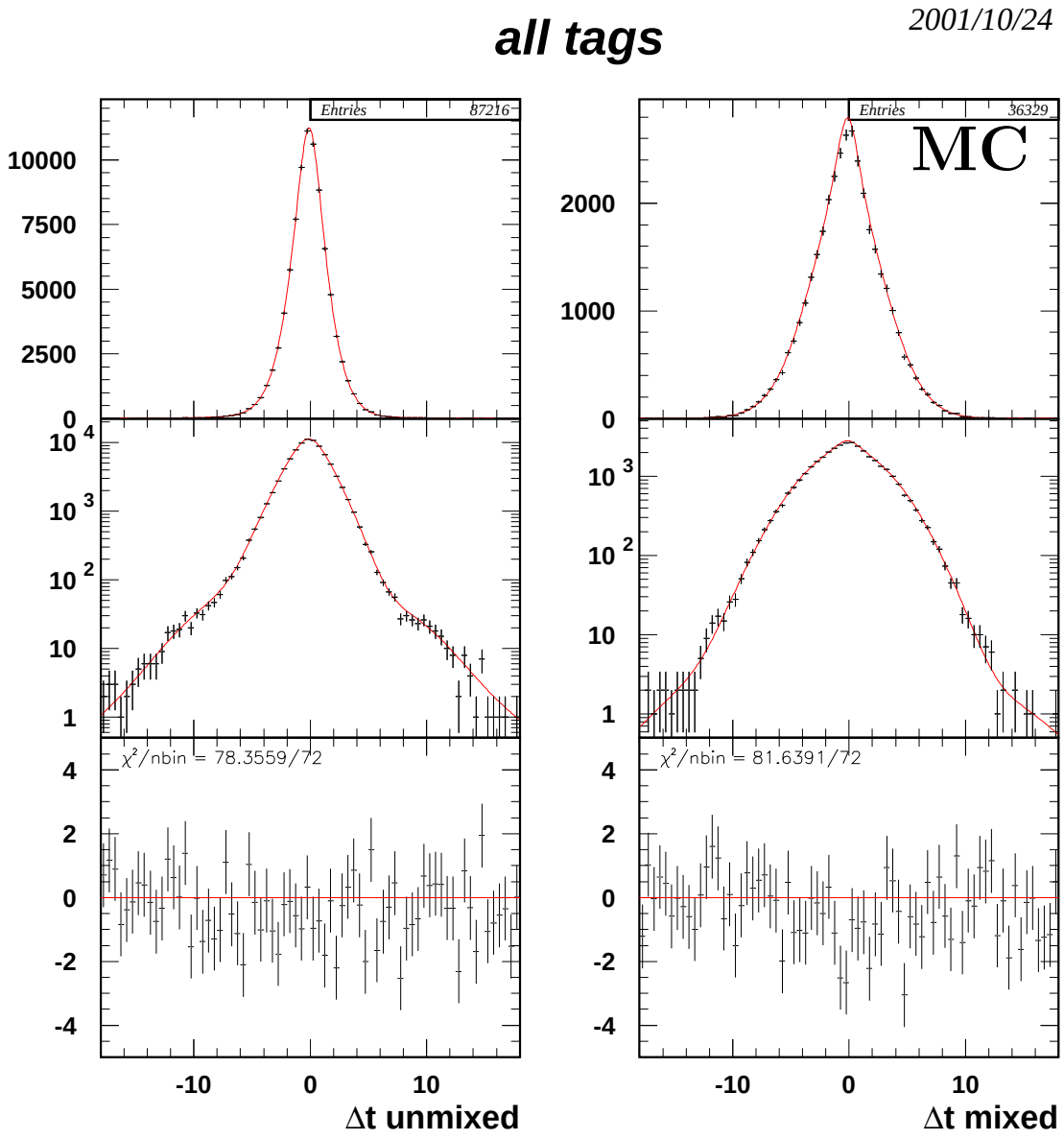


Figure 4: $\Delta t$ distributions in signal Monte Carlo for the selected hadronic $B$ decays (after truth association and for $m_{\rm ES} > 5.27\,{\rm GeV}$) separately for unmixed and mixed candidates. The fitted $\Delta t$ shapes for these candidates are overlaid. In addition, the fit residuals (in the form of Poisson $\chi^2$) are shown.

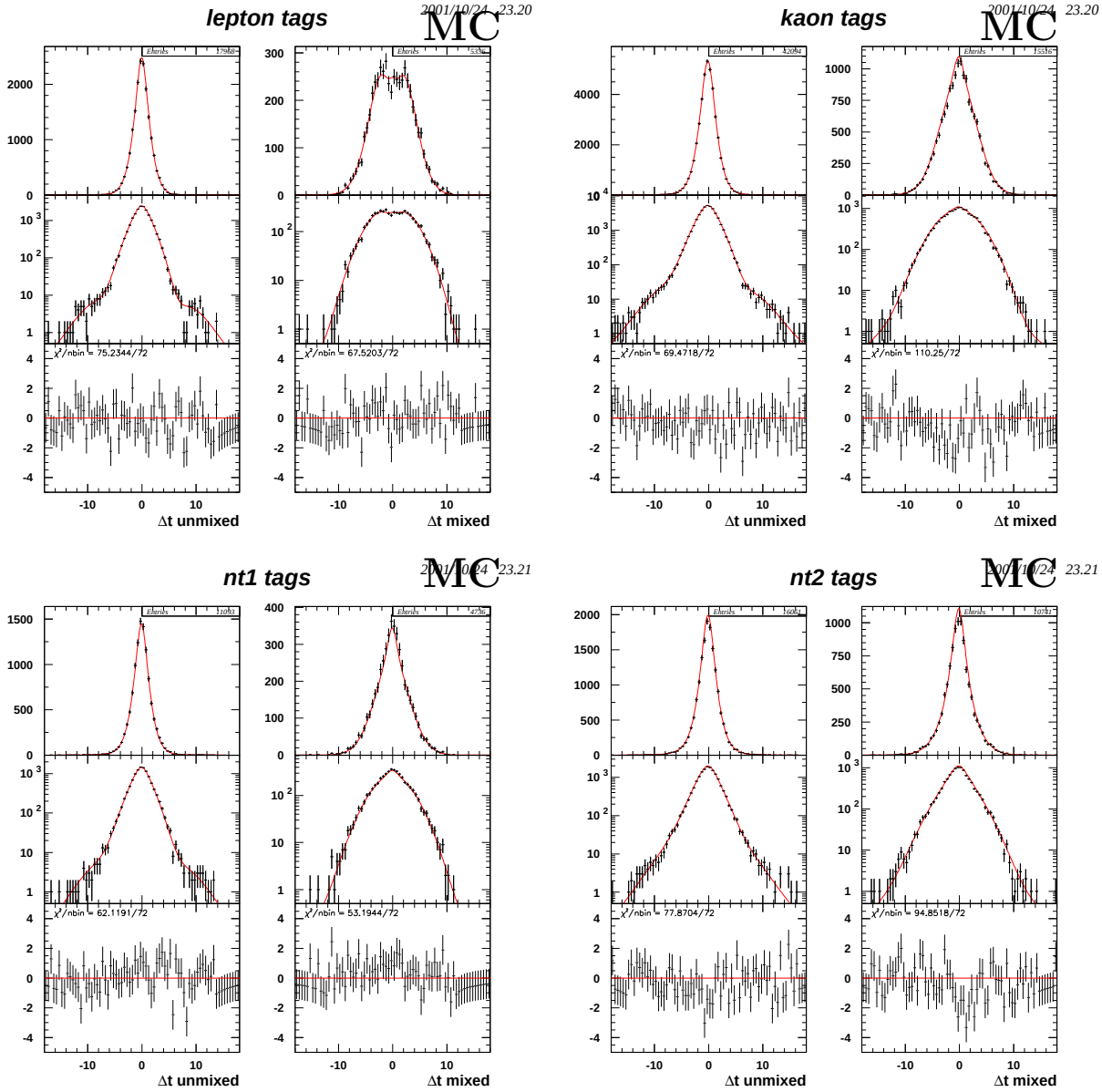


Figure 5: $\Delta t$ distributions in signal Monte Carlo for the selected hadronic $B$ decays (after truth association and for $m_{\rm ES} > 5.27\,{\rm GeV}$) separated by tagging category and separately for unmixed and mixed candidates. The fitted $\Delta t$ shapes for these candidates are overlaid. In addition, the fit residuals (in the form of Poisson $\chi^2$) are shown.

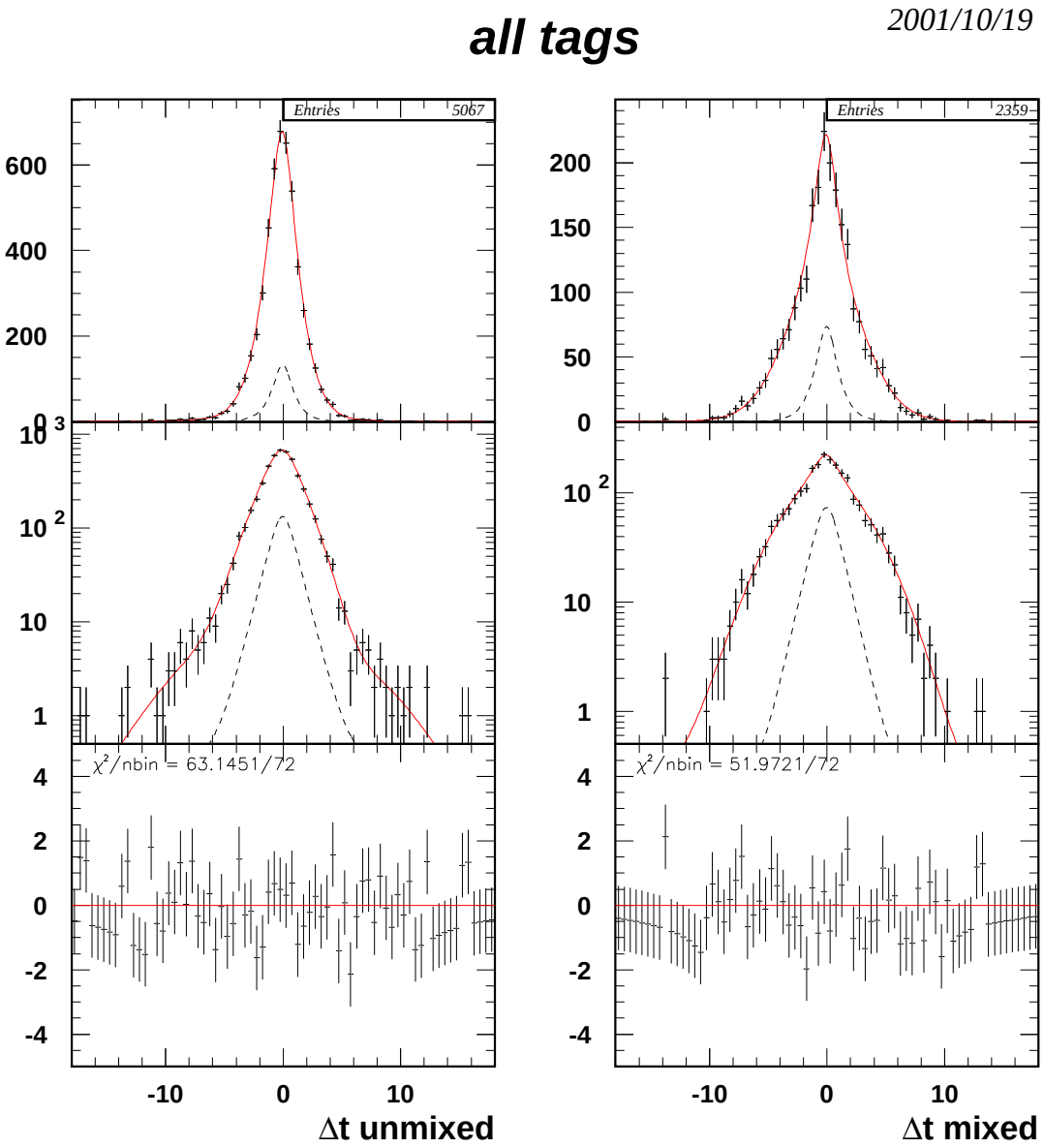


Figure 6: $\Delta t$ distributions in data for the selected hadronic $B$ decays ($m_{\rm ES} > 5.27$) separately for unmixed and mixed candidates. The fitted $\Delta t$ shapes for the selected candidates and for the fraction of background candidates are overlaid. In addition, Poisson $\chi^2$ distributions from the fits to the $\Delta t$ distributions are shown.

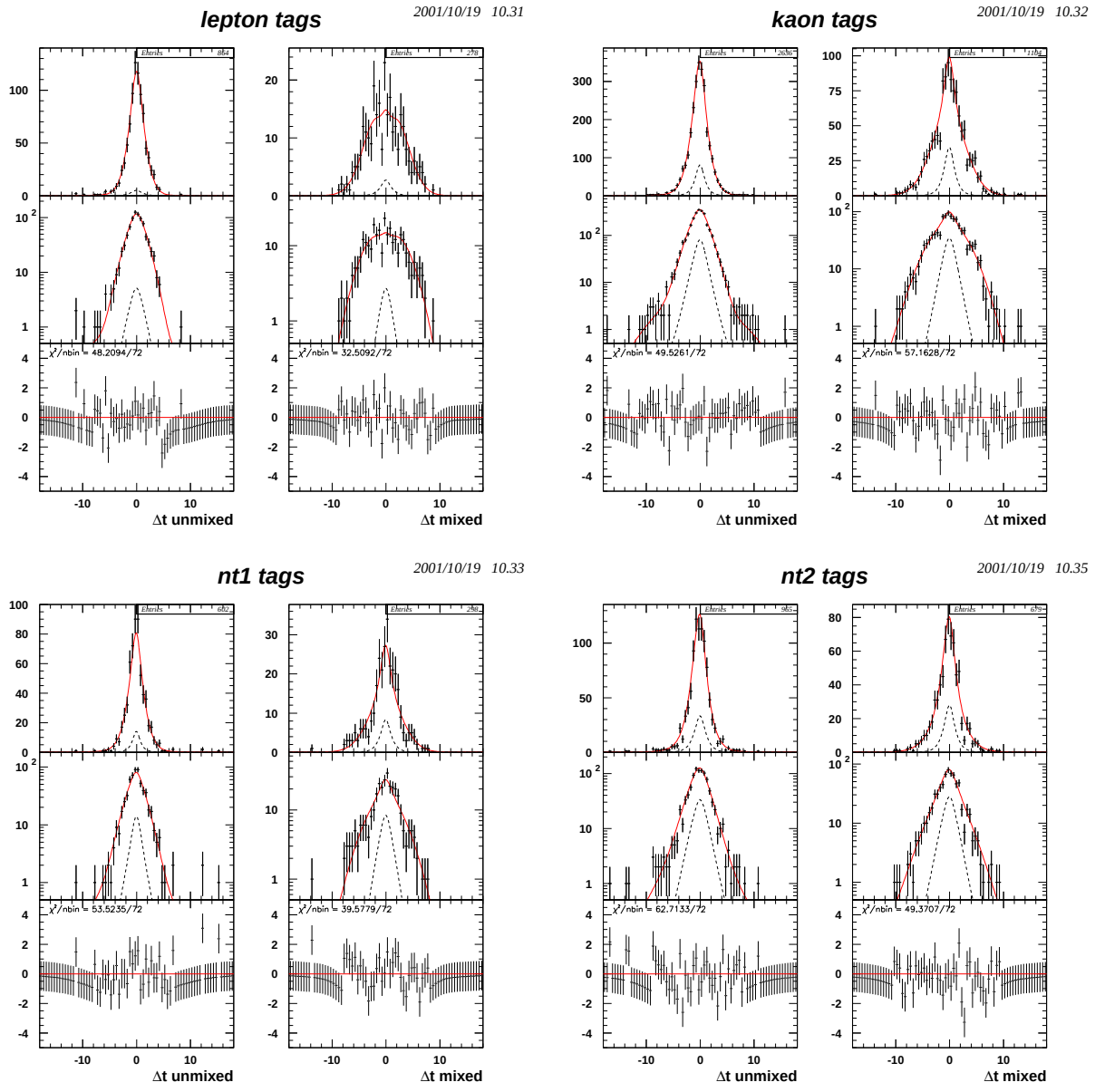


Figure 7: $\Delta t$ distributions in data for the selected hadronic $B$ decays in the signal region $m_{\rm ES} > 5.27\,{\rm GeV}$ separated by tagging category and separately for unmixed and mixed candidates. The fitted $\Delta t$ shapes for the selected candidates and for the fraction of background candidates are overlaid. In addition, Poisson $\chi^2$ distributions from the fits to the $\Delta t$ distributions are shown.

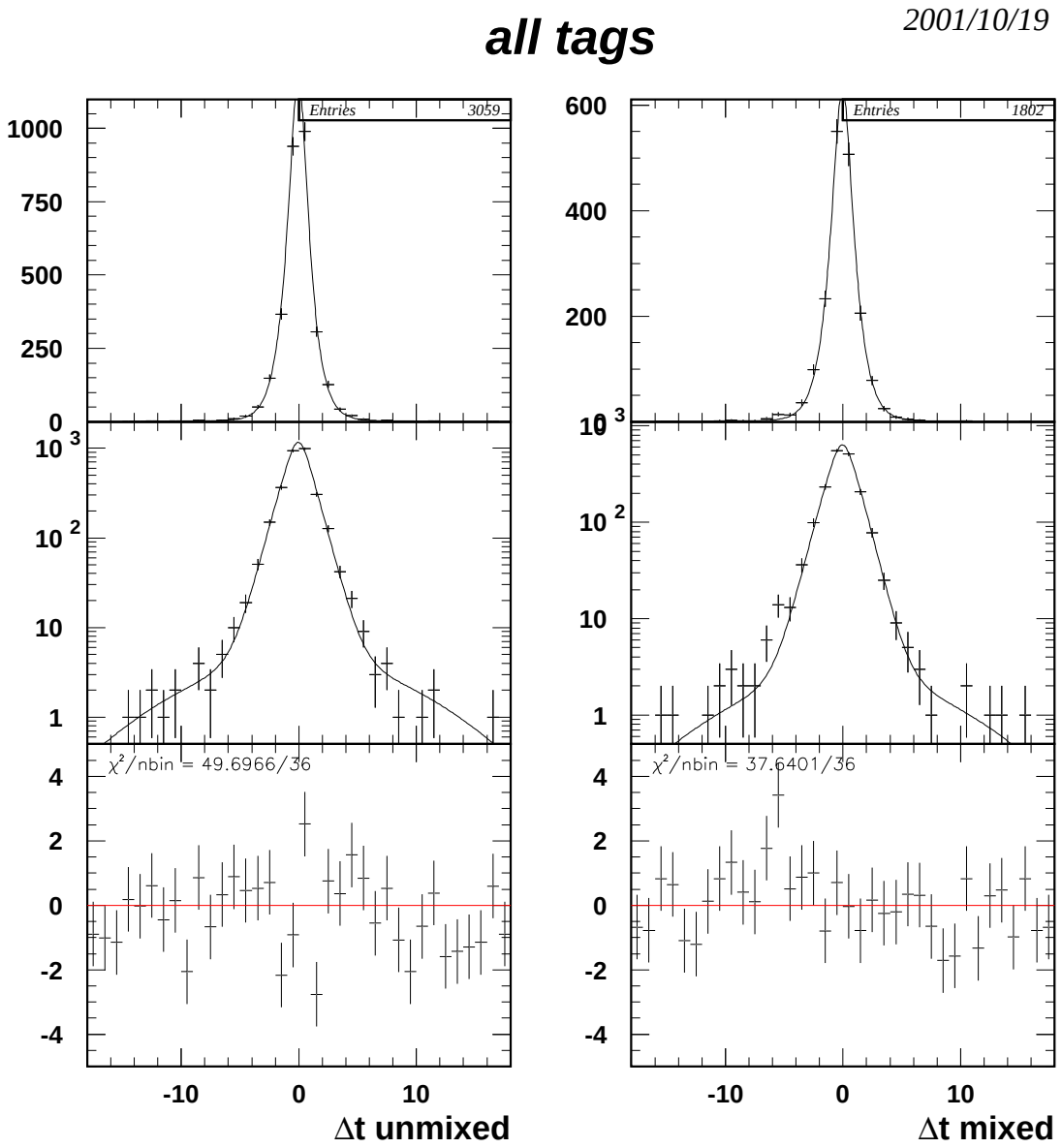


Figure 8: $\Delta t$ distributions in data for the background candidates with $m_{\rm ES} < 5.27\,{\rm GeV}$ with tagging information separately for unmixed and mixed candidates. The fitted $\Delta t$ shapes for these candidates are overlaid. In addition, Poisson $\chi^2$ distributions from the fits to the $\Delta t$ distributions in data are shown.

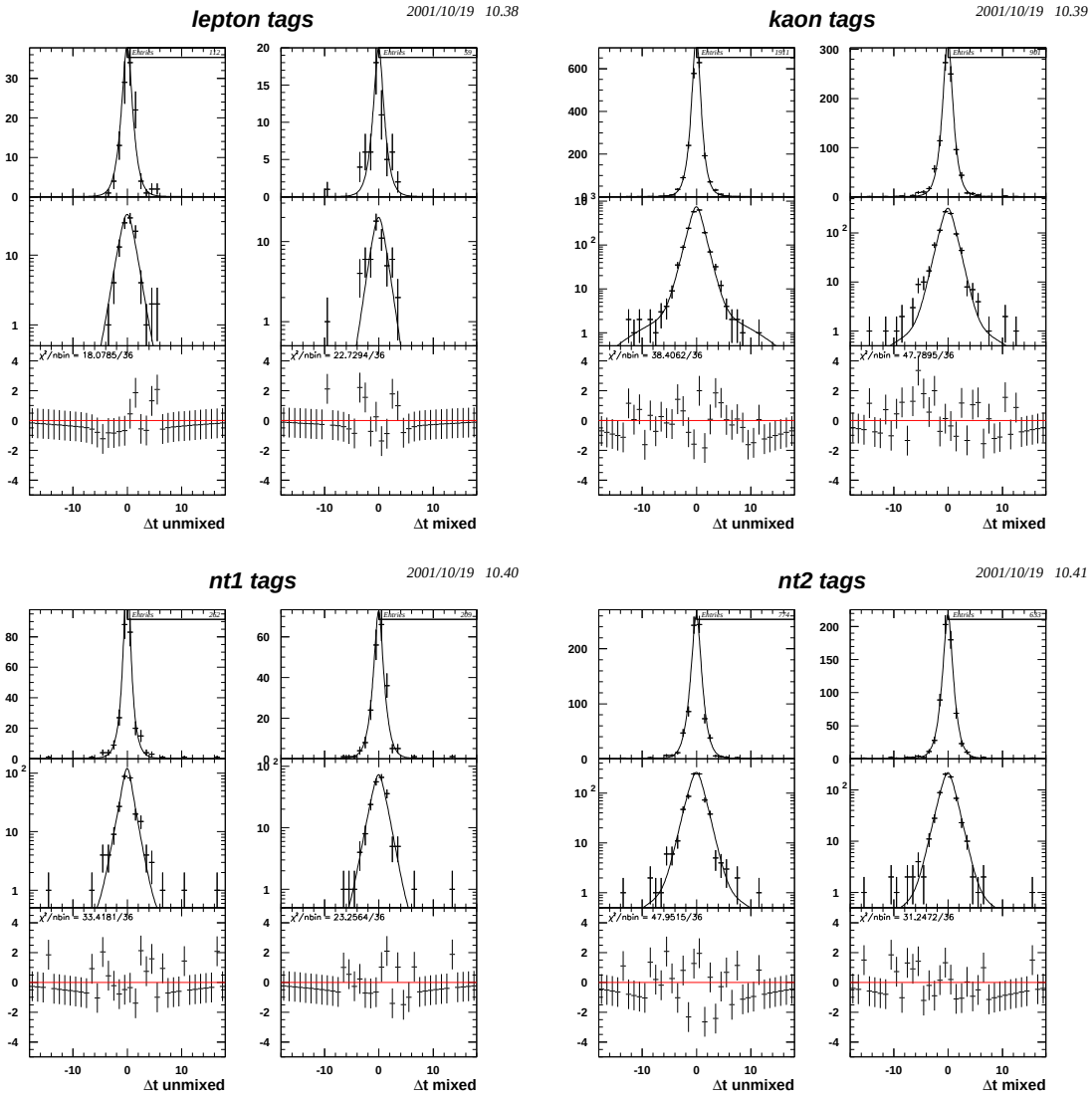


Figure 9: $\Delta t$ distributions in data for the background candidates with $m_{\rm ES} < 5.27\,{\rm GeV}$ separated by tagging category and separately for unmixed and mixed candidates. The fitted $\Delta t$ shapes for those candidates are overlaid.

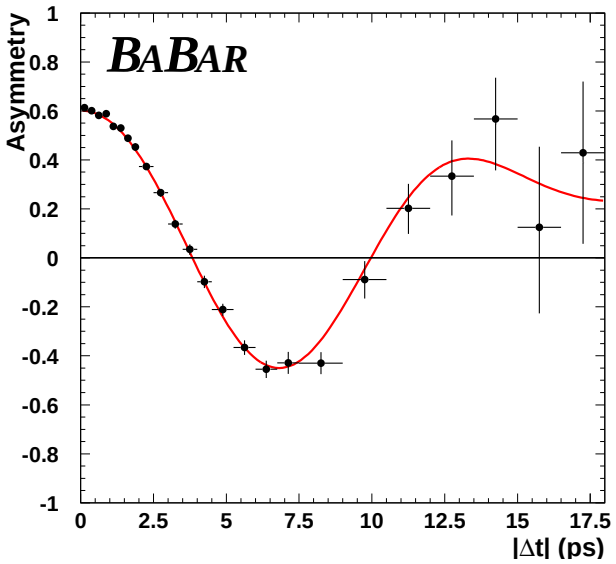


Figure 10: Time-dependent asymmetry $A_{\rm mixing}(|\Delta t|)$ (as defined in 4) between unmixed and mixed events in hadronic $B$ decays for signal Monte Carlo. Note that the presence of finite detector resolution distorts the observed asymmetry.

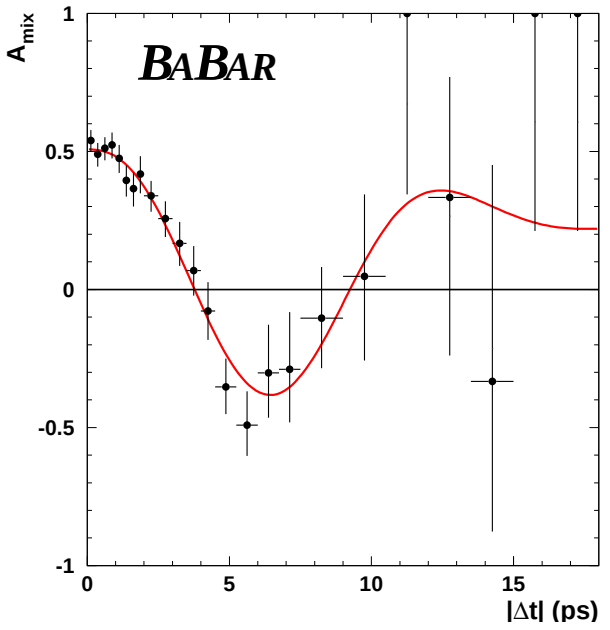


Figure 11: Time-dependent asymmetry $A_{\rm mixing}(|\Delta t|)$ (as defined in 4between unmixed and mixed events in hadronic $B$ decays for data. Note, that the presence of backgrounds in the data sample and the finite resolution change the observed time-dependence of the asymmetry.

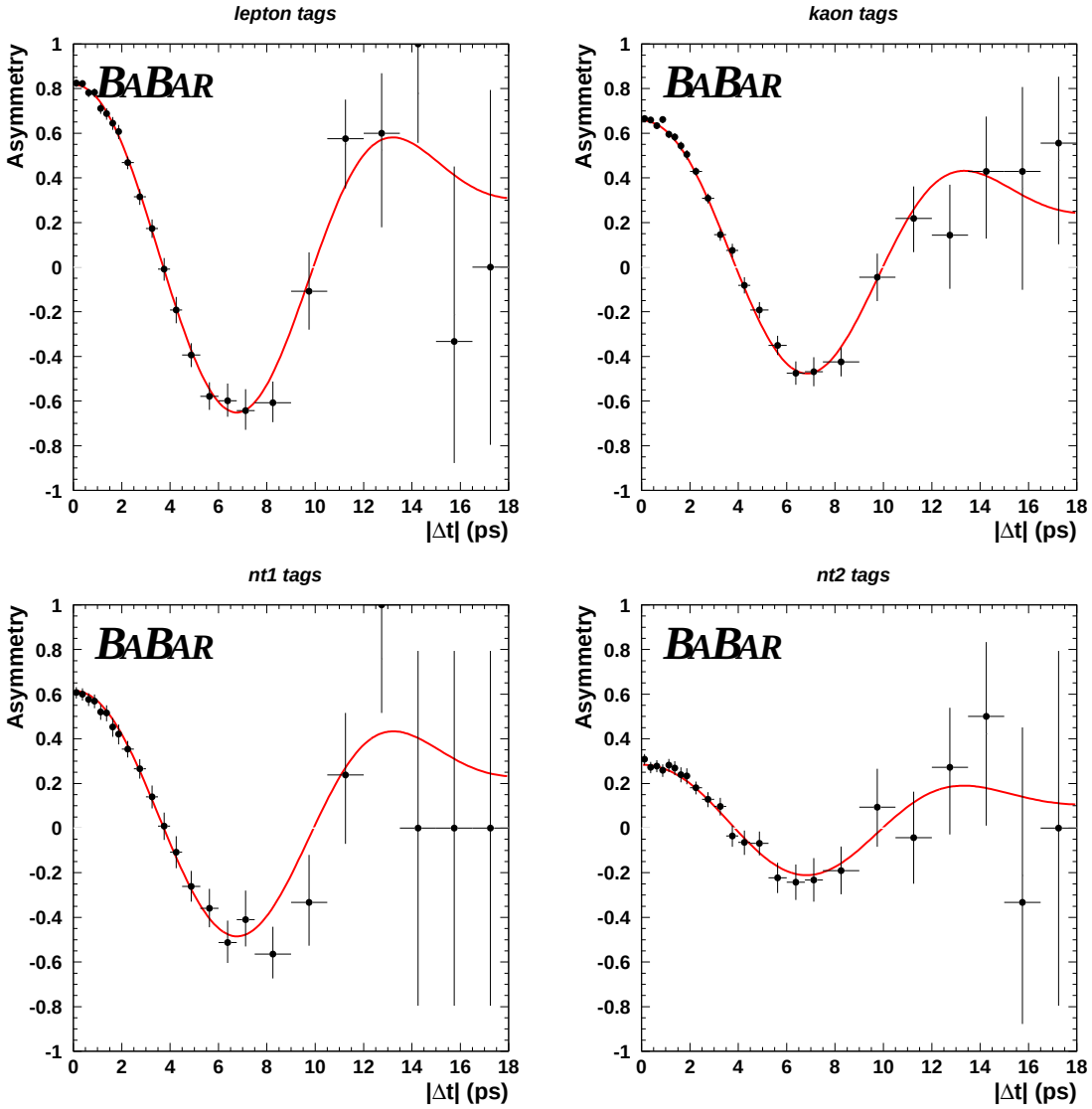


Figure 12: Time-dependent asymmetries $A_{\rm mixing}(|\Delta t|)$ between unmixed and mixed events in hadronic $B$ decays for signal MC, per tagging category.

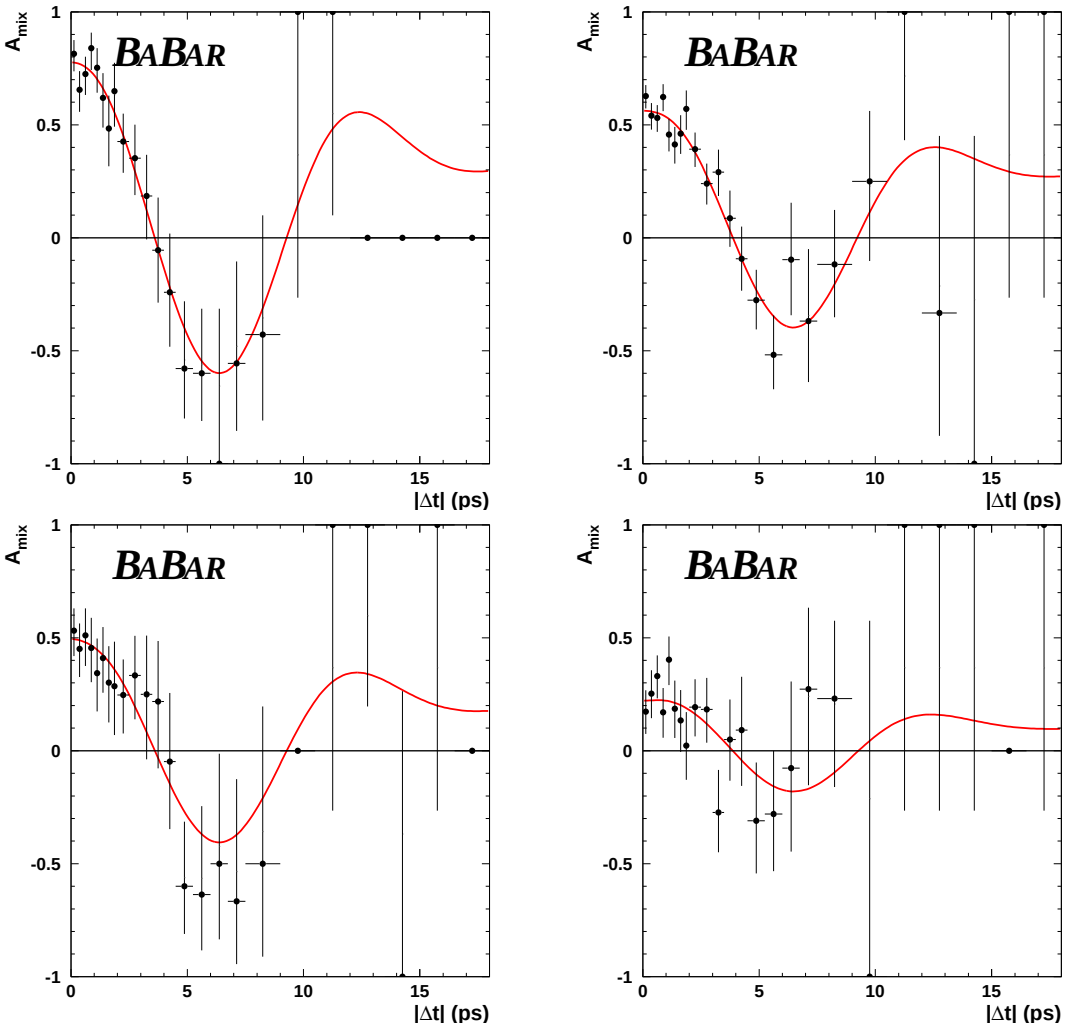


Figure 13: Time-dependent asymmetries $A_{\rm mixing}(|\Delta t|)$ between unmixed and mixed events in hadronic $B$ decays for data, per tagging category.

# 6 Consistency Checks

We have performed various checks of the consistency of the measurement including splitting of the data in sub-samples by several key variables.

## 6.1 $B^0$ Lifetime from Mixing Fits

In the nominal likelihood fits, we fix the $B^0$ lifetime to the PDG average of 1.548±0.032 ps [10]. We check if our $\Delta t$ distributions are consistent with the $\tau_{B^0}$ PDG average by allowing the $B^0$ lifetime to float. The fit results are listed in Table 4. The measured value for $\tau_{B^0}$ (1.502±0.031) is 1.0 $\sigma$ below the PDG value [2]. The changes in the tagging dilutions are negligible compared to their statistical uncertainties and the change in $\Delta m_d$ of -0.007 ±0.008 is due to a negative correlation between $\Delta m_d$ and $\tau_{B^0}$ and the correlations of both $\Delta m_d$ and $\tau_{B^0}$ with the resolution function parameters.

Table 4: Variation of $\Delta m_d$ for the likelihood fit with $\tau_{B^0}$ fixed to the PDG value and and as a free fit parameter in data. The error on the quoted difference includes the uncertainty on the PDG value of 0.032 ps.

| Variable | $\tau_{B^0}$ fixed | $\tau_{B^0}$ float | difference |
|---|---|---|---|
| $\tau(B^0)$ | 1.548 (fixed) | 1.502 ±0.031 | -0.046 ± 0.044 (-1.0$\sigma$) |
| $\Delta m_d$ [$\hbar\,\mathrm{ps}^{-1}$] | —— ± 0.016 | —— ± 0.017 | 0.008 ± 0.007 (1.3$\sigma$) |

## 6.2 MC split into data-sized subsamples

In addition to performing this check on the full cocktail MC sample, we also split the cocktail MC into 20 samples, and compare the effect of floating the lifetime. Table 5 lists the results, and they are illustrated in Figure 14. The fitted value for $\Delta m_d$, averaged over the 20 subsamples, is consistent with result from the full cocktail Monte Carlo sample (Table 5), both with and without a floating $B^0$ lifetime. There appear to be no bias effects related to sample size.

If we use only the MC generated with the correct value of $\chi_d$ (i.e. BReco events with a run number larger than 480000), we find 60K events, and a value of $\Delta m_d$ of 0.4756 ±0.0046. Fitting only the events which required re-weighting yield 0.4815 ±0.0045.

## 6.3 MC truth fits

We first perform a series of fits using the MC truth to check against possible selection biases. Starting from the reconstructed events and adding the requirement that $m_{\mathrm{ES}} > 5.27\,\mathrm{GeV}/c^2$

[2] the quoted "-1.0$\sigma$" includes the PDG 2000 error of 0.032 ps

Table 5: $\Delta m_d$ for likelihood fit with $\tau_{B^0}$ fixed to the PDG value and as a free fit parameter for cocktail signal MC. The error on the difference in $\Delta m_d$, $\delta\Delta m_d$ is computed using $\sqrt{|\sigma^2_{i,float} - \sigma^2_{i,fixed}|}$.

| Sample | $\tau_{B^0}$ fixed to PDG | $\tau_{B^0}$ Floating | | $\delta\Delta m_d$ |
|---|---|---|---|---|
| | $\Delta m_d$ | $\tau_{B^0}$ | $\Delta m_d$ | |
| 0 | 0.4709 ±0.0143 | 1.5337 ±0.0315 | 0.4730 ±0.0152 | 0.0021 ±0.0052 (0.4 ) |
| 1 | 0.4922 ±0.0142 | 1.5867 ±0.0327 | 0.4857 ±0.0150 | -0.0065 ±0.0048 (-1.3) |
| 2 | 0.4747 ±0.0145 | 1.5015 ±0.0327 | 0.4854 ±0.0169 | 0.0107 ±0.0087 (1.2 ) |
| 3 | 0.4735 ±0.0138 | 1.5258 ±0.0318 | 0.4782 ±0.0155 | 0.0047 ±0.0071 (0.7 ) |
| 4 | 0.4930 ±0.0140 | 1.5385 ±0.0326 | 0.4951 ±0.0160 | 0.0021 ±0.0077 (0.3 ) |
| 5 | 0.4850 ±0.0138 | 1.5384 ±0.0307 | 0.4868 ±0.0151 | 0.0018 ±0.0061 (0.3 ) |
| 6 | 0.4701 ±0.0139 | 1.5261 ±0.0333 | 0.4746 ±0.0157 | 0.0045 ±0.0073 (0.6 ) |
| 7 | 0.4646 ±0.0145 | 1.5813 ±0.0322 | 0.4502 ±0.0145 | -0.0144 ±0.000? ( ??? ) |
| 8 | 0.4725 ±0.0147 | 1.4774 ±0.0339 | 0.4865 ±0.0172 | 0.0140 ±0.0089 ( 1.6 ) |
| 9 | 0.4920 ±0.0142 | 1.5167 ±0.0321 | 0.4985 ±0.0160 | 0.0065 ±0.0074 ( 0.9 ) |
| 10 | 0.4726 ±0.0143 | 1.5402 ±0.0323 | 0.4741 ±0.0158 | 0.0015 ±0.0067 ( 0.2 ) |
| 11 | 0.4863 ±0.0127 | 1.1006 ±0.0318 | Fit failed | |
| 12 | 0.5029 ±0.0154 | 1.4777 ±0.0326 | 0.5218 ±0.0179 | 0.0189 ±0.0091 ( 2.1 ) |
| 13 | 0.4839 ±0.0145 | 1.5786 ±0.0316 | 0.4608 ±0.0098 | -0.0231 ±0.0107 (-2.2) |
| 14 | 0.4719 ±0.0139 | 1.5414 ±0.0321 | 0.4733 ±0.0156 | 0.0014 ±0.0071 ( 0.2 ) |
| 15 | 0.4844 ±0.0138 | 1.5641 ±0.0322 | 0.4812 ±0.0152 | -0.0032 ±0.0064 (-0.5) |
| 16 | 0.4638 ±0.0142 | 1.5464 ±0.0336 | 0.4642 ±0.0166 | 0.0004 ±0.0086 ( 0.0) |
| 17 | 0.4451 ±0.0149 | 1.5188 ±0.0334 | 0.4511 ±0.0167 | 0.0060 ±0.0075 ( 0.8) |
| 18 | 0.4837 ±0.0139 | 1.5780 ±0.0318 | 0.4782 ±0.0148 | -0.0055 ±0.0051 (-1.1) |
| 19 | Fit Failed | 1.5276 ±0.0304 | 0.4901 ±0.0135 | |
| Average | 0.4782 ±0.0032 | | 0.4776 ±0.0034 | |
| Full sample | 0.4786 ±0.0032 | | | |

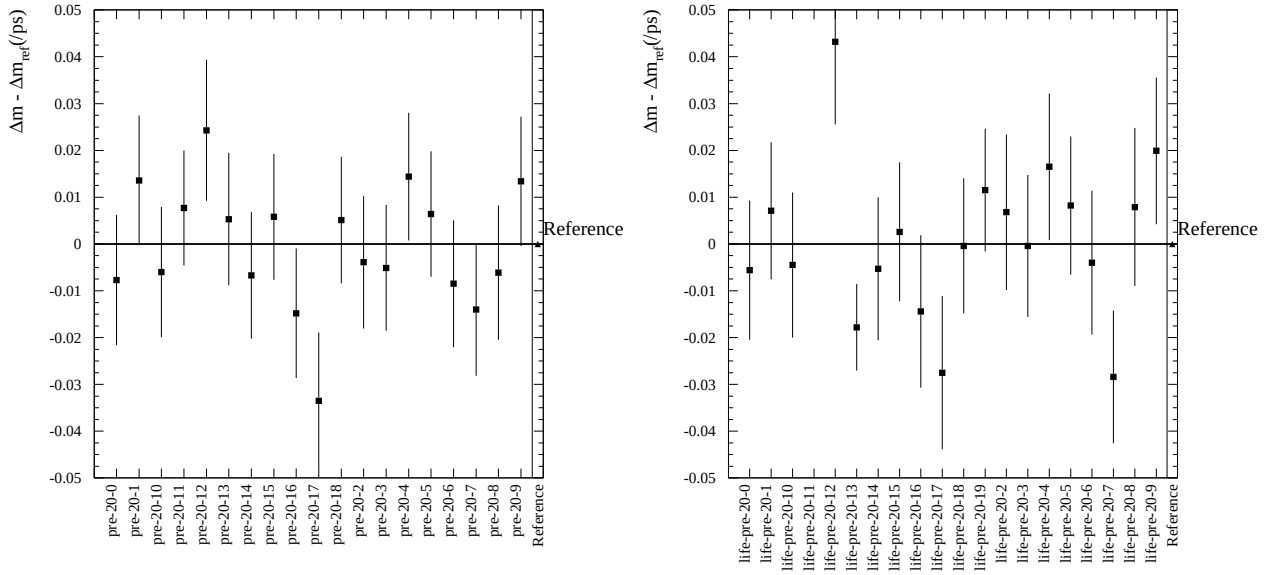


Figure 14: $\Delta m_d$ for likelihood fit with $\tau_{B^0}$ fixed to the PDG value and and as a free fit parameter for cocktail signal MC split into 20 samples.

and that there be a MC truth association for the event yields 123722 tagged events. Replacing both the reconstructed $\Delta t$ and reconstructed flavor tag with the MC truth, we obtain a deviation[3] of $\Delta m_d$ from its generated value of 0.472 of $+0.0008 \pm 0.0012$ (or $+0.7\sigma$). If in addition the lifetime is fitted, we obtain the same value for $\Delta m_d$ and a deviation of $\tau_{B^0}$ from its generated value of 1.548 ps of $+0.010 \pm 0.004$ (or $+2.2\sigma$).

We also check individual tag and reco B generated lifetime distributions by looking at the true $z$ production and decay positions and $\overline{B}^0$ momenta (see Figure 15).

Next the reconstructed flavor tag is used (while keeping the MC truth for the resolution), and the fit includes in addition to $\Delta m_d$ the mistag rates. The result is summarized and compared to MC truth in Table 6; The deviation of $\Delta m_d$ in this case is given by $\delta\Delta m_d$ =-0.0020 $\pm 0.0024 \hbar\,\mathrm{ps}^{-1}$.

## 6.4 MC characterization from counting

To check the MC and the event selection, we perform some simple test using MC truth counting to see if the fraction of mixed events ($\chi_d$) is correct and whether there are any differences between $B^0$ and $\overline{B}^0$. The results split up by fully reconstructed decay mode are shown in Table 7; split up by reconstructed tagging category in Table 8. We see that the sample tagged by leptons has a fraction of mixed events which is significantly higher than expected (resulting by itself in an increase in the apparent value of $\Delta m_d$). Splitting the

[3]defined as measured minus generated

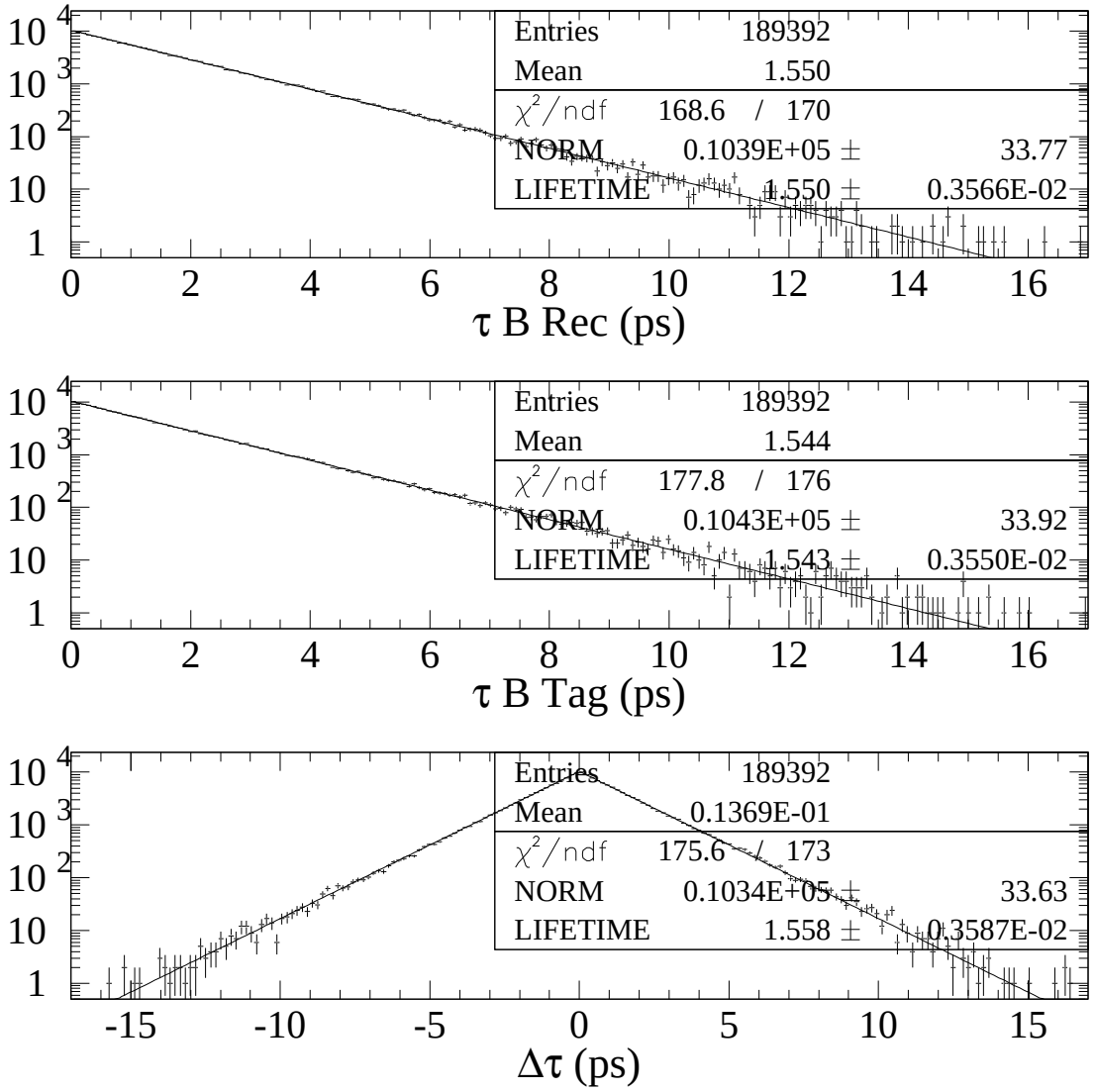


Figure 15: Monte Carlo Truth lifetime checks for reco (upper), tag (center), and $\Delta t$ in cocktail MC events.

Table 6: Values of dilution obtained from a) counting of MC truth information; b) the mixing fit using the true MC true $\Delta t$; c) the mixing fit using the reconstructed $\Delta t$, with the resolution fcn fixed to the values obtained from the fit to the MC $\Delta t$ residuals; d) the full mixing fit using the reconstructed $\Delta t$; In all cases using events with $m_{\rm ES} > 5.27\,{\rm GeV}/c^2$, $\sigma_{\Delta t} < 1.4\,{\rm ps}$ and with a succesfull MC truth match

| Variable | Counting using MC truth | Fit to true $\Delta t$ distribution | Fit with fixed $\Delta t$ res fcn | Full fit |
|---|---|---|---|---|
| D(lepton) | 0.859 ±0.003 | 0.847 ±0.005 | 0.852 ±0.006 | 0.853 ±0.006 |
| D(kaon) | 0.692 ±0.003 | 0.698 ±0.004 | 0.707 ±0.004 | 0.708 ±0.004 |
| D(NT1) | 0.614 ±0.006 | 0.614 ±0.008 | 0.624 ±0.009 | 0.625 ±0.009 |
| D(NT2) | 0.306 ±0.006 | 0.307 ±0.007 | 0.310 ±0.008 | 0.310 ±0.008 |
| ΔD(lepton) | 0.007 ±0.007 | 0.009 ±0.009 | 0.005 ±0.009 | 0.005 ±0.009 |
| ΔD(kaon) | 0.031 ±0.006 | 0.039 ±0.007 | 0.037 ±0.007 | 0.037 ±0.007 |
| ΔD(NT1) | -0.036 ±0.013 | -0.050 ±0.014 | -0.051 ±0.014 | -0.051 ±0.014 |
| ΔD(NT2) | 0.071 ±0.012 | 0.067 ±0.012 | 0.070 ±0.012 | 0.070 ±0.012 |

lepton tags further, it is clear that the main effect is in the case of lepton tags which also contain a (confirming) kaon tag. There is no significant difference between electrons and muons.

In addition we check the difference in reconstruction and tagging efficiencies, respectively, for $B^0$ and $\overline{B}^0$. Following the recipe of Ref. [18] (adopting the same notation), we find a relative difference in $B^0$ reconstruction efficiencies $\nu = 0.0059 \pm 0.0024 (+2.5\sigma)$ and tagging efficiency $\mu = 0.0057 \pm 0.0024 (+2.4\sigma)$, with a tagging efficiency $T = 0.6980 \pm 0.0011$.

## 6.5 Performing a counting experiment

The fraction of mixed events, $\chi_d$ is given by $\frac{1}{2}\frac{x_d}{1+x_d^2}$ where $x_d = \Delta m_d \cdot \tau_{B^0}$. As a result, given the mistag rates, one can compute $\Delta m_d$ from counting. Taking the dilutions from the time-dependent fit, the result of the counting experiment on data yields a value which is different from the full time-dependent fit by -0.003±0.013 $\hbar\,{\rm ps}^{-1}$, where the quoted uncertainty is the difference in quadrature between the error from the counting measurement and the error from the time-dependent fit with $\Delta m_d$ as the only free parameter. We conclude that for data the fraction of mixed events is consistent with the fitted value of $\Delta m_d$.

## 6.6 Fitting using the $\Delta t$ shapes only

The normalization of the default fit is such that the fraction of mixed events is forced to be consistent with the values of $\tau_B^0$ and $\Delta m_d$ (see Ref. [14] for more details). Taking out this constraint one can fit just the shapes of the various $\Delta t$ distributions, and even fit only the

Table 7: MC sample composition split by reconstructed decay mode. The $\chi_d^{rmtrue}$ reported is the fraction of mixed events, where (un)mixed is determined using MC truth. The values in parenthesis are the number of $\sigma$ that the reported value deviates from the expected value, computed from the input $B^0$ lifetime and $\Delta m_d$ to the event generator.

| $B^0$ decay mode | $B^0$ tag | $\overline{B}^0$ tag | f($B^0$ tag) | $\chi_d^{\rm true}$ |
|---|---|---|---|---|
| $D^-$ $(K^+\ \pi^+\ \pi^-)\pi^+$ | 27269 | 26779 | 0.505 ±0.004 ( 1.21) | 0.174 ±0.002 (-0.21) |
| $D^-$ $(K^+\ \pi^+\ \pi^-)\ a_1^+$ | 6596 | 6420 | 0.507 ±0.008 ( 0.88) | 0.173 ±0.003 (-0.35) |
| $D^-$ $(K^+\ \pi^+\ \pi^-)\rho^+$ | 14043 | 14091 | 0.499 ±0.005 (-0.17) | 0.178 ±0.002 ( 1.65) |
| $D^-$ $(K_S^0\ \pi^-)\pi^+$ | 2588 | 2535 | 0.505 ±0.012 ( 0.42) | 0.175 ±0.005 ( 0.27) |
| $D^-$ $(K_S^0\ \pi^-)\rho^+$ | 1133 | 1229 | 0.480 ±0.017 (-1.17) | 0.172 ±0.008 (-0.28) |
| $D^-$ $(K_S^0\ \pi^-)\ a_1^+$ | 704 | 697 | 0.502 ±0.023 ( 0.11) | 0.163 ±0.010 (-1.07) |
| $D^{*-}$ $(D^0\ (K^+\ \pi^-)\pi^-)\pi^+$ | 6672 | 6473 | 0.508 ±0.008 ( 0.99) | 0.176 ±0.003 ( 0.58) |
| $D^{*-}$ $(D^0\ (K^+\ \pi^-)\ \pi^-,)a_1^+$ | 5064 | 4975 | 0.504 ±0.009 ( 0.51) | 0.173 ±0.004 (-0.19) |
| $D^{*-}$ $(D^0\ (K^+\ \pi^-\ \pi^+\ \pi^-)\pi^-)a_1^+$ | 671 | 648 | 0.509 ±0.024 ( 0.36) | 0.170 ±0.010 (-0.41) |
| $D^{*-}$ $(D^0\ (K^+\ \pi^-\ \pi^+\ \pi^-)\pi^-)\pi^+$ | 1055 | 1066 | 0.497 ±0.019 (-0.14) | 0.190 ±0.009 ( 1.82) |
| $D^{*-}$ $(D^0\ (K^+\ \pi^-\ \pi^0)\pi^-)\pi^+$ | 4703 | 4831 | 0.493 ±0.009 (-0.76) | 0.173 ±0.004 (-0.36) |
| $D^{*-}$ $(D^0\ (K^+\ \pi^-\ \pi^0)\ \pi^-)a_1^+$ | 3536 | 3468 | 0.505 ±0.010 ( 0.47) | 0.168 ±0.004 (-1.44) |
| $D^{*-}$ $(D^0\ (K^+\ \pi^-)\ \pi^-)\rho^+$ | 3685 | 3615 | 0.505 ±0.010 ( 0.47) | 0.175 ±0.004 ( 0.23) |
| $D^{*-}$ $(D^0\ (K^+\ \pi^-\ \pi^+\ \pi^-)\pi^-)\rho^+$ | 571 | 587 | 0.493 ±0.025 (-0.27) | 0.152 ±0.011 (-2.09) |
| $D^{*-}$ $(D^0\ (K^+\ \pi^-\ \pi^0)\ \pi^-)\rho^+$ | 2734 | 2772 | 0.497 ±0.012 (-0.30) | 0.183 ±0.005 ( 1.80) |
| $D^{*-}$ $(D^0\ (K_S^0\ \pi^+\ \pi^-)\pi^-)\pi^+$ | 1274 | 1316 | 0.492 ±0.017 (-0.48) | 0.159 ±0.007 (-2.14) |
| $D^{*-}$ $(D^0\ (K_S^0\ \pi^+\ \pi^-)\pi^-)a_1^+$ | 889 | 865 | 0.507 ±0.021 ( 0.33) | 0.173 ±0.009 (-0.08) |
| $D^{*-}$ $(D^0\ (K_S^0\ \pi^+\ \pi^-)\ \pi^-)\rho^+$ | 725 | 683 | 0.515 ±0.024 ( 0.63) | 0.173 ±0.010 (-0.07) |
| $J/\psi$ $(e^+e^-)K^{*0}$ $(K^+\ \pi^-)$ | 2250 | 2219 | 0.503 ±0.013 ( 0.27) | 0.177 ±0.006 ( 0.52) |
| $J/\psi$ $(\mu^+\mu^-)K^{*0}$ $(K^+\ \pi^-)$ | 2989 | 2842 | 0.513 ±0.012 ( 1.09) | 0.171 ±0.005 (-0.69) |
| all | 89151 | 88111 | 0.503 ±0.002 ( 1.42) | 0.174 ±0.001 ( 0.21) |

Table 8: MC sample composition split by tagging category. In the top half of the table, MC truth is used to determine whether an event is mixed or unmixed. In the bottom half, the reconstructed $B_{\rm rec}$ and the result of the flavor tagging algorithm is used. The value of $\chi_d^{corrected}$ is determined from the observed $\chi_d^{observed}$, and then corrected using the mistag rate determined by comparing the reconstructed flavour tag and MC truth. Finally, the column labeled ($\chi_d$ pull) is the deviation in units of $\sigma$ from the expected value.

| TRUTH | mixed | unmixed | $\chi_d$ ($\chi_d$ pull) |
|---|---|---|---|
| lepton | 4271 | 19050 | 0.183 ±0.003 (3.60) |
| elec(kaon) | 2295 | 10119 | 0.185 ±0.003 (3.11) |
| muon(kaon) | 1976 | 8931 | 0.181 ±0.004 (1.94) |
| lepton *without* kaon | 3050 | 13837 | 0.181 ±0.003 (2.23) |
| lepton *with* kaon | 1221 | 5213 | 0.190 ±0.005 (3.22) |
| kaon | 9878 | 47830 | 0.171 ±0.002 (-1.82) |
| NT1 | 2798 | 13043 | 0.177 ±0.003 (0.86) |
| NT2 | 4723 | 22129 | 0.176 ±0.002 (0.80) |
| none | 9211 | 44329 | 0.172 ±0.002 (-1.22) |
| ave | 30881 | 146381 | 0.174 ±0.001 (0.21) |
| RECO | mixed | unmixed | $\chi_d^{\rm observed}$ $\chi_d^{\rm corrected}$ ($\chi_d$ pull) |
| lep reco | 5339 | 17982 | 0.229 0.184 ±0.003 (3.04) |
| electron(k) | 2833 | 9581 | 0.228 0.187 ±0.005 (2.72) |
| muon(k) | 2506 | 8401 | 0.230 0.182 ±0.005 (1.55) |
| lepton *without* kaon | 4077 | 12810 | 0.241 0.181 ±0.004 (1.67) |
| lepton *with* kaon | 1262 | 5172 | 0.196 0.191 ±0.005 (3.35) |
| kaon reco | 15560 | 42148 | 0.270 0.167 ±0.003 (-2.31) |
| NT1 reco | 4745 | 11096 | 0.300 0.174 ±0.007 (-0.05) |
| NT2 reco | 10766 | 16086 | 0.401 0.176 ±0.012 (0.17) |
| ave reco | 62793 | 114469 | 0.354 0.171 ±0.003 (-1.03) |

mixed or only the unmixed events. The results of these fits for several samples are shown in Table 9 and Table 10.

Table 9: Result of likelihood fits on MC using only the $\Delta t$ shape;

| sample | $\Delta m_d$ |
|---|---|
| shape | 0.4786 ±0.0032 |
| mixed-shape | 0.4786 ±0.0032 CHECK |
| unmixed-shape | 0.4786 ±0.0032 CHECK |
| bbarrec-shape | 0.4689 ±0.0069 |
| brec-shape | 0.4777 ±0.0065 |
| bbartag-shape | 0.4781 ±0.0045 |
| btag-shape | 0.4790 ±0.0046 |
| Lep-shape | 0.4875 ±0.0056 |
| Kaon-shape | 0.4730 ±0.0047 |
| NT1-shape | 0.4691 ±0.0090 |
| NT2-shape | 0.4849 ±0.0145 |

## 6.7 Other unbinned likelihood fit implementations

In order to check that there are no implementation specific problems in the likelihood fit, the $\Delta m_d$ MC fit is repeated using both CPExtract and RooFitTools/Core. Of course, all three programs are intended to implement the same likelihood functions, and all three use MINUIT to perform their minimization. Using RooFitCore, performing the MC fit, we obtain an answer consistent with the tFit result. In addition results from CPExtract have been reported in [19]. We conclude that all three implementations are consistent with one another.

## 6.8 Decay Modes

We perform the likelihood fit separately on sub-samples of different $B$ decay modes. We separate by the $B$ decay mode ($\pi/\rho/a_1$) and by the state of the charmed meson ($D^{*-}$ or a $D^-$). We also fit the $B \to J/\psi K^{*0}$ events separately. The results are listed in Table 11. No significant discrepancy is seen among these subsamples.

## 6.9 Tagging Category

We perform the likelihood fit for each tagging category individually. In these fits, we let, for example, the resolution function parameters and the background lifetime float. As a result, small differences in the tagging dilutions from these fits compared with the fit to the total

Table 10: Result of likelihood fits on Data using only the $\Delta t$ shape;

| sample | $\Delta m_d$- nominal |
|---|---|
| all | XX+0.003 ±0.015 |
| lepton | XX+ 0.004 ±0.024 |
| kaon | XX+ 0.009 ±0.021 |
| nt1 | XX -0.019 ±0.039 |
| nt2 | XX+ 0.189 ±0.092 |
| unmixed | XX+0.003 ±0.015 (CHECK!) |
| mixed | XX+0.003 ±0.015 (CHECK!) |
| bbartag | XX+ 0.015 ±0.021 |
| btag | XX+-0.016 ±0.020 |
| bbarrec | XX+ (CHECK!) |
| brec | XX+-0.010 ±0.021 |

Table 11: Variation of $\Delta m_d$ for different decay modes in data. As the value of $\Delta m_d$ is still blind, the values of $\Delta m_d$ are reported as 'XX' (representing the blind result from the nominal fit) plus the difference. The error reported is on the value itself, and *not* on the difference with the reference value.

| mode | $\Delta m_{d\text{mode}} - \Delta m_{d\text{all}}$ |
|---|---|
| $D^*\pi$ | -0.029 ±0.030 |
| $D^*\rho$ | +0.017 ±0.039 |
| $D^*a_1^+$ | +0.066 ±0.063 |
| $D\pi$ | +0.022 ±0.030 |
| $D\rho$ | -0.031 ±0.038 |
| $Da_1^+$ | -0.033 ±0.041 |
| $D^*$ $X$ | 0.000 ±0.025 |
| $D$ $X$ | -0.005 ±0.023 |
| $J/\psi K^{*0}$ | |

sample are possible. The results are listed in Table 12. No significant discrepancy is seen among these subsamples. For MC, the results are shown in Table 13.

## 6.10 $B^0$ vs. $\overline{B}^0$

We split the data sample in two, depending on whether the reconstructed $B$ is a $B^0$ or a $\overline{B}^0$. In addition we split the sample depending on the flavor of the tagging $B$. The results of these four fits is summarized in Table 14. No significant discrepancy is seen between these subsamples.

## 6.11 Resolution Model

To motivate the choice of scaling the bias, as described in Sec. 4.2, the sample is sliced in bins of $\sigma_{\Delta t}$, and for each slice the MC residual ($\Delta t$- $\Delta t_{\rm true}$) distribution is plotted in a range of $\pm 5$ times the maximum $\sigma_{\Delta t}$ in the slice under consideration. The mean values and RMS deviations obtained from the individual slices are shown as a function of the per-event error (for this we take the center of the slice) in Fig. 16. From this plot we conclude that one should scale the bias with the per-event error. An explanation of this behaviour can be found in [6], with additional information in [15]. In addition, we require the per-event $\sigma_{\Delta t}$ to be less than 1.4 ps to avoid the region where this scaling no longer holds.

Fitting this resolution model on the MC residual $\delta\Delta t$ distributions, and constraining the resolution function to those parameters in a mixing fit, we obtain a $\Delta m_d$ of 0.4777 $\pm$0.0029 $\hbar\,\mathrm{ps}^{-1}$.

For the nominal fit to MC, where the parameters of the resolution model are floating free in the fit and are determined without the help of the knowledge of the MC truth $\Delta t$, we find the values listed in Table 2. The value of $\Delta m_d$ is 0.4786 $\pm$0.0032 $\hbar\,\mathrm{ps}^{-1}$. The main change in the resolution function parameters between the two configurations is the increase in the two scale factors in the nominal fit wrt. the fit on $\delta\Delta t$, and the change in the tail fraction.

We perform the fits to the $\Delta t$ residual distributions separately for each tagging category because the $\Delta t$ resolution can generally depend on the tagging category. The fit results are listed in Table 15. The $\Delta t$ resolutions are very similar for the four tagging categories as demonstrated in Fig. 17 where a global residual fit and fits to individual tagging category residuals are compared; The largest difference occurs in the biases. Therefore we use the same resolution function parameters in the likelihood fit for all tagging categories, but allow for seperate bias in each tagging category. The $\Delta t$ residual distributions overlaid with both the residual and nominal mixing fit results for simulated tagged events are shown in Fig. 18 for all tagging categories combined.

**Resolution vs.** $\Delta t_{\rm true}$ In addition we check on MC that the $\Delta t$ resolution does not depend on the value of $\Delta t$ by slicing $\Delta t_{\rm true}$ into 10 regions, each with approximately 10% of the events and fitting the resolution model on the MC residuals. The results are listed in Table 16; No evidence for a dependence of the resolution on $|\Delta t_{\rm true}|$ is observed. Note that

Table 12: $\Delta m_d$ and tagging dilutions for different tagging categories. XX represent the blind value of $\Delta m_d$. The error quoted on $\Delta m_d$ is error on the fit to the specific sample, and it is *not* the error on the difference with the nominal blind fit.

| | lepton | kaon | NT1 | NT2 |
|---|---|---|---|---|
| $S_{core,SigRun1}$ | 1.428 ±0.158 | 1.047 ±0.189 | 1.126 ±0.227 | 1.307 ±0.178 |
| $S_{core,SigRun2}$ | 0.100 ±8.820 | 1.126 ±0.148 | 1.132 ±0.463 | 1.148 ±0.317 |
| $b_{core,SigLepRun1}$ | 0.013 ±0.118 | | | |
| $b_{core,SigKaonRun1}$ | -0.058 ±0.145 | | | |
| $b_{core,SigNT1Run1}$ | | -0.283 ±0.108 | | |
| $b_{core,SigNT2Run1}$ | | -0.217 ±0.106 | | |
| $b_{core,SigLepRun2}$ | | | -0.102 ±0.143 | |
| $b_{core,SigKaonRun2}$ | | | -0.532 ±0.208 | |
| $b_{core,SigNT1Run2}$ | | | | -0.482 ±0.113 |
| $b_{core,SigNT2Run2}$ | | | | -0.184 ±0.256 |
| $b_{tail,SigRun1}$ | | -0.190 ±0.397 | | -10.000 ±2.505 |
| $b_{tail,SigRun2}$ | | -5.861 ±3.187 | | -0.826 ±3.625 |
| $F_{tail,SigRun1}$ | | 0.232 ±0.066 | | 0.009 ±0.008 |
| $F_{tail,SigRun2}$ | | 0.028 ±0.027 | | 0.082 ±0.147 |
| $F_{outl,SigRun1}$ | 0.000 ±0.014 | 0.003 ±0.004 | 0.015 ±0.010 | 0.006 ±0.010 |
| $F_{outl,SigRun2}$ | 0.000 ±0.007 | 0.008 ±0.008 | 0.000 ±0.007 | 0.000 ±0.007 |
| $D_{SigLep}$ | 0.838 ±0.029 | | | |
| $D_{SigKaon}$ | 0.675 ±0.025 | | | |
| $D_{SigNT1}$ | | 0.552 ±0.044 | | |
| $D_{SigNT2}$ | | | 0.338 ±0.048 | |
| $\delta D_{Sig,Lep}$ | -0.005 ±0.045 | | | |
| $\delta D_{Sig,Kaon}$ | | 0.023 ±0.033 | | |
| $\delta D_{Sig,NT1}$ | | | -0.087 ±0.068 | |
| $\delta D_{Sig,NT2}$ | | 0.098 ±0.060 | | |
| $S_{core,BkgRun1}$ | 0.650 ±0.290 | 1.350 ±0.047 | 1.173 ±0.157 | 1.125 ±0.112 |
| $S_{core,BkgRun2}$ | 0.834 ±0.180 | 1.213 ±0.053 | 1.134 ±0.155 | 1.220 ±0.108 |
| $b_{core,BkgRun1}$ | -0.176 ±0.172 | -0.130 ±0.039 | -0.142 ±0.099 | -0.135 ±0.059 |
| $b_{core,BkgRun2}$ | 0.397 ±0.225 | -0.047 ±0.047 | 0.355 ±0.136 | -0.094 ±0.075 |
| $F_{outl,BkgRun1}$ | 0.006 ±0.028 | 0.014 ±0.005 | 0.016 ±0.011 | 0.026 ±0.009 |
| $F_{outl,BkgRun2}$ | 0.000 ±0.028 | 0.019 ±0.007 | 0.048 ±0.026 | 0.047 ±0.013 |
| $\tau_{\rm nonpromptBkg}$ | 1.355 ±0.190 | 1.303 ±0.129 | 1.030 ±0.157 | 0.710 ±0.064 |
| $D_{Bkg1,Lep}$ | 0.298 ±0.352 | | | |
| $D_{Bkg1,Kaon}$ | 0.441 ±0.036 | | | |
| $D_{Bkg1,NT1}$ | | 0.425 ±0.218 | | |
| $D_{Bkg1,NT2}$ | | -0.095 ±0.173 | | |
| $D_{Bkg2,Lep}$ | 0.334 ±0.107 | | | |
| $D_{Bkg2,Kaon}$ | 0.216 ±0.067 | | | |
| $D_{Bkg2,NT1}$ | | -0.081 ±0.114 | | |
| $D_{Bkg2,NT2}$ | | 0.127 ±0.031 | | |
| $f_{\tau=0,BkgLep}$ | 0.191 ±0.094 | | | |
| $f_{\tau=0,BkgKaon}$ | 0.673 ±0.047 | | | |
| $f_{\tau=0,BkgNT1}$ | | 0.429 ±0.135 | | |
| $f_{\tau=0,BkgNT2}$ | | 0.285 ±0.131 | | |
| $\Delta m_d$ | XX+0.005 ±0.026 | XX+0.002 ±0.023 | XX-0.032 ±0.044 | XX+0.12 ±0.10 |

Table 13: $\Delta m_d$ and tagging dilutions for different tagging categories for MC.

| | lepton | kaon | NT1 | NT2 |
|---|---|---|---|---|
| Scale core Sig | 1.226 ±0.036 | 1.098 ±0.030 | 1.067 ±0.063 | 1.155 ±0.051 |
| Bias core Sig Lep | -0.089 ±0.021 | | | |
| Bias core Sig Kaon | | -0.218 ±0.018 | | |
| Bias core Sig NT1 | | | -0.143 ±0.033 | |
| Bias core Sig NT2 | | | | -0.185 ±0.031 |
| Scale tail Sig | 6.317 ±1.248 | 3.257 ±0.376 | 3.747 ±0.524 | 3.223 ±0.655 |
| Bias tail Sig | -2.827 ±1.165 | -2.152 ±0.598 | -2.027 ±1.088 | -2.293 ±1.578 |
| Frac tail Sig | 0.016 ±0.006 | 0.042 ±0.014 | 0.045 ±0.022 | 0.044 ±0.027 |
| Frac outl Sig | 0.001 ±0.001 | 0.005 ±0.001 | 0.002 ±0.001 | 0.006 ±0.001 |
| aveD Sig Lep | 0.857 ±0.006 | | | |
| aveD Sig Kaon | | 0.705 ±0.005 | | |
| aveD Sig NT1 | | | 0.621 ±0.009 | |
| aveD Sig NT2 | | | | 0.311 ±0.008 |
| DeltaD Sig, Lep | 0.005 ±0.009 | | | |
| DeltaD Sig, Kaon | | 0.037 ±0.007 | | |
| DeltaD Sig, NT1 | | | -0.051 ±0.014 | |
| DeltaD Sig, NT2 | | | | 0.070 ±0.012 |
| DeltaM Sig | 0.487 ±0.006 | 0.473 ±0.005 | 0.469 ±0.009 | 0.485 ±0.015 |

Table 14: Variation of $\Delta m_d$ observed in data depending on the flavor of either the fully reconstructed $B^0$ or the tagging $B^0$. $\Delta m_d$ is reported as the blinded value of the nominal fit ("X") plus the difference between the fit using the subsample and the nominal fit. The reported error is the statistical error of the fit using the subsample.

| Category | $\Delta m_d$ |
|---|---|
| $B^0$ rec | X -0.019±0.031 |
| $\overline{B}^0$ rec | X +0.015±0.031 |
| $B^0$ tag | X -0.018±0.023 |
| $\overline{B}^0$ tag | X +0.012±0.024 |

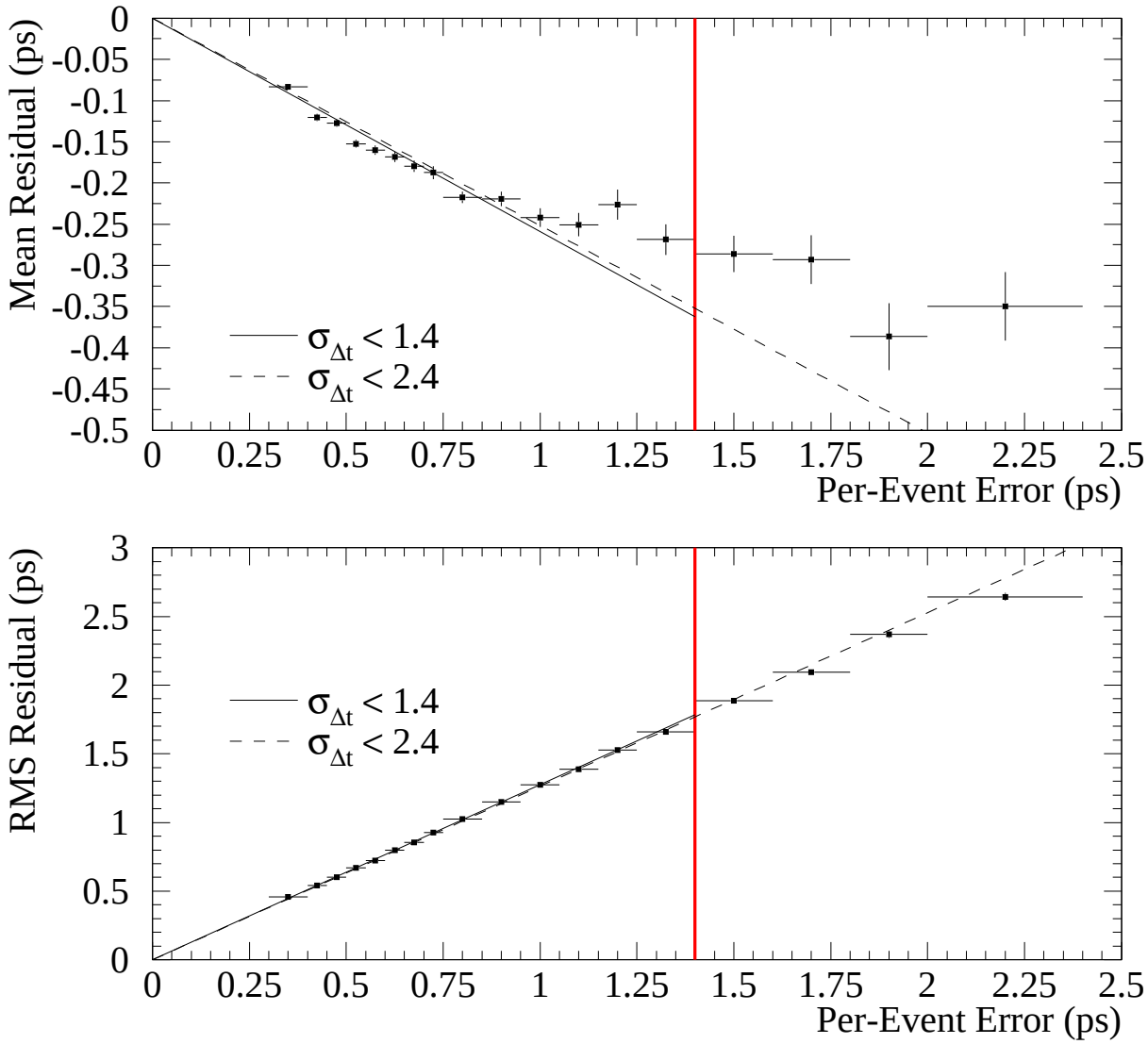


Figure 16: Mean and width of the MC $\Delta t$ residual in bins of the per-event error $\sigma_{\Delta t}$. Fits are shown to a line constrained to pass through the origin for $\sigma_{\Delta t} < 1.4$ and $\sigma_{\Delta t} < 2.4$ ps.

Table 15: Fitting the MC $\Delta t$ residuals with the nominal resolution model, which scales all biases with the per-event error, and which has individual core biases seperately for each tagging category, using only events with a per-event error less than 1.4 ps.

| Variable | all | lepton | kaon | NT1 | NT2 |
|---|---|---|---|---|---|
| $S_{\rm core}$ | 1.058 ±0.005 | 1.036 ±0.011 | 1.060 ±0.007 | 1.079 ±0.011 | 1.054 ±0.011 |
| $\delta_{\rm core,Lepton}$ | -0.088 ±0.008 | -0.101 ±0.009 | | | |
| $\delta_{\rm core,Kaon}$ | -0.210 ±0.006 | | -0.201 ±0.006 | | |
| $\delta_{\rm core,NT1}$ | -0.134 ±0.010 | | | -0.148 ±0.011 | |
| $\delta_{\rm core,NT2}$ | -0.186 ±0.008 | | | | -0.181 ±0.009 |
| $S_{\rm tail}$ | 2.310 ±0.038 | 2.308 ±0.110 | 2.248 ±0.051 | 2.659 ±0.120 | 2.208 ±0.073 |
| $\delta_{\rm tail}$ | -1.031 ±0.041 | -0.723 ±0.087 | -1.186 ±0.064 | -1.147 ±0.133 | -0.889 ±0.074 |
| $f_{\rm tail}$ | 0.106 ±0.005 | 0.096 ±0.012 | 0.109 ±0.007 | 0.082 ±0.009 | 0.134 ±0.013 |
| $f_{\rm outl}$ | 0.008 ±0.000 | 0.006 ±0.001 | 0.009 ±0.001 | 0.005 ±0.001 | 0.011 ±0.001 |

Table 16: Parameters of fit of the signal resolution model to the $\Delta t$ residual $(\Delta t_{\rm reco} - \Delta t_{\rm true})$ distributions for simulated hadronic $B$ cocktail events for slices of $\Delta t_{\rm true}$.

| $\Delta t_{\rm true}$ interval | $(-\infty, -2.48]$ | $(-2.48, -1.41]$ | $(-1.41, -0.79]$ | $(-0.79, -0.34]$ | $(-0.34 : 0]$ |
|---|---|---|---|---|---|
| $S_{\rm core}$ | 1.052 ±0.016 | 1.040 ±0.013 | 1.055 ±0.014 | 1.051 ±0.013 | 1.060 ±0.017 |
| $\delta_{\rm core,Lepton}$ | -0.073 ±0.026 | -0.080 ±0.025 | -0.101 ±0.026 | -0.084 ±0.026 | -0.084 ±0.028 |
| $\delta_{\rm core,Kaon}$ | -0.207 ±0.018 | -0.168 ±0.017 | -0.227 ±0.017 | -0.211 ±0.017 | -0.183 ±0.019 |
| $\delta_{\rm core,NT1}$ | -0.164 ±0.032 | -0.114 ±0.031 | -0.131 ±0.032 | -0.103 ±0.030 | -0.104 ±0.033 |
| $\delta_{\rm core,NT2}$ | -0.171 ±0.025 | -0.200 ±0.024 | -0.207 ±0.025 | -0.207 ±0.025 | -0.196 ±0.027 |
| $S_{\rm tail}$ | 2.280 ±0.115 | 2.465 ±0.120 | 2.393 ±0.132 | 2.488 ±0.128 | 2.089 ±0.113 |
| $\delta_{\rm tail}$ | -0.819 ±0.102 | -0.963 ±0.115 | -0.963 ±0.131 | -1.204 ±0.139 | -0.813 ±0.117 |
| $f_{\rm tail}$ | 0.124 ±0.018 | 0.111 ±0.013 | 0.100 ±0.015 | 0.093 ±0.012 | 0.127 ±0.023 |
| $f_{\rm outl}$ | 0.009 ±0.001 | 0.009 ±0.001 | 0.007 ±0.001 | 0.008 ±0.001 | 0.009 ±0.001 |
| $\Delta t_{\rm true}$ interval | $(0, 0.34]$ | $(0.34, 0.79]$ | $(0.79, 1.41]$ | $(1.41, 2.48]$ | $(2.48, \infty)$ |
| $S_{\rm core}$ | 1.023 ±0.018 | 1.081 ±0.013 | 1.068 ±0.013 | 1.058 ±0.015 | 1.075 ±0.015 |
| $\delta_{\rm core,Lepton}$ | -0.096 ±0.028 | -0.062 ±0.026 | -0.058 ±0.026 | -0.098 ±0.026 | -0.137 ±0.026 |
| $\delta_{\rm core,Kaon}$ | -0.207 ±0.019 | -0.219 ±0.017 | -0.236 ±0.017 | -0.212 ±0.018 | -0.227 ±0.018 |
| $\delta_{\rm core,NT1}$ | -0.112 ±0.034 | -0.163 ±0.032 | -0.128 ±0.031 | -0.137 ±0.033 | -0.171 ±0.031 |
| $\delta_{\rm core,NT2}$ | -0.160 ±0.027 | -0.187 ±0.025 | -0.157 ±0.025 | -0.184 ±0.025 | -0.183 ±0.025 |
| $S_{\rm tail}$ | 2.055 ±0.101 | 2.371 ±0.128 | 2.357 ±0.107 | 2.244 ±0.105 | 2.284 ±0.128 |
| $\delta_{\rm tail}$ | -0.873 ±0.107 | -1.165 ±0.157 | -1.158 ±0.138 | -1.117 ±0.131 | -1.269 ±0.164 |
| $f_{\rm tail}$ | 0.146 ±0.024 | 0.085 ±0.013 | 0.097 ±0.013 | 0.117 ±0.016 | 0.093 ±0.015 |
| $f_{\rm outl}$ | 0.009 ±0.001 | 0.007 ±0.001 | 0.007 ±0.001 | 0.009 ±0.001 | 0.009 ±0.001 |

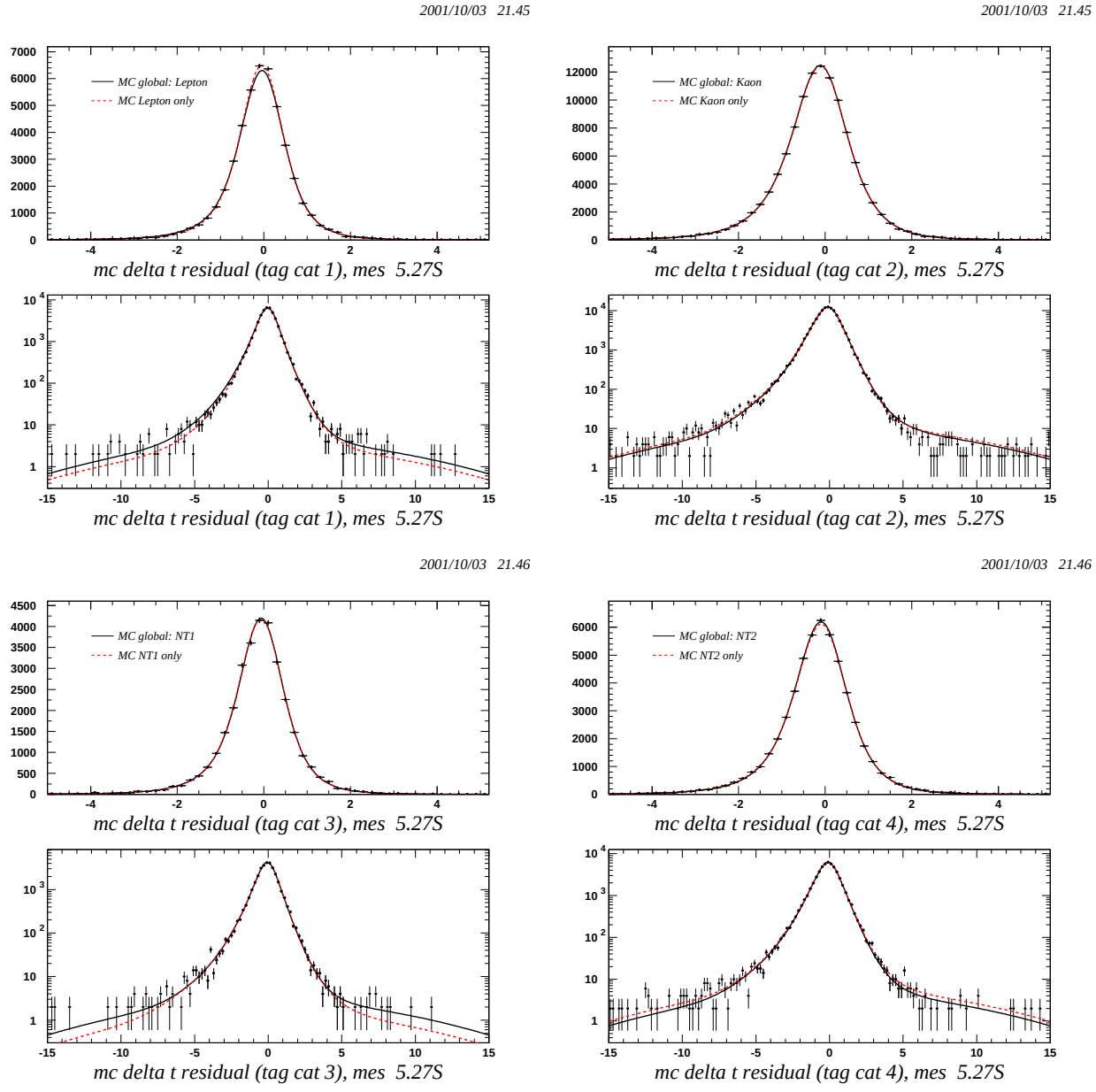


Figure 17: Distribution of $\Delta t$ residuals for each tagging category for selected $B$ candidates in signal MC, overlaid with the fitted resolution model. Note that for each tagging category both a linear and log plot are shown. The solid line is the global fit to the residuals (corresponding to the 'all' column in Table 15), while the dashed line are the fits to the individual tagging categories (*i.e.* the other columns in Table 15). Note that only on the log scale plots a small difference can be seen between these fits.

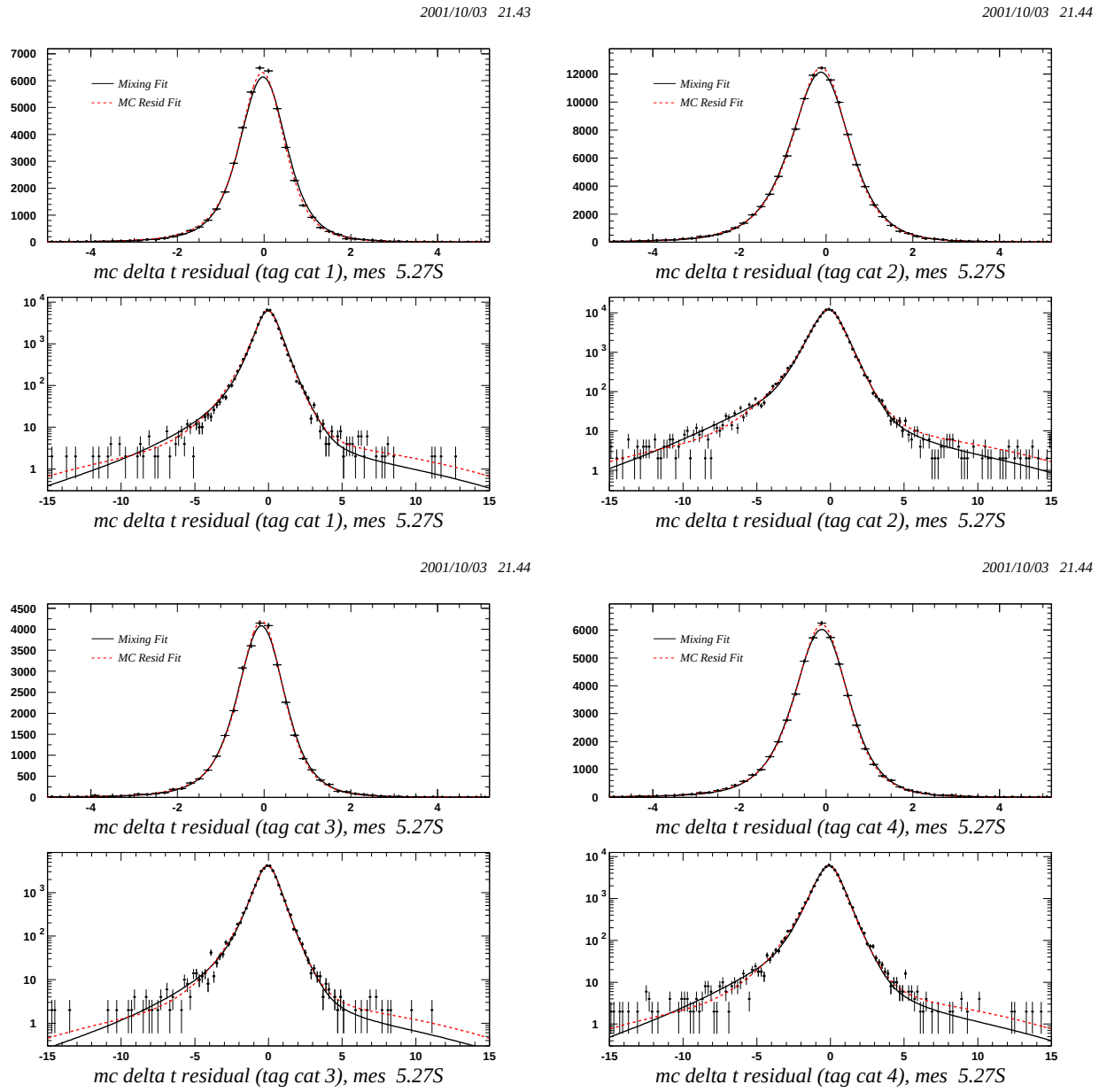


Figure 18: Distribution of $\Delta t$ residuals for selected $B$ candidates in signal MC, overlaid with the fitted resolution model. The solid line is the fit to the residuals (corresponding to the 'all' column in Table 15, and also shown as the solid line in Fig. 17), while the dashed line is the nominal mixing fit (corresponding to Table 2)

if one were to slice in bins of *reconstructed* $\Delta t$ one does observe (as expected and described by the fitmodel!) a dependence due to the fact that outlier events (or just events with large $\sigma_{\Delta t}$) tend to migrate from small $\Delta t$ to large $\Delta t$.

## 6.12 Charm Lifetime Studies

We divide the cocktail signal Monte Carlo cocktail into subsamples containing different upper bounds on the true flight distances for the charm daughters of the $B$ to check whether the measured value of $\Delta m_d$ has any dependence the charm meson ($D^0, D^+, D_s^+$) flight distance. The results of this check are shown in Tables 17-21, and is illustrated graphically in Figs 19-21.

We observe the measured value of $\Delta m_d$ to be unchanged when we vary the bound on the true flight distance of the tag-side $D$ in the event. See Section 7.1.2 for a discussion of systematics associated with $D$ lifetimes.

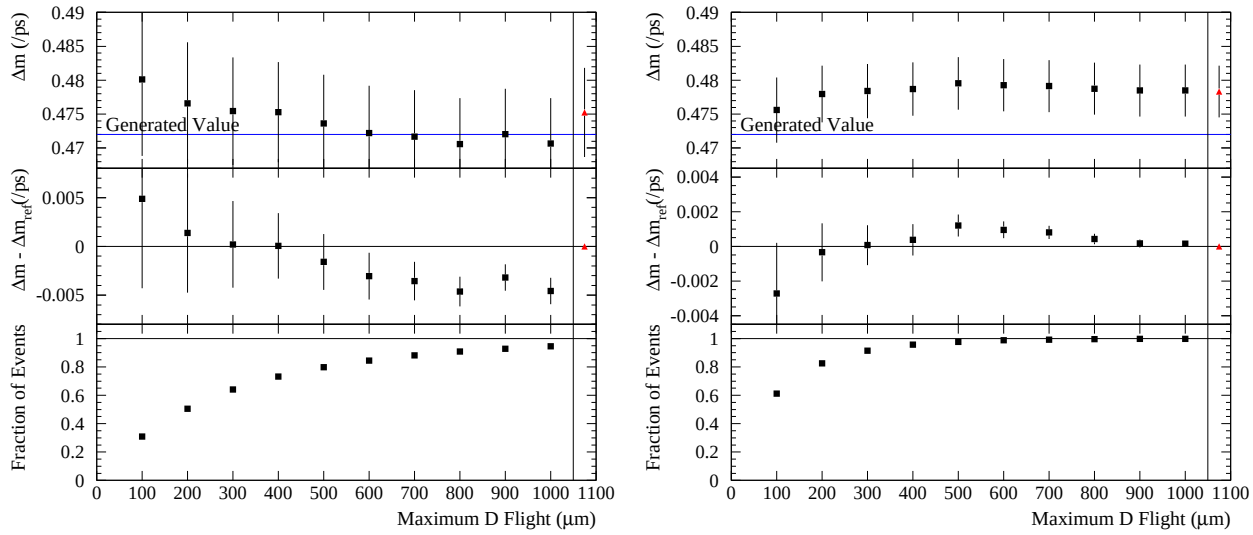


Figure 19: Results from the likelihood fits to the $\Delta t$ distributions of the hadronic $B$ decays in 2.8 million simulated signal cocktail events (no $B \to J/\psi K^*$) for different values of upper bound on true 3-dimensional charm flight distance, $l_c$, for events with at least one true $D^+$ on the tag side (left) and at least one $D^0$ on the tag side (right). (Both include double charm decays). The reference fits (red triangles) have $l_c = \infty$. The errors shown on the middle plot are computed as the difference in quadrature from the reference.

We also categorize the sample according to which species of charm is generated on the tag side, and perform separate fits to these samples. For this study, events are selected for

Table 17: Results from the likelihood fits to the $\Delta t$ distributions of the hadronic $B$ decays in 2.8 million simulated signal cocktail events (no $B \to J/\psi K^*$) for different values of upper bound on true 3-dimensional charm flight distance, $l_c$, for events with at least one true $D^+$ on the tag side (includes double charm decays).

| Parameter | $D^+, l_c < 0.0100$ | $D^+, l_c < 0.0200$ | $D^+, l_c < 0.0300$ | $D^+, l_c < 0.0400$ | $D^+, l_c < 0.0500$ | $D^+, l_c < 0.0600$ |
|---|---|---|---|---|---|---|
| $\mathcal{S}_{\text{core, sig}}$ | .282 ±.000 | 1.10 ±.053 | .894 ±.262 | 1.15 ±.037 | 1.16 ±.043 | 1.17 ±.042 |
| $\delta^L_{\text{core, sig}}$ | -.010 ±.263 | -.018 ±.047 | -.118 ±.101 | -.078 ±.039 | -.091 ±.038 | -.091 ±.038 |
| $\delta^K_{\text{core, sig}}$ | -.230 ±.139 | -.134 ±.032 | -.333 ±.160 | -.247 ±.026 | -.284 ±.027 | -.301 ±.026 |
| $\delta^{NT1}_{\text{core, sig}}$ | .189 ±.002 | .034 ±.068 | .004 ±.138 | -.022 ±.055 | -.042 ±.054 | -.053 ±.053 |
| $\delta^{NT2}_{\text{core, sig}}$ | -.142 ±.196 | -.162 ±.048 | -.384 ±.199 | -.278 ±.040 | -.301 ±.039 | -.314 ±.039 |
| $\mathcal{S}_{\text{tail, sig}}$ | 1.43 ±.106 | 4.22 ±1.15 | 1.60 ±.439 | 4.66 ±1.35 | 3.93 ±1.11 | 3.90 ±.901 |
| $\delta_{\text{tail, sig}}$ | -.028 ±.062 | -1.41 ±1.15 | .003 ±.208 | -1.27 ±.968 | -1.40 ±1.07 | -1.39 ±.874 |
| $f_{\text{tail}}$ | .725 ±.080 | .026 ±.020 | .368 ±.364 | .019 ±.012 | .022 ±.018 | .027 ±.018 |
| $f_{\text{outlier}}$ | .006 ±.002 | .004 ±.002 | .007 ±.001 | .004 ±.002 | .004 ±.001 | .004 ±.001 |
| $D_{\text{L}}$ | .809 ±.017 | .796 ±.014 | .798 ±.012 | .793 ±.011 | .794 ±.011 | .789 ±.011 |
| $D_{\text{K}}$ | .566 ±.016 | .568 ±.012 | .571 ±.011 | .573 ±.010 | .566 ±.010 | .569 ±.010 |
| $D_{\text{NT1}}$ | .448 ±.032 | .467 ±.024 | .475 ±.021 | .475 ±.020 | .485 ±.019 | .483 ±.018 |
| $D_{\text{NT2}}$ | .122 ±.025 | .110 ±.019 | .111 ±.017 | .108 ±.016 | .110 ±.015 | .111 ±.015 |
| $\Delta D_{\text{L}}$ | .034 ±.028 | .010 ±.022 | .012 ±.020 | .007 ±.018 | .014 ±.018 | .012 ±.017 |
| $\Delta D_{\text{K}}$ | .033 ±.024 | .039 ±.019 | .033 ±.017 | .028 ±.016 | .027 ±.015 | .031 ±.015 |
| $\Delta D_{\text{NT1}}$ | .087 ±.049 | .073 ±.038 | .046 ±.033 | .046 ±.031 | .044 ±.029 | .036 ±.029 |
| $\Delta D_{\text{NT2}}$ | .142 ±.038 | .114 ±.030 | .130 ±.027 | .132 ±.025 | .129 ±.024 | .115 ±.023 |
| $\Delta m_d$ | .4801 ±.0113 | .4766 ±.0090 | .4754 ±.0079 | .4753 ±.0074 | .4736 ±.0072 | .4722 ±.0070 |
| Events | 12337 | 20089 | 25543 | 29176 | 31777 | 33650 |

| Parameter | $D^+, l_c < 0.0700$ | $D^+, l_c < 0.0800$ | $D^+, l_c < 0.0900$ | $D^+, l_c < 0.1000$ | $D^+, l_c < 50.0$ |
|---|---|---|---|---|---|
| $\mathcal{S}_{\text{core, sig}}$ | 1.20 ±.040 | 1.21 ±.035 | 1.21 ±.038 | 1.20 ±.040 | 1.21 ±.034 |
| $\delta^L_{\text{core, sig}}$ | -.079 ±.037 | -.086 ±.036 | -.078 ±.036 | -.073 ±.037 | -.071 ±.036 |
| $\delta^K_{\text{core, sig}}$ | -.316 ±.027 | -.323 ±.026 | -.332 ±.026 | -.331 ±.027 | -.328 ±.026 |
| $\delta^{NT1}_{\text{core, sig}}$ | -.062 ±.052 | -.074 ±.050 | -.085 ±.051 | -.088 ±.051 | -.097 ±.049 |
| $\delta^{NT2}_{\text{core, sig}}$ | -.324 ±.038 | -.321 ±.037 | -.333 ±.038 | -.327 ±.038 | -.309 ±.037 |
| $\mathcal{S}_{\text{tail, sig}}$ | 3.80 ±.757 | 4.01 ±.634 | 3.78 ±.554 | 3.61 ±.450 | 4.04 ±.341 |
| $\delta_{\text{tail, sig}}$ | -1.69 ±.985 | -2.06 ±1.04 | -1.91 ±.902 | -1.71 ±.669 | -2.48 ±.579 |
| $f_{\text{tail}}$ | .027 ±.017 | .025 ±.013 | .032 ±.015 | .044 ±.018 | .052 ±.012 |
| $f_{\text{outlier}}$ | .004 ±.001 | .004 ±.001 | .004 ±.001 | .004 ±.001 | .004 ±.001 |
| $D_{\text{L}}$ | .791 ±.011 | .793 ±.010 | .794 ±.010 | .793 ±.010 | .792 ±.010 |
| $D_{\text{K}}$ | .568 ±.010 | .567 ±.009 | .567 ±.009 | .566 ±.009 | .570 ±.009 |
| $D_{\text{NT1}}$ | .489 ±.018 | .491 ±.017 | .492 ±.017 | .495 ±.017 | .505 ±.016 |
| $D_{\text{NT2}}$ | .115 ±.015 | .118 ±.014 | .121 ±.014 | .122 ±.014 | .131 ±.014 |
| $\Delta D_{\text{L}}$ | .013 ±.017 | .015 ±.016 | .016 ±.016 | .015 ±.016 | .015 ±.016 |
| $\Delta D_{\text{K}}$ | .033 ±.015 | .036 ±.014 | .037 ±.014 | .036 ±.014 | .038 ±.014 |
| $\Delta D_{\text{NT1}}$ | .036 ±.028 | .039 ±.027 | .040 ±.027 | .042 ±.027 | .034 ±.026 |
| $\Delta D_{\text{NT2}}$ | .112 ±.023 | .116 ±.022 | .117 ±.022 | .119 ±.022 | .115 ±.021 |
| $\Delta m_d$ | .4717 ±.0069 | .4706 ±.0067 | .4720 ±.0067 | .4707 ±.0067 | .4752 ±.0066 |
| Events | 35123 | 36193 | 36987 | 37636 | 39825 |

Table 18: Results from the likelihood fits to the $\Delta t$ distributions of the hadronic $B$ decays in 2.8 million simulated signal cocktail events (no $B \to J/\psi K^*$) for different values of upper bound on true 3-dimensional charm flight distance, $l_c$, for events with at least one true $D^0$ on the tag side (includes double charm decays).

| Parameter | $D^0, l_c < 0.0100$ | $D^0, l_c < 0.0200$ | $D^0, l_c < 0.0300$ | $D^0, l_c < 0.0400$ | $D^0, l_c < 0.0500$ | $D^0, l_c < 0.0600$ |
|---|---|---|---|---|---|---|
| $\mathcal{S}_{\text{core, sig}}$ | .884 ±.186 | .969 ±.083 | .938 ±.106 | .973 ±.092 | .978 ±.085 | .988 ±.075 |
| $\delta^L_{\text{core, sig}}$ | .196 ±.267 | .050 ±.081 | .091 ±.108 | .057 ±.094 | .050 ±.086 | .034 ±.074 |
| $\delta^K_{\text{core, sig}}$ | .081 ±.209 | -.053 ±.066 | -.039 ±.084 | -.080 ±.075 | -.088 ±.069 | -.106 ±.060 |
| $\delta^{NT1}_{\text{core, sig}}$ | .004 ±.184 | -.106 ±.073 | -.095 ±.085 | -.126 ±.078 | -.120 ±.074 | -.139 ±.066 |
| $\delta^{NT2}_{\text{core, sig}}$ | .170 ±.254 | .004 ±.076 | .034 ±.100 | -.020 ±.087 | -.039 ±.079 | -.063 ±.068 |
| $\mathcal{S}_{\text{tail, sig}}$ | 1.34 ±.387 | 1.80 ±.478 | 1.63 ±.322 | 1.80 ±.457 | 1.85 ±.459 | 2.00 ±.527 |
| $\delta_{\text{tail, sig}}$ | -.933 ±1.49 | -1.10 ±.972 | -.822 ±.561 | -1.000 ±.690 | -1.07 ±.700 | -1.13 ±.654 |
| $f_{\text{tail}}$ | .202 ±.599 | .099 ±.113 | .180 ±.170 | .125 ±.132 | .115 ±.116 | .097 ±.091 |
| $f_{\text{outlier}}$ | .006 ±.001 | .005 ±.001 | .005 ±.001 | .005 ±.001 | .004 ±.001 | .005 ±.001 |
| $D_{\text{L}}$ | .940 ±.008 | .939 ±.007 | .939 ±.006 | .936 ±.006 | .936 ±.006 | .938 ±.006 |
| $D_{\text{K}}$ | .807 ±.007 | .809 ±.006 | .806 ±.006 | .808 ±.006 | .808 ±.006 | .809 ±.006 |
| $D_{\text{NT1}}$ | .819 ±.013 | .808 ±.011 | .811 ±.011 | .812 ±.010 | .813 ±.010 | .813 ±.010 |
| $D_{\text{NT2}}$ | .503 ±.014 | .514 ±.012 | .517 ±.011 | .517 ±.011 | .518 ±.011 | .517 ±.011 |
| $\Delta D_{\text{L}}$ | -.008 ±.013 | -.005 ±.012 | -.005 ±.011 | -.003 ±.011 | -.004 ±.011 | -.004 ±.011 |
| $\Delta D_{\text{K}}$ | .042 ±.011 | .040 ±.010 | .040 ±.009 | .040 ±.009 | .040 ±.009 | .041 ±.009 |
| $\Delta D_{\text{NT1}}$ | -.080 ±.022 | -.083 ±.019 | -.059 ±.018 | -.057 ±.017 | -.061 ±.017 | -.060 ±.017 |
| $\Delta D_{\text{NT2}}$ | .032 ±.022 | .026 ±.019 | .031 ±.018 | .033 ±.017 | .034 ±.017 | .038 ±.017 |
| $\Delta m_d$ | .4756 ±.0048 | .4780 ±.0042 | .4784 ±.0040 | .4787 ±.0039 | .4795 ±.0039 | .4793 ±.0039 |
| Events | 36826 | 49624 | 55039 | 57538 | 58725 | 59399 |

| Parameter | $D^0, l_c < 0.0700$ | $D^0, l_c < 0.0800$ | $D^0, l_c < 0.0900$ | $D^0, l_c < 0.1000$ | $D^0, l_c < 50.0$ |
|---|---|---|---|---|---|
| $\mathcal{S}_{\text{core, sig}}$ | .997 ±.066 | .995 ±.068 | .998 ±.069 | 1.00 ±.066 | 1.00 ±.063 |
| $\delta^L_{\text{core, sig}}$ | .021 ±.065 | .021 ±.066 | .019 ±.067 | .015 ±.064 | .016 ±.061 |
| $\delta^K_{\text{core, sig}}$ | -.113 ±.053 | -.112 ±.053 | -.114 ±.055 | -.117 ±.052 | -.119 ±.050 |
| $\delta^{NT1}_{\text{core, sig}}$ | -.143 ±.060 | -.146 ±.060 | -.149 ±.061 | -.151 ±.059 | -.151 ±.057 |
| $\delta^{NT2}_{\text{core, sig}}$ | -.073 ±.060 | -.075 ±.060 | -.077 ±.062 | -.081 ±.059 | -.082 ±.057 |
| $\mathcal{S}_{\text{tail, sig}}$ | 2.10 ±.534 | 2.09 ±.530 | 2.11 ±.563 | 2.15 ±.571 | 2.16 ±.542 |
| $\delta_{\text{tail, sig}}$ | -1.20 ±.623 | -1.19 ±.622 | -1.21 ±.648 | -1.23 ±.640 | -1.24 ±.626 |
| $f_{\text{tail}}$ | .087 ±.073 | .089 ±.076 | .086 ±.077 | .083 ±.072 | .083 ±.067 |
| $f_{\text{outlier}}$ | .004 ±.001 | .005 ±.001 | .005 ±.001 | .004 ±.001 | .004 ±.001 |
| $D_{\text{L}}$ | .938 ±.006 | .938 ±.006 | .938 ±.006 | .938 ±.006 | .937 ±.006 |
| $D_{\text{K}}$ | .809 ±.006 | .809 ±.006 | .809 ±.006 | .809 ±.006 | .809 ±.006 |
| $D_{\text{NT1}}$ | .813 ±.010 | .813 ±.010 | .814 ±.010 | .814 ±.010 | .813 ±.010 |
| $D_{\text{NT2}}$ | .518 ±.011 | .518 ±.011 | .518 ±.011 | .518 ±.011 | .518 ±.011 |
| $\Delta D_{\text{L}}$ | -.003 ±.011 | -.003 ±.011 | -.003 ±.011 | -.004 ±.011 | -.003 ±.011 |
| $\Delta D_{\text{K}}$ | .041 ±.009 | .041 ±.009 | .041 ±.009 | .041 ±.009 | .040 ±.009 |
| $\Delta D_{\text{NT1}}$ | -.064 ±.017 | -.064 ±.017 | -.063 ±.017 | -.063 ±.017 | -.063 ±.017 |
| $\Delta D_{\text{NT2}}$ | .039 ±.017 | .040 ±.017 | .041 ±.017 | .041 ±.017 | .041 ±.017 |
| $\Delta m_d$ | .4791 ±.0038 | .4787 ±.0038 | .4785 ±.0038 | .4785 ±.0038 | .4783 ±.0038 |
| Events | 59735 | 59910 | 60002 | 60067 | 60153 |

Table 19: Results from the likelihood fits to the $\Delta t$ distributions of the hadronic $B$ decays in 2.8 million simulated signal cocktail events (no $B \to J/\psi K^*$) for different values of upper bound on true 3-dimensional charm flight distance, $l_c$, for events with at least one true $D_s$ on the tag side

| Parameter | $D_s^+, l_c < 0.0200$ | $D_s^+, l_c < 0.0300$ | $D_s^+, l_c < 0.0500$ | $D_s^+, l_c < 0.0600$ | $D_s^+, l_c < 0.0800$ | $D_s^+, l_c < 0.0900$ |
|---|---|---|---|---|---|---|
| $\mathcal{S}_{\text{core, sig}}$ | 1.11 ±.148 | 1.10 ±.140 | 1.14 ±.150 | 1.12 ±.187 | 1.14 ±.102 | 1.14 ±.100 |
| $\delta^L_{\text{core, sig}}$ | -.003 ±.300 | -.126 ±.293 | -.368 ±.286 | -.358 ±.304 | -.362 ±.243 | -.397 ±.240 |
| $\delta^K_{\text{core, sig}}$ | -.317 ±.143 | -.289 ±.152 | -.357 ±.144 | -.352 ±.155 | -.378 ±.073 | -.382 ±.071 |
| $\delta^{NT1}_{\text{core, sig}}$ | -.189 ±.185 | -.226 ±.185 | -.336 ±.179 | -.360 ±.185 | -.380 ±.139 | -.382 ±.138 |
| $\delta^{NT2}_{\text{core, sig}}$ | -.166 ±.169 | -.168 ±.165 | -.265 ±.159 | -.278 ±.167 | -.290 ±.098 | -.298 ±.096 |
| $\mathcal{S}_{\text{tail, sig}}$ | 2.40 ±1.17 | 2.15 ±.962 | 2.58 ±1.32 | 2.59 ±1.34 | 2.77 ±.649 | 2.79 ±.638 |
| $\delta_{\text{tail, sig}}$ | -1.99 ±1.74 | -2.16 ±1.71 | -1.67 ±1.03 | -1.48 ±.829 | -1.55 ±.751 | -1.55 ±.753 |
| $f_{\text{tail}}$ | .094 ±.121 | .101 ±.125 | .095 ±.127 | .114 ±.163 | .098 ±.070 | .096 ±.068 |
| $f_{\text{outlier}}$ | .001 ±.002 | .001 ±.002 | .000 ±.004 | .001 ±.002 | .001 ±.002 | .001 ±.002 |
| $D_{\text{L}}$ | .174 ±.089 | .161 ±.082 | .142 ±.080 | .136 ±.080 | .115 ±.079 | .119 ±.079 |
| $D_{\text{K}}$ | .724 ±.018 | .721 ±.016 | .731 ±.016 | .730 ±.016 | .728 ±.016 | .727 ±.016 |
| $D_{\text{NT1}}$ | .537 ±.052 | .529 ±.048 | .534 ±.046 | .527 ±.046 | .528 ±.046 | .528 ±.046 |
| $D_{\text{NT2}}$ | .213 ±.034 | .226 ±.032 | .225 ±.030 | .226 ±.030 | .226 ±.030 | .227 ±.030 |
| $\Delta D_{\text{L}}$ | .044 ±.136 | .104 ±.128 | .110 ±.122 | .125 ±.121 | .107 ±.121 | .113 ±.121 |
| $\Delta D_{\text{K}}$ | .032 ±.025 | .042 ±.024 | .038 ±.023 | .038 ±.023 | .034 ±.023 | .035 ±.022 |
| $\Delta D_{\text{NT1}}$ | -.261 ±.082 | -.259 ±.077 | -.272 ±.073 | -.262 ±.073 | -.265 ±.073 | -.265 ±.073 |
| $\Delta D_{\text{NT2}}$ | .059 ±.050 | .041 ±.048 | .037 ±.046 | .036 ±.046 | .040 ±.045 | .041 ±.045 |
| $\Delta m_d$ | .5043 ±.0164 | .4972 ±.0152 | .5030 ±.0146 | .5008 ±.0147 | .4983 ±.0146 | .4982 ±.0146 |
| Events | 6555 | 7315 | 7878 | 7968 | 8053 | 8069 |

| Parameter | $D_s^+, l_c < 0.1000$ | $D_s^+, l_c < 50.0$ |
|---|---|---|
| $\mathcal{S}_{\text{core, sig}}$ | 1.14 ±.099 | 1.14 ±.099 |
| $\delta^L_{\text{core, sig}}$ | -.399 ±.239 | -.399 ±.239 |
| $\delta^K_{\text{core, sig}}$ | -.383 ±.070 | -.385 ±.070 |
| $\delta^{NT1}_{\text{core, sig}}$ | -.391 ±.138 | -.392 ±.137 |
| $\delta^{NT2}_{\text{core, sig}}$ | -.301 ±.096 | -.297 ±.096 |
| $\mathcal{S}_{\text{tail, sig}}$ | 2.80 ±.638 | 2.81 ±.636 |
| $\delta_{\text{tail, sig}}$ | -1.55 ±.753 | -1.55 ±.754 |
| $f_{\text{tail}}$ | .094 ±.067 | .094 ±.067 |
| $f_{\text{outlier}}$ | .001 ±.002 | .001 ±.002 |
| $D_{\text{L}}$ | .119 ±.079 | .117 ±.079 |
| $D_{\text{K}}$ | .727 ±.016 | .727 ±.016 |
| $D_{\text{NT1}}$ | .530 ±.046 | .531 ±.046 |
| $D_{\text{NT2}}$ | .226 ±.030 | .226 ±.030 |
| $\Delta D_{\text{L}}$ | .113 ±.121 | .127 ±.120 |
| $\Delta D_{\text{K}}$ | .035 ±.022 | .035 ±.022 |
| $\Delta D_{\text{NT1}}$ | -.262 ±.073 | -.260 ±.072 |
| $\Delta D_{\text{NT2}}$ | .043 ±.045 | .043 ±.045 |
| $\Delta m_d$ | .4979 ±.0146 | .4982 ±.0146 |
| Events | 8072 | 8079 |

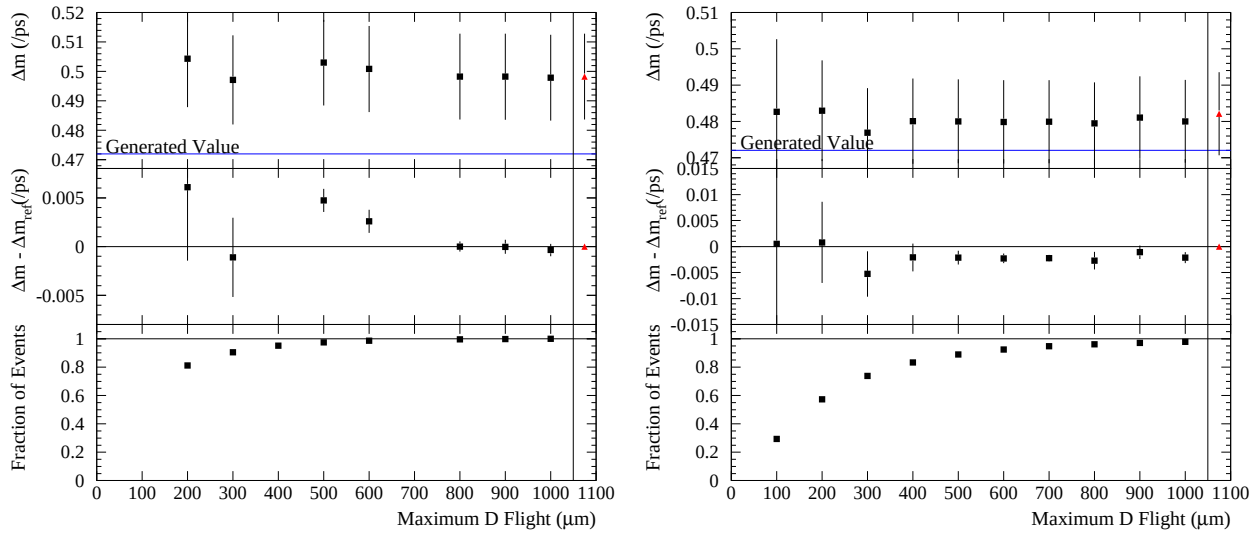


Figure 20: Results from the likelihood fits to the $\Delta t$ distributions of the hadronic $B$ decays in 2.8 million simulated signal cocktail events (no $B \to J/\psi K^*$) for different values of upper bound on true 3-dimensional charm flight distance, $l_c$, for events with at least one true $D_s$ on the tag side (includes double charm decays) (left), and for events with two true $D$ mesons on the tag side (right). The reference fit (red triangle) has $l_c = \infty$. The errors shown on the middle plot are computed as the difference in quadrature from the reference.

Table 20: Results from the likelihood fits to the $\Delta t$ distributions of the hadronic $B$ decays in 2.8 million simulated signal cocktail events (no $B \to J/\psi K^*$) for different values of upper bound on true 3-dimensional charm flight distance, $l_c$, for events with two true $D$ mesons on the tag side.

| Parameter | DD -0.0100 | DD -0.0200 | DD -0.0300 | DD -0.0400 | DD -0.0500 | DD -0.0600 |
|---|---|---|---|---|---|---|
| $\mathcal{S}_{\text{core, sig}}$ | 1.02 ±.097 | 1.02 ±.051 | 1.05 ±.049 | 1.07 ±.044 | 1.10 ±.046 | 1.09 ±.055 |
| $\delta^L_{\text{core, sig}}$ | .058 ±.330 | -.186 ±.204 | -.215 ±.177 | -.292 ±.165 | -.378 ±.161 | -.366 ±.161 |
| $\delta^K_{\text{core, sig}}$ | -.150 ±.057 | -.231 ±.034 | -.311 ±.034 | -.355 ±.031 | -.376 ±.034 | -.365 ±.041 |
| $\delta^{NT1}_{\text{core, sig}}$ | -.054 ±.158 | -.222 ±.107 | -.353 ±.098 | -.415 ±.091 | -.472 ±.090 | -.469 ±.093 |
| $\delta^{NT2}_{\text{core, sig}}$ | -.078 ±.094 | -.224 ±.061 | -.338 ±.057 | -.411 ±.052 | -.438 ±.054 | -.457 ±.058 |
| $\mathcal{S}_{\text{tail, sig}}$ | 3.34 ±1.11 | 3.79 ±.716 | 3.48 ±.879 | 3.81 ±.922 | 3.40 ±.963 | 2.98 ±.794 |
| $\delta_{\text{tail, sig}}$ | -.637 ±.695 | -1.92 ±1.10 | -2.13 ±1.34 | -1.82 ±.950 | -2.15 ±1.44 | -2.03 ±1.12 |
| $f_{\text{tail}}$ | .066 ±.055 | .036 ±.017 | .032 ±.020 | .032 ±.016 | .031 ±.020 | .047 ±.031 |
| $f_{\text{outlier}}$ | .004 ±.003 | .004 ±.002 | .005 ±.002 | .004 ±.002 | .004 ±.002 | .004 ±.002 |
| $D_{\text{L}}$ | .385 ±.112 | .199 ±.076 | .205 ±.066 | .165 ±.062 | .155 ±.060 | .165 ±.058 |
| $D_{\text{K}}$ | .553 ±.018 | .565 ±.013 | .561 ±.012 | .560 ±.011 | .557 ±.011 | .555 ±.011 |
| $D_{\text{NT1}}$ | .491 ±.059 | .500 ±.041 | .482 ±.036 | .479 ±.034 | .468 ±.033 | .453 ±.032 |
| $D_{\text{NT2}}$ | .216 ±.036 | .231 ±.025 | .229 ±.022 | .235 ±.021 | .230 ±.020 | .225 ±.020 |
| $\Delta D_{\text{L}}$ | .099 ±.180 | .008 ±.119 | .083 ±.104 | .141 ±.096 | .113 ±.093 | .112 ±.090 |
| $\Delta D_{\text{K}}$ | .085 ±.027 | .070 ±.019 | .068 ±.017 | .064 ±.016 | .061 ±.016 | .062 ±.015 |
| $\Delta D_{\text{NT1}}$ | -.253 ±.094 | -.309 ±.066 | -.348 ±.057 | -.345 ±.054 | -.358 ±.052 | -.333 ±.051 |
| $\Delta D_{\text{NT2}}$ | .014 ±.055 | .034 ±.039 | .046 ±.035 | .029 ±.032 | .047 ±.031 | .040 ±.031 |
| $\Delta m_d$ | .4827 ±.0200 | .4829 ±.0139 | .4769 ±.0123 | .4801 ±.0118 | .4800 ±.0115 | .4799 ±.0115 |
| Events | 6237 | 12174 | 15640 | 17655 | 18872 | 19603 |

| Parameter | DD -0.0700 | DD -0.0800 | DD -0.0900 | DD -0.1000 | DD -50.0 |
|---|---|---|---|---|---|
| $\mathcal{S}_{\text{core, sig}}$ | 1.09 ±.065 | 1.08 ±.096 | 1.09 ±.069 | 1.10 ±.071 | 1.10 ±.055 |
| $\delta^L_{\text{core, sig}}$ | -.332 ±.165 | -.354 ±.181 | -.417 ±.164 | -.426 ±.164 | -.436 ±.155 |
| $\delta^K_{\text{core, sig}}$ | -.363 ±.049 | -.358 ±.076 | -.370 ±.050 | -.374 ±.054 | -.380 ±.036 |
| $\delta^{NT1}_{\text{core, sig}}$ | -.453 ±.096 | -.436 ±.113 | -.453 ±.097 | -.479 ±.098 | -.494 ±.090 |
| $\delta^{NT2}_{\text{core, sig}}$ | -.443 ±.064 | -.441 ±.084 | -.459 ±.064 | -.464 ±.066 | -.449 ±.055 |
| $\mathcal{S}_{\text{tail, sig}}$ | 2.75 ±.677 | 2.63 ±.940 | 2.81 ±.642 | 2.80 ±.694 | 3.01 ±.382 |
| $\delta_{\text{tail, sig}}$ | -1.89 ±.896 | -1.81 ±.877 | -1.93 ±.778 | -1.91 ±.781 | -2.12 ±.666 |
| $f_{\text{tail}}$ | .067 ±.045 | .079 ±.078 | .073 ±.047 | .073 ±.050 | .080 ±.030 |
| $f_{\text{outlier}}$ | .004 ±.002 | .004 ±.002 | .004 ±.002 | .005 ±.002 | .005 ±.002 |
| $D_{\text{L}}$ | .150 ±.057 | .159 ±.057 | .150 ±.056 | .149 ±.056 | .144 ±.055 |
| $D_{\text{K}}$ | .555 ±.011 | .555 ±.010 | .553 ±.010 | .553 ±.010 | .554 ±.010 |
| $D_{\text{NT1}}$ | .456 ±.032 | .457 ±.032 | .458 ±.032 | .459 ±.031 | .455 ±.031 |
| $D_{\text{NT2}}$ | .226 ±.020 | .227 ±.020 | .226 ±.019 | .224 ±.019 | .223 ±.019 |
| $\Delta D_{\text{L}}$ | .114 ±.089 | .135 ±.088 | .137 ±.087 | .132 ±.086 | .129 ±.085 |
| $\Delta D_{\text{K}}$ | .062 ±.015 | .062 ±.015 | .064 ±.015 | .064 ±.015 | .064 ±.015 |
| $\Delta D_{\text{NT1}}$ | -.332 ±.051 | -.329 ±.050 | -.334 ±.050 | -.328 ±.050 | -.312 ±.049 |
| $\Delta D_{\text{NT2}}$ | .045 ±.030 | .043 ±.030 | .043 ±.030 | .044 ±.030 | .044 ±.029 |
| $\Delta m_d$ | .4799 ±.0114 | .4795 ±.0113 | .4811 ±.0114 | .4800 ±.0114 | .4821 ±.0115 |
| Events | 20091 | 20383 | 20611 | 20756 | 21210 |

Table 21: Results from the likelihood fits to the $\Delta t$ distributions of the hadronic $B$ decays in 2.8 million simulated signal cocktail events (no $B \to J/\psi K^*$) for different values of upper bound on true 3-dimensional charm flight distance, $l_c$, for all events.

| Parameter | all -0.0100 | all -0.0200 | all -0.0300 | all -0.0500 | all -0.0600 | all -0.0700 |
|---|---|---|---|---|---|---|
| $\mathcal{S}_{\text{core, sig}}$ | 1.10 ±.020 | 1.07 ±.081 | 1.10 ±.021 | 1.11 ±.020 | 1.11 ±.030 | 1.12 ±.022 |
| $\delta^{L}_{\text{core, sig}}$ | -.015 ±.028 | -.031 ±.038 | -.049 ±.024 | -.064 ±.023 | -.062 ±.025 | -.058 ±.023 |
| $\delta^{K}_{\text{core, sig}}$ | -.072 ±.016 | -.118 ±.032 | -.165 ±.014 | -.206 ±.014 | -.212 ±.017 | -.217 ±.015 |
| $\delta^{NT1}_{\text{core, sig}}$ | -.080 ±.036 | -.097 ±.045 | -.126 ±.029 | -.147 ±.028 | -.148 ±.029 | -.146 ±.028 |
| $\delta^{NT2}_{\text{core, sig}}$ | -.029 ±.026 | -.080 ±.037 | -.128 ±.022 | -.178 ±.021 | -.189 ±.023 | -.193 ±.021 |
| $\mathcal{S}_{\text{tail, sig}}$ | 10.00 ±6.21 | 4.34 ±6.91 | 4.29 ±.945 | 3.87 ±.612 | 3.60 ±.876 | 3.45 ±.432 |
| $\delta_{\text{tail, sig}}$ | -.697 ±1.07 | -1.34 ±1.15 | -1.28 ±.602 | -1.54 ±.596 | -1.47 ±.578 | -1.50 ±.477 |
| $f_{\text{tail}}$ | .006 ±.002 | .017 ±.039 | .016 ±.007 | .019 ±.007 | .025 ±.016 | .029 ±.010 |
| $f_{\text{outlier}}$ | .003 ±.001 | .004 ±.002 | .004 ±.001 | .004 ±.001 | .004 ±.001 | .004 ±.001 |
| $D_{\text{L}}$ | .878 ±.008 | .871 ±.007 | .869 ±.006 | .861 ±.006 | .858 ±.006 | .857 ±.006 |
| $D_{\text{K}}$ | .738 ±.006 | .731 ±.006 | .724 ±.005 | .716 ±.005 | .715 ±.005 | .714 ±.005 |
| $D_{\text{NT1}}$ | .593 ±.013 | .616 ±.011 | .624 ±.010 | .625 ±.009 | .621 ±.009 | .622 ±.009 |
| $D_{\text{NT2}}$ | .310 ±.011 | .322 ±.009 | .320 ±.009 | .313 ±.008 | .310 ±.008 | .310 ±.008 |
| $\Delta D_{\text{L}}$ | -.003 ±.013 | -.005 ±.011 | -.004 ±.010 | .000 ±.010 | -.000 ±.010 | .000 ±.010 |
| $\Delta D_{\text{K}}$ | .040 ±.010 | .038 ±.008 | .037 ±.008 | .035 ±.007 | .037 ±.007 | .038 ±.007 |
| $\Delta D_{\text{NT1}}$ | -.047 ±.021 | -.057 ±.017 | -.051 ±.016 | -.052 ±.015 | -.052 ±.015 | -.053 ±.015 |
| $\Delta D_{\text{NT2}}$ | .054 ±.017 | .051 ±.015 | .062 ±.014 | .066 ±.013 | .064 ±.013 | .064 ±.013 |
| $\Delta m_d$ | .4775 ±.0044 | .4786 ±.0055 | .4785 ±.0035 | .4788 ±.0034 | .4781 ±.0034 | .4778 ±.0033 |
| Events | 56965 | 80737 | 93723 | 105720 | 108716 | 110789 |

| Parameter | all -0.0800 | all -0.0900 | all -0.1000 | all -50.0 |
|---|---|---|---|---|
| $\mathcal{S}_{\text{core, sig}}$ | 1.12 ±.030 | 1.12 ±.030 | 1.12 ±.028 | 1.13 ±.020 |
| $\delta^{L}_{\text{core, sig}}$ | -.063 ±.025 | -.059 ±.025 | -.058 ±.025 | -.058 ±.022 |
| $\delta^{K}_{\text{core, sig}}$ | -.221 ±.017 | -.223 ±.017 | -.224 ±.017 | -.227 ±.014 |
| $\delta^{NT1}_{\text{core, sig}}$ | -.150 ±.029 | -.153 ±.030 | -.154 ±.029 | -.158 ±.027 |
| $\delta^{NT2}_{\text{core, sig}}$ | -.196 ±.023 | -.200 ±.023 | -.200 ±.023 | -.197 ±.021 |
| $\mathcal{S}_{\text{tail, sig}}$ | 3.51 ±.717 | 3.43 ±.646 | 3.37 ±.525 | 3.72 ±.284 |
| $\delta_{\text{tail, sig}}$ | -1.59 ±.553 | -1.61 ±.526 | -1.58 ±.453 | -2.06 ±.398 |
| $f_{\text{tail}}$ | .029 ±.016 | .032 ±.017 | .036 ±.016 | .037 ±.008 |
| $f_{\text{outlier}}$ | .004 ±.001 | .004 ±.001 | .004 ±.001 | .004 ±.001 |
| $D_{\text{L}}$ | .857 ±.006 | .857 ±.006 | .856 ±.006 | .854 ±.006 |
| $D_{\text{K}}$ | .712 ±.005 | .711 ±.005 | .710 ±.005 | .710 ±.005 |
| $D_{\text{NT1}}$ | .622 ±.009 | .622 ±.009 | .623 ±.009 | .623 ±.009 |
| $D_{\text{NT2}}$ | .309 ±.008 | .309 ±.008 | .308 ±.008 | .308 ±.008 |
| $\Delta D_{\text{L}}$ | .002 ±.010 | .003 ±.009 | .001 ±.009 | .002 ±.009 |
| $\Delta D_{\text{K}}$ | .039 ±.007 | .039 ±.007 | .039 ±.007 | .040 ±.007 |
| $\Delta D_{\text{NT1}}$ | -.051 ±.014 | -.050 ±.014 | -.049 ±.014 | -.049 ±.014 |
| $\Delta D_{\text{NT2}}$ | .066 ±.012 | .068 ±.012 | .070 ±.012 | .069 ±.012 |
| $\Delta m_d$ | .4773 ±.0034 | .4776 ±.0034 | .4771 ±.0034 | .4788 ±.0033 |
| Events | 112226 | 113250 | 114048 | 116539 |

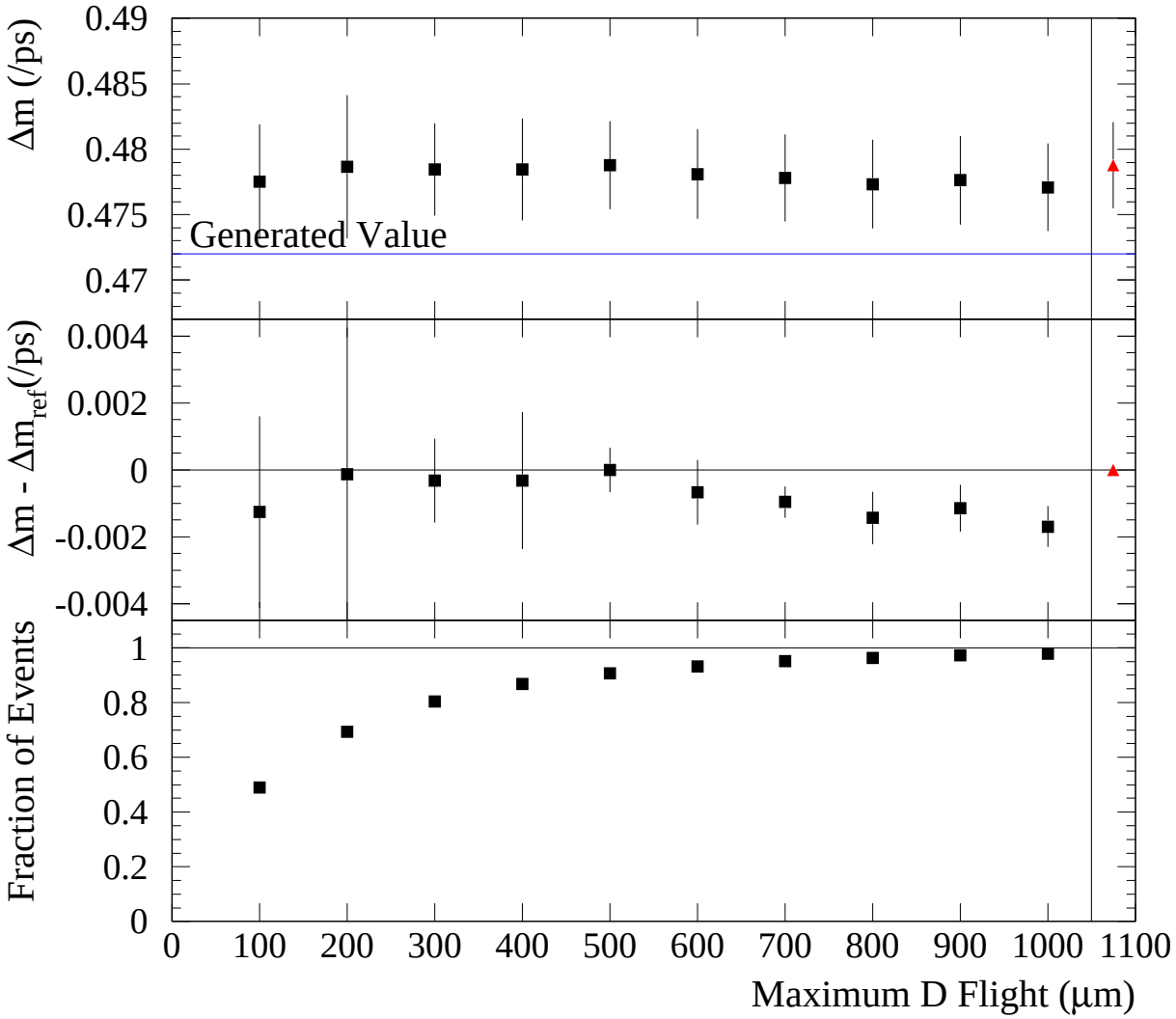


Figure 21: Results from the likelihood fits to the $\Delta t$ distributions of the hadronic $B$ decays in 2.8 million simulated signal cocktail events (no $B \to J/\psi K^*$) for different values of upper bound on true 3-dimensional charm flight distance, $l_c$, for all events. The reference fit (red triangle) has $l_c = \infty$. The errors shown on the middle plot are computed as the difference in quadrature from the reference.

a category by the minimal requirement that *at least* one of the species be present on the tag side, and therefore always include double-charm decays. The "No charm" category includes decays to charmed baryons and charmonium final states, as well as true cases of $b \to u$ and $b \to s$ transitions. The results of those fits are in Table 22 and Figure 22.

Table 22: Results from the likelihood fits to the $\Delta t$ distributions of the hadronic $B$ decays in 2.8 million simulated signal cocktail events(including $B \to J/\psi K^*$) for different true species of charm on the tag side. (The $D^+, D^0$ and $D_s$ categories require at least one of the $D$ species under study to be in the event on the tag side, and therefore include double charm decays).

| Parameter | $D^+, l_c < 50.0$ | $D^0, l_c < 50.0$ | $D_s^+, l_c < 50.0$ | DD -50.0 | nonD -50.0 | all -50.0 |
|---|---|---|---|---|---|---|
| $\mathcal{S}_{\text{core, sig}}$ | 1.21 ±.034 | 1.00 ±.063 | 1.14 ±.099 | 1.10 ±.055 | 1.12 ±.138 | 1.13 ±.020 |
| $\delta^L_{\text{core, sig}}$ | -.071 ±.036 | .016 ±.061 | -.399 ±.239 | -.436 ±.155 | -.115 ±.250 | -.058 ±.022 |
| $\delta^K_{\text{core, sig}}$ | -.328 ±.026 | -.119 ±.050 | -.385 ±.070 | -.380 ±.036 | -.126 ±.179 | -.227 ±.014 |
| $\delta^{NT1}_{\text{core, sig}}$ | -.097 ±.049 | -.151 ±.057 | -.392 ±.137 | -.494 ±.090 | -.077 ±.212 | -.158 ±.027 |
| $\delta^{NT2}_{\text{core, sig}}$ | -.309 ±.037 | -.082 ±.057 | -.297 ±.096 | -.449 ±.055 | -.181 ±.183 | -.197 ±.021 |
| $\mathcal{S}_{\text{tail, sig}}$ | 4.04 ±.341 | 2.16 ±.542 | 2.81 ±.636 | 3.01 ±.382 | .643 ±.962 | 3.72 ±.284 |
| $\delta_{\text{tail, sig}}$ | -2.48 ±.579 | -1.24 ±.626 | -1.55 ±.754 | -2.12 ±.666 | 2.48 ±1.58 | -2.06 ±.398 |
| $f_{\text{tail}}$ | .052 ±.012 | .083 ±.067 | .094 ±.067 | .080 ±.030 | .041 ±.085 | .037 ±.008 |
| $f_{\text{outlier}}$ | .004 ±.001 | .004 ±.001 | .001 ±.002 | .005 ±.002 | .012 ±.003 | .004 ±.001 |
| $D_{\text{L}}$ | .792 ±.010 | .937 ±.006 | .117 ±.079 | .144 ±.055 | .373 ±.054 | .854 ±.006 |
| $D_{\text{K}}$ | .570 ±.009 | .809 ±.006 | .727 ±.016 | .554 ±.010 | .534 ±.020 | .710 ±.005 |
| $D_{\text{NT1}}$ | .505 ±.016 | .813 ±.010 | .531 ±.046 | .455 ±.031 | -.128 ±.037 | .623 ±.009 |
| $D_{\text{NT2}}$ | .131 ±.014 | .518 ±.011 | .226 ±.030 | .223 ±.019 | .004 ±.025 | .308 ±.008 |
| $\Delta D_{\text{L}}$ | .015 ±.016 | -.003 ±.011 | .127 ±.120 | .129 ±.085 | -.048 ±.084 | .002 ±.009 |
| $\Delta D_{\text{K}}$ | .038 ±.014 | .040 ±.009 | .035 ±.022 | .064 ±.015 | .044 ±.029 | .040 ±.007 |
| $\Delta D_{\text{NT1}}$ | .034 ±.026 | -.063 ±.017 | -.260 ±.072 | -.312 ±.049 | -.064 ±.057 | -.049 ±.014 |
| $\Delta D_{\text{NT2}}$ | .115 ±.021 | .041 ±.017 | .043 ±.045 | .044 ±.029 | .049 ±.038 | .069 ±.012 |
| $\Delta m_d$ | .4752 ±.0066 | .4783 ±.0038 | .4982 ±.0146 | .4821 ±.0115 | .4835 ±.0235 | .4788 ±.0033 |
| Events | 39825 | 60153 | 8079 | 21210 | 8482 | 116539 |

## 6.13 Dilution vs. per event error and other variables

A correlation between the mistag rate and the per-event $\Delta t$ error exists. See Figure 23. If we include a linear dependence on the mistag rate in the likelihood fit, we obtain (for data) a value of $\Delta m_d$ which is 0.0054 ±0.0030 lower than ignoring this dependence (the error is the difference in quadrature between the two fits). For MC, we observe a value which is 0.0032 ±0.0004 lower. As a result, after performing the correction from the MC, we would find a value of $\Delta m_d$ which is 0.0022 ±0.0030 lower than we would conclude ignoring the correlation. The fitted dilutions and their dependence on the per-event error are listed in Table 23.

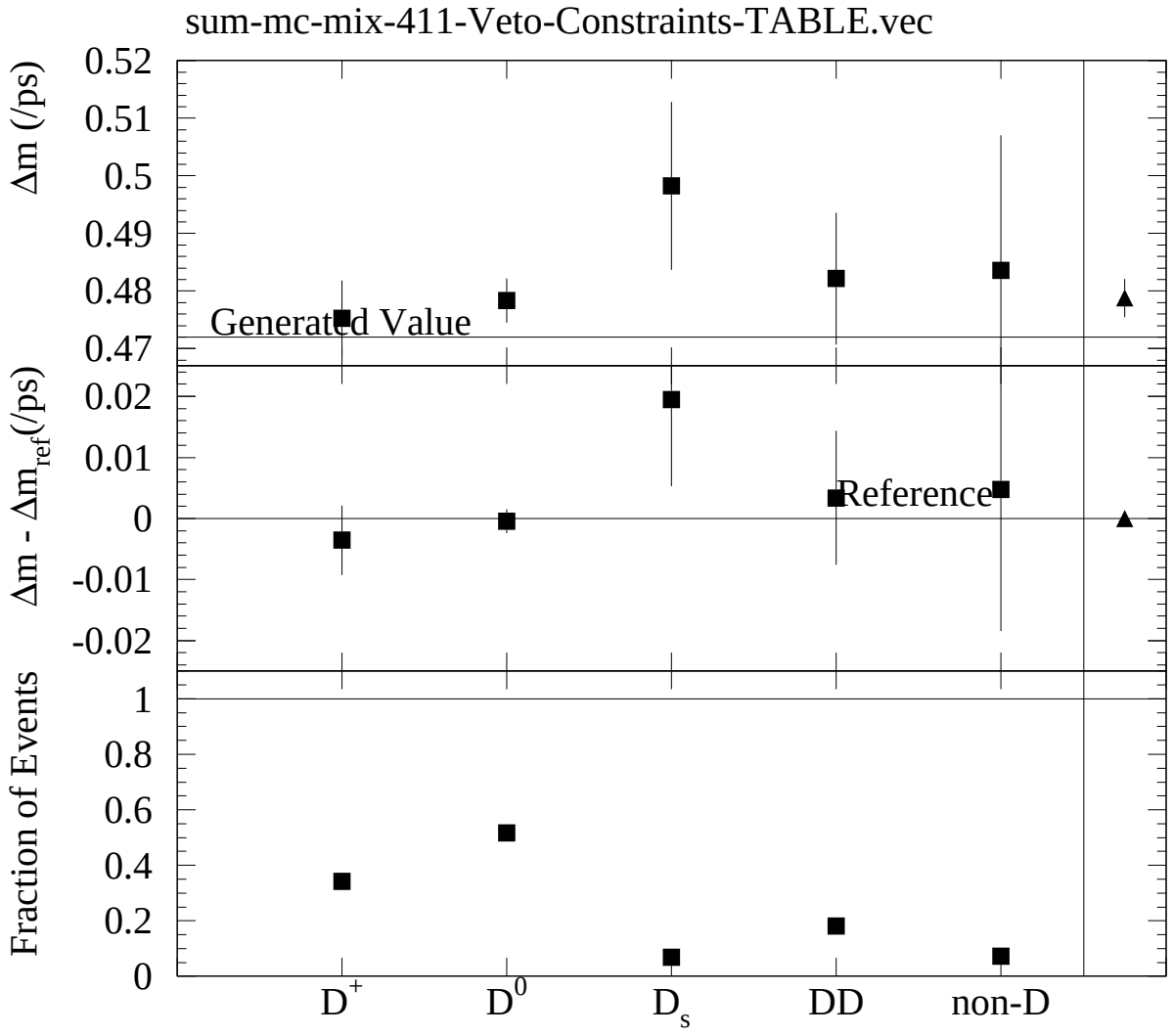


Figure 22: Results from the likelihood fits to the $\Delta t$ distributions of the hadronic $B$ decays in various subsets of 2.8 million simulated signal cocktail events (no $B \to J/\psi K^*$) which have different true species of charm on the tag side. (The $D^+, D^0$ and $D_s$ categories include double charm decays). The reference is a fit to the nominal 2.8 million events. The errors shown on the middle plot are computed as the difference in quadrature from the reference.

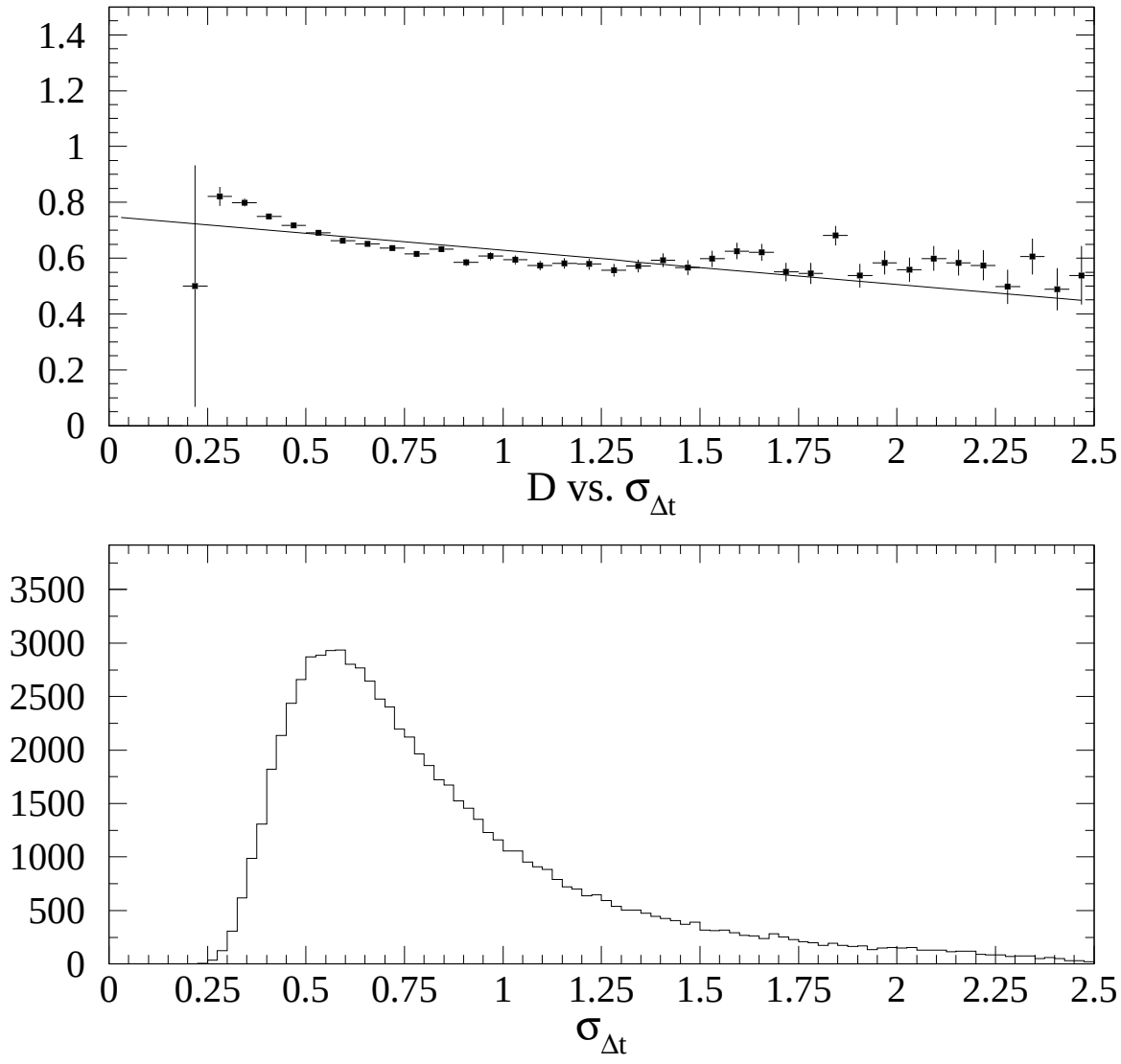


Figure 23: Correlation between the Dilution and per-event error (top) for the `Kaon` tagging category in a sub-sample of the cocktail signal MC. The dilution is obtained by counting, within sample defined by the slice in $\Delta t$ given by the bin, the fraction of wrong-tags (defined as those events where the reconstructed flavour tag does not match the MC truth). To *illustrate* the dependence, a linear fit to the points is also shown. For comparison, the distribution of per-event errors for the same sample is also shown (bottom).

Table 23: Results from likelihood fits (both data and MC) which include the correlation between the mistag rate and the per-event error.

| | data | MC |
|---|---|---|
| D($\sigma_{\Delta t} = 0$) Lep | 0.834 ±0.079 | 0.847 ±0.018 |
| D($\sigma_{\Delta t} = 0$) Kaon | 0.840 ±0.068 | 0.854 ±0.013 |
| D($\sigma_{\Delta t} = 0$) NT1 | 0.723 ±0.132 | 0.672 ±0.025 |
| D($\sigma_{\Delta t} = 0$) NT2 | 0.308 ±0.121 | 0.363 ±0.023 |
| slopeD Lep | 0.011 ±0.133 | 0.009 ±0.029 |
| slopeD Kaon | -0.252 ±0.095 | -0.207 ±0.019 |
| slopeD NT1 | -0.289 ±0.221 | -0.083 ±0.041 |
| slopeD NT2 | 0.004 ±0.172 | -0.079 ±0.032 |
| DeltaD Lep | -0.006 ±0.045 | 0.005 ±0.009 |
| DeltaD Kaon | 0.023 ±0.033 | 0.036 ±0.007 |
| DeltaD NT1 | -0.087 ±0.068 | -0.050 ±0.014 |
| DeltaD NT2 | 0.101 ±0.060 | 0.070 ±0.012 |
| $\Delta m_d$ | XX-0.0054±0.016 | 0.475 ±0.003 |

As the correlation seems to be well described by the MC, and causes for possible disagreement of the size of this effect between data and MC (such as charm meson fractions, wrong sign kaon decays) are specifically included in the systematics, this effect is assumed to be fully corrected for by the MC correction, and no additional systematic error is added.

Other variables which may exhibit a similar correlation have been explored. The effect seems to come from the correlation between the wrong-sign Kaon rates of a given $D$ species and e.g. decay multiplicity, momentum spectrum, etc. In particular, for the $D^+$, the ratio of wrong to right-sign Kaons is more than twice that for $D^0$s. Just from charge-conservation and phase-space arguments, the $D^+$ favors higher charge-multiplicity decays than the $D^0$, which combined with the wrong-sign kaon differences would introduce a correlation between the per-event error(which depends on multiplicity) and the wrong-tag rate. This has been confirmed in MC studies.

In an effort to better parametrize the effect, we have found an observable which seems to be correlated with the per-event wrong-tag rate for the `Kaon` category. It is defined as

$$\alpha \;=\; \frac{1}{\sqrt{\sum_{\mathrm{tag-side\,tracks}} p_{\perp i}^2}}, \tag{13}$$

where $p_{\perp i}$ is the transverse momentum component of the $i$th track. This variable also shows a correlation with dilution (see Fig 24.) Again, as a check, we fit the entire MC sample, allowing for a linear dependence on $\alpha$ in the `Kaon` category, and again allowing a linear dependence in all tagging categories. See Table 24. It is clear from Fig 24 and 23 that a linear parameterization of the dilution on $\alpha$ yields a better description of this effect then a linear parameterization as a function of $\sigma_{\Delta t}$.

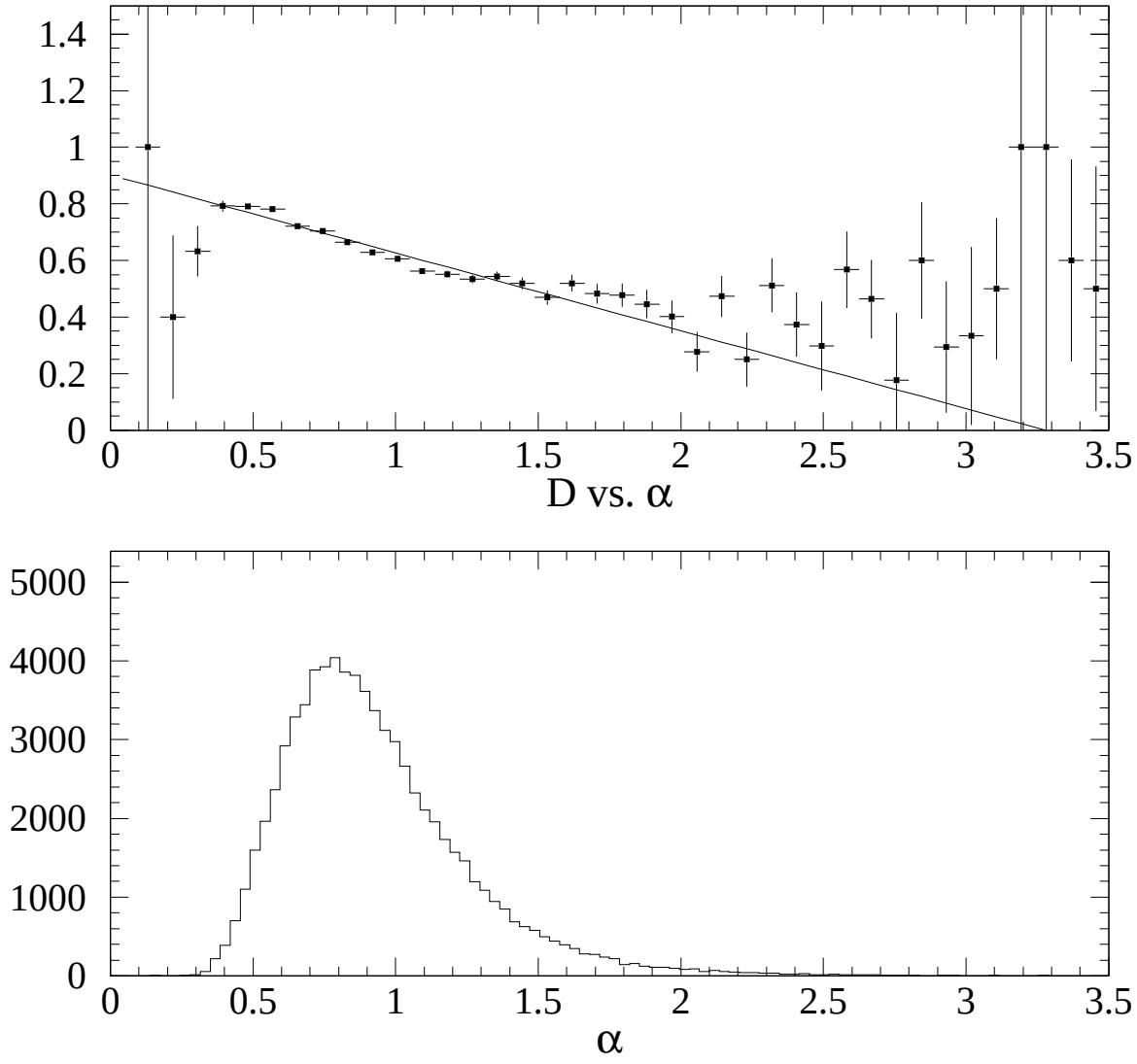


Figure 24: Correlation between the Dilution and $\alpha$ (see equation 13 for the definition of $\alpha$) (top) for the `Kaon` tagging category in a sub-sample of the cocktail signal MC. The dilution is obtained by counting, within sample defined by the slice in $\Delta t$ given by the bin, the fraction of wrong-tags (defined as those events where the reconstructed flavour tag does not match the MC truth). To *illustrate* the dependence, a linear fit to the points is also shown. For comparison, the distribution of $\alpha$ for the same sample is also shown (bottom).

Table 24: Results from the likelihood fits to the $\Delta t$ distributions of the hadronic $B$ decays in 2.8 million simulated signal cocktail events (no $B \to J/\psi K^*$). Here, we allow the dilution to depend on the variable $\alpha$ in the fit for all categories (See equation 13 for the definition of $\alpha$). and just the `Kaon` category. The errors shown on the middle plot are computed as the difference in quadrature from the reference.

| Parameter | all slope | kaon slope | kaon noSlope |
|---|---|---|---|
| $\mathcal{S}_{\text{core, sig}}$ | 1.131 ±.020 | 1.130 ±.020 | 1.129 ±.021 |
| $\delta^L_{\text{core, sig}}$ | -.059 ±.023 | -.059 ±.023 | -.058 ±.023 |
| $\delta^K_{\text{core, sig}}$ | -.228 ±.014 | -.228 ±.014 | -.227 ±.014 |
| $\delta^{NT1}_{\text{core, sig}}$ | -.159 ±.027 | -.160 ±.027 | -.158 ±.028 |
| $\delta^{NT2}_{\text{core, sig}}$ | -.198 ±.021 | -.198 ±.021 | -.197 ±.021 |
| $\mathcal{S}_{\text{tail, sig}}$ | 3.722 ±.335 | 3.735 ±.335 | 3.717 ±.316 |
| $\delta_{\text{tail, sig}}$ | -2.243 ±.465 | -2.208 ±.450 | -2.060 ±.395 |
| $f_{\text{tail}}$ | .033 ±.008 | .034 ±.008 | .037 ±.008 |
| $f_{\text{outlier}}$ | .004 ±.001 | .004 ±.001 | .004 ±.001 |
| $D_{\text{L}}$ | .919 ±.030 | .853 ±.006 | .854 ±.006 |
| $D_{\text{K}}$ | .982 ±.015 | .982 ±.015 | .710 ±.005 |
| $D_{\text{NT1}}$ | .622 ±.029 | .622 ±.009 | .623 ±.009 |
| $D_{\text{NT2}}$ | .298 ±.023 | .307 ±.008 | .308 ±.008 |
| $\Delta D_{\text{L}}$ | .002 ±.009 | .002 ±.009 | .002 ±.009 |
| $\Delta D_{\text{K}}$ | .039 ±.007 | .039 ±.007 | .040 ±.007 |
| $\Delta D_{\text{NT1}}$ | -.049 ±.014 | -.049 ±.014 | -.049 ±.014 |
| $\Delta D_{\text{NT2}}$ | .068 ±.012 | .069 ±.012 | .069 ±.012 |
| $\alpha D_{\text{L}}$ | -.098 ±.044 | | |
| $\alpha D_{\text{K}}$ | -.308 ±.017 | -.308 ±.017 | |
| $\alpha D_{\text{NT1}}$ | -.000 ±.037 | | |
| $\alpha D_{\text{NT2}}$ | .010 ±.023 | | |
| $\Delta m_d$ | .4757 ±.0033 | .4760 ±.0033 | .4788 ±.0033 |
| Events | 116539 | 116539 | 116539 |

# 7 Systematic Uncertainties

This section contains the results of the studies of systematic uncertainties in the measurement of $\Delta m_d$.

## 7.1 Monte Carlo Tests

The analysis procedure is tested at various levels of complexity. First, we check the likelihood fit algorithm with high-statistics toy Monte Carlo. Next, we check the resolution function in fully simulated events by comparing the reconstructed $\Delta t$ to the true value. Finally, we perform the full analysis chain on simulated events including the likelihood fit to the $\Delta t$ distributions. A global systematic bias due to the measurement technique (event selection, $\Delta t$ reconstruction and likelihood fit) is measured with fully simulated events as the difference between the fitted values and the true value of $\Delta m_d$ and the mistag rates. We correct for these biases and the corresponding statistical uncertainties are considered as systematic errors.

Table 25: Parameters of the per-event error distributions

| | Run 1 | | Run 2 | |
|---|---|---|---|---|
| | Landau peak (ps) | Landau width (ps) | Landau peak (ps) | Landau width (ps) |
| Leptons, signal | 0.43 | 0.073 | 0.42 | 0.070 |
| Kaons, signal | 0.57 | 0.116 | 0.57 | 0.117 |
| NT1, signal | 0.44 | 0.077 | 0.44 | 0.081 |
| NT2, signal | 0.53 | 0.102 | 0.51 | 0.099 |
| Leptons, background | 0.48 | 0.093 | 0.50 | 0.107 |
| Kaons, background | 0.63 | 0.145 | 0.62 | 0.134 |
| NT1, background | 0.49 | 0.103 | 0.51 | 0.117 |
| NT2, background | 0.57 | 0.123 | 0.54 | 0.115 |

### 7.1.1 Toy Monte Carlo Checks

We check the likelihood fit program `tFit` for systematic biases in the central values of the fit parameters and in their calculated statistical uncertainties with high-statistics toy Monte Carlo. To this end, we generate 2000 toy MC samples with a size and parametrization identical to the data sample. The actual parameters used for the generation are therefore the ones listed in Table 2. In addition, the per-event errors are generated from a Landau distribution with parameters obtained from the data, seperately for background (obtained from the $m_{\rm ES} < 5.27\,{\rm GeV}/c^2$ sideband) and the signal (obtained from the sideband subtracted signal region $m_{\rm ES} > 5.27\,{\rm GeV}/c^2$), and seperately for each tagging category (see Table 25). The values generated for $m_{\rm ES}$ for the combinatorial background use the Argus parameters

obtained from a fit to the $m_{\rm ES}$ distribution of the combined tagged sample ($\xi = -29$). All events use the same value of $\xi$, and only tagged events are generated.

The distributions of the fitted signal parameters and their pull distributions are shown in Fig. 25 and 26, and for the background parameters in Fig. 27. Even though several of the background parameters show a bias, no bias is observed in the signal parameters. Note that for the toy MC fits the dilution of the prompt lepton background was fixed to 0, to avoid a non-negligble number of fit failures (there are O(10) events generated in this category). When fixing this parameter to 0 for data, no change in the log-likelihood value nor in $\Delta m_d$ are observed.

Figure 25: Distributions of the signal fit parameters and their pull in toy MC. The vertical line corresponds to the generated value.

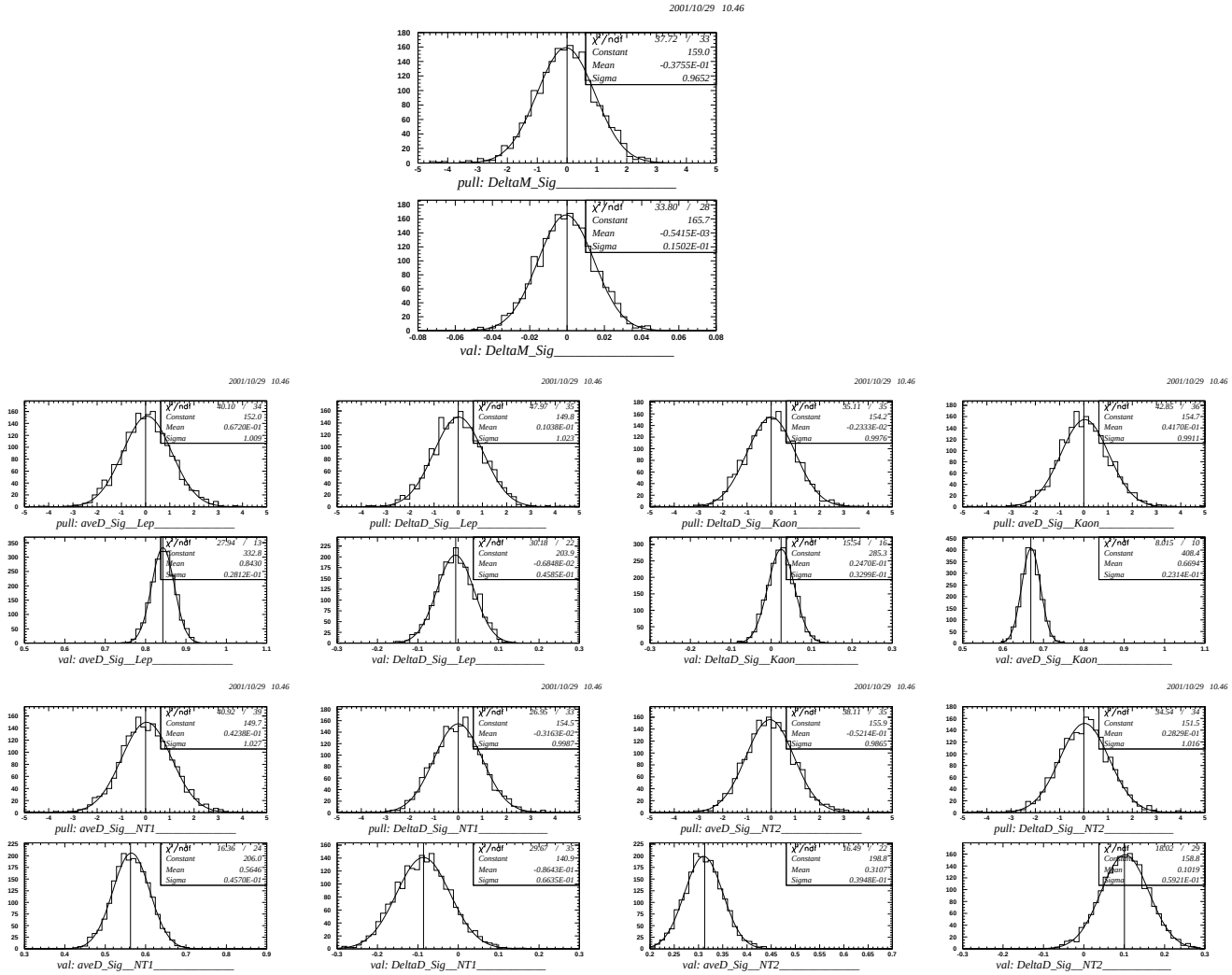

Figure 26: Distributions of the signal resolution function fit parameters and their pull in toy MC. The vertical line corresponds to the generated value.

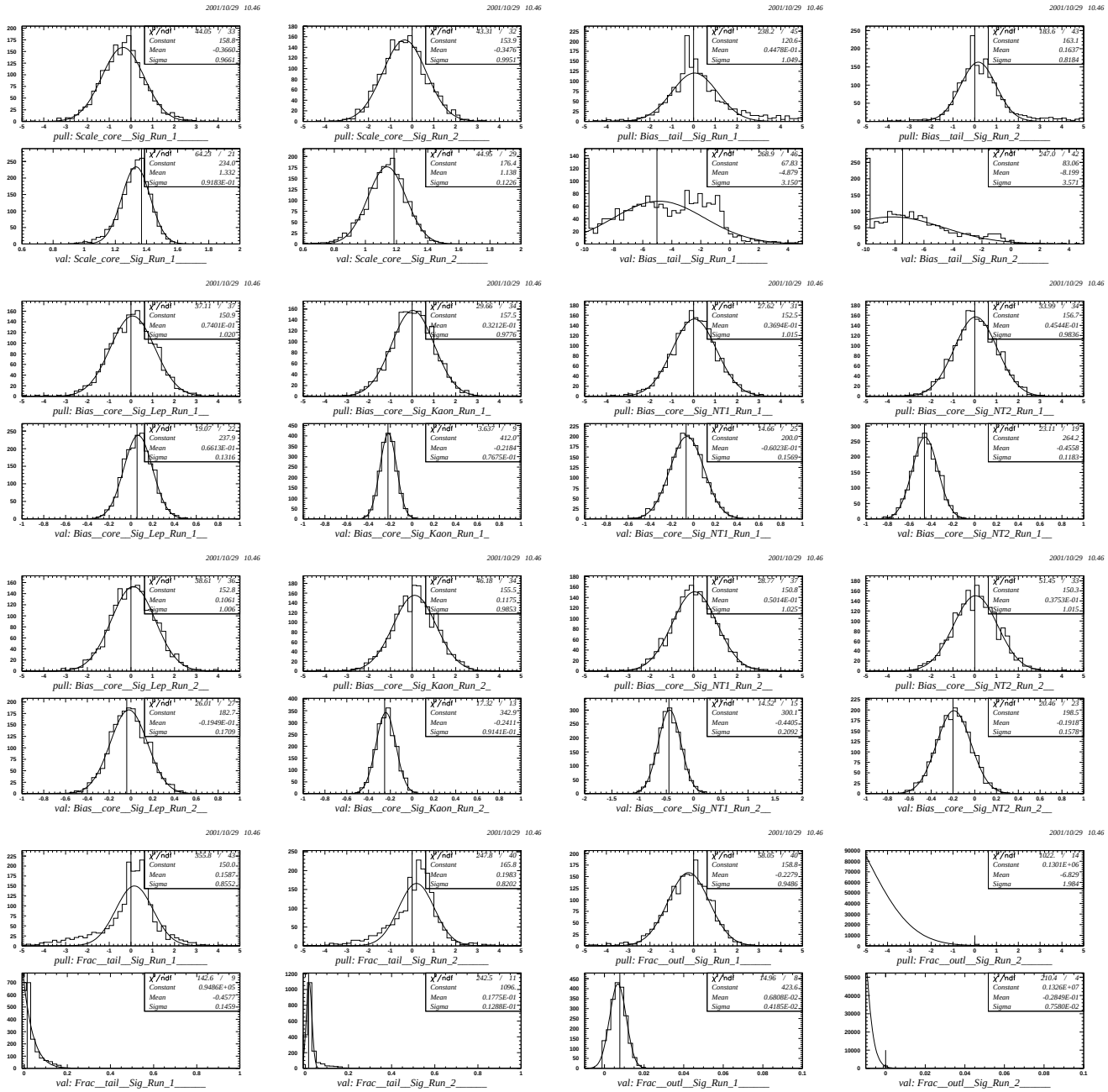

Figure 27: Distributions of the background fit parameters and their pull in toy MC. The vertical line corresponds to the generated value.

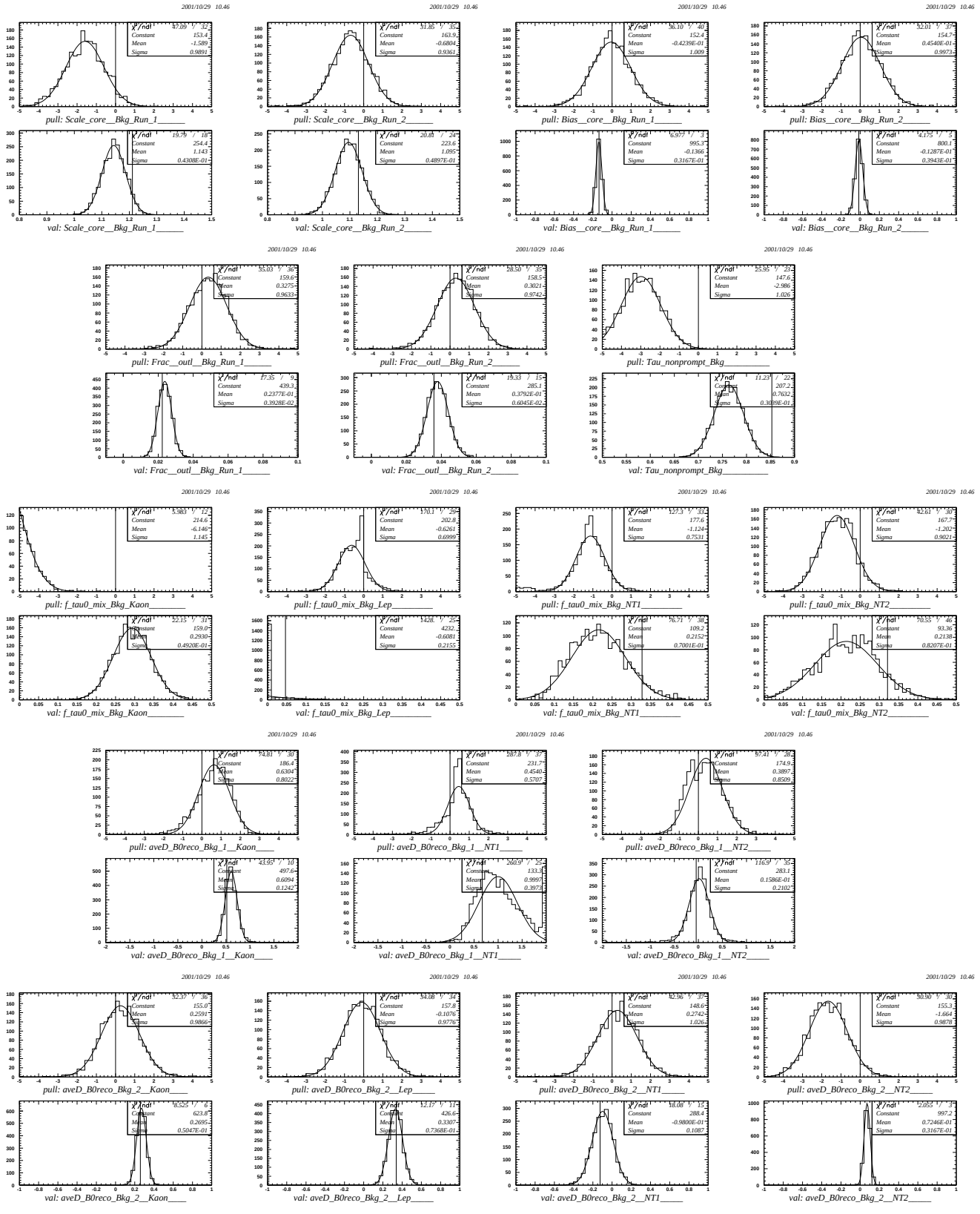

### 7.1.2 Signal Monte Carlo Analysis

We perform the complete analysis chain including event reconstruction, candidate selection and the likelihood fit with fully simulated signal events. We compare the fitted resolution functions and the fitted dilutions to the values obtained using MC truth information. In the following, we describe how we use MC truth to obtain the resolution functions and the dilutions and we discuss the likelihood fit result for $\Delta m_d$.

**$\Delta t$ Measurement** We extract a detector resolution function for the selected $B$ candidates in simulated events by fitting the distribution of the residual $\Delta t = \Delta t_{\rm reco} - \Delta t_{\rm gen}$ with the resolution function model described in section 4.2, *i.e.* two Gaussians (using the calculated error on $\Delta t$) with 5 free fit parameters and a third Gaussian with fixed width (8 ps) and mean (0 ps) for a total of 9 free fit parameters. If the calculated event-by-event error on $\Delta t$ is a good estimate of the true error, the normalized residual distribution (pull) of $\Delta t$ should be a Gaussian with a mean of zero and an RMS of one (unit Gaussian). Due to non-Gaussian measurement errors, the pull distribution will generally not be described by such a unit Gaussian.

For the sin2$\beta$ measurement, it was decided *not* to float the tail width due to the high global correlation coefficients of these two parameters, leading to "difficult" fits. For this measurement we do the same, but check the effect of floating these parameters. The value of $\Delta m_d$ changes by -0.0008, with no change in the error. Also, the value of the log likelihood changes only slightly: from -30440.8 to -30438.3.

**ADD GEXP RESULT**

Table 26: Parameters of fit of the signal resolution model to the $\Delta t$ residual ($\Delta t_{\rm reco} - \Delta t_{\rm true}$) distributions for simulated hadronic $B$ cocktail events for all tags, all correct tags, all wrong tags, all unmixed event and all mixed events (where (un)mixed is defined using the reconstructed flavor tag).

| | ALL | RIGHT | WRONG | unmixed | mixed |
|---|---|---|---|---|---|
| Bias core Sig Kaon | -0.210 ±0.006 | -0.210 ±0.006 | -0.215 ±0.015 | -0.207 ±0.011 | -0.212 ±0.006 |
| Bias core Sig Lep | -0.088 ±0.008 | -0.081 ±0.009 | -0.207 ±0.033 | -0.112 ±0.018 | -0.082 ±0.009 |
| Bias core Sig NT1 | -0.134 ±0.010 | -0.128 ±0.011 | -0.161 ±0.024 | -0.140 ±0.019 | -0.132 ±0.012 |
| Bias core Sig NT2 | -0.186 ±0.008 | -0.168 ±0.010 | -0.217 ±0.014 | -0.203 ±0.013 | -0.173 ±0.010 |
| Bias tail Sig | -1.031 ±0.041 | -0.963 ±0.045 | -1.268 ±0.097 | -1.085 ±0.073 | -1.006 ±0.050 |
| Frac outl Sig | 0.008 ±0.000 | 0.007 ±0.000 | 0.013 ±0.001 | 0.011 ±0.001 | 0.007 ±0.000 |
| Frac tail Sig | 0.106 ±0.005 | 0.104 ±0.006 | 0.120 ±0.010 | 0.122 ±0.010 | 0.100 ±0.006 |
| Scale core Sig | 1.058 ±0.005 | 1.054 ±0.005 | 1.076 ±0.011 | 1.060 ±0.009 | 1.057 ±0.005 |
| Scale tail Sig | 2.310 ±0.038 | 2.262 ±0.042 | 2.462 ±0.083 | 2.280 ±0.066 | 2.324 ±0.047 |

**Restricted $\Delta t$ fit ranges** To check whether $\Delta m_d$ measurement is independent of the $\Delta t$ fit range (for example, due to an imperfect description of outliers in the $\Delta t$ measurement), we repeat the fit on the data in restricted $\Delta t$ ranges $[-t_{bound}, +t_{bound}]$, varying the value of $t_{bound}$ between 8 and 40 ps. The results (both leaving *all* parameters floating and only leaving $\Delta m_d$ floating) are shown in Fig. 28. No systematic error due to this cut is assigned.

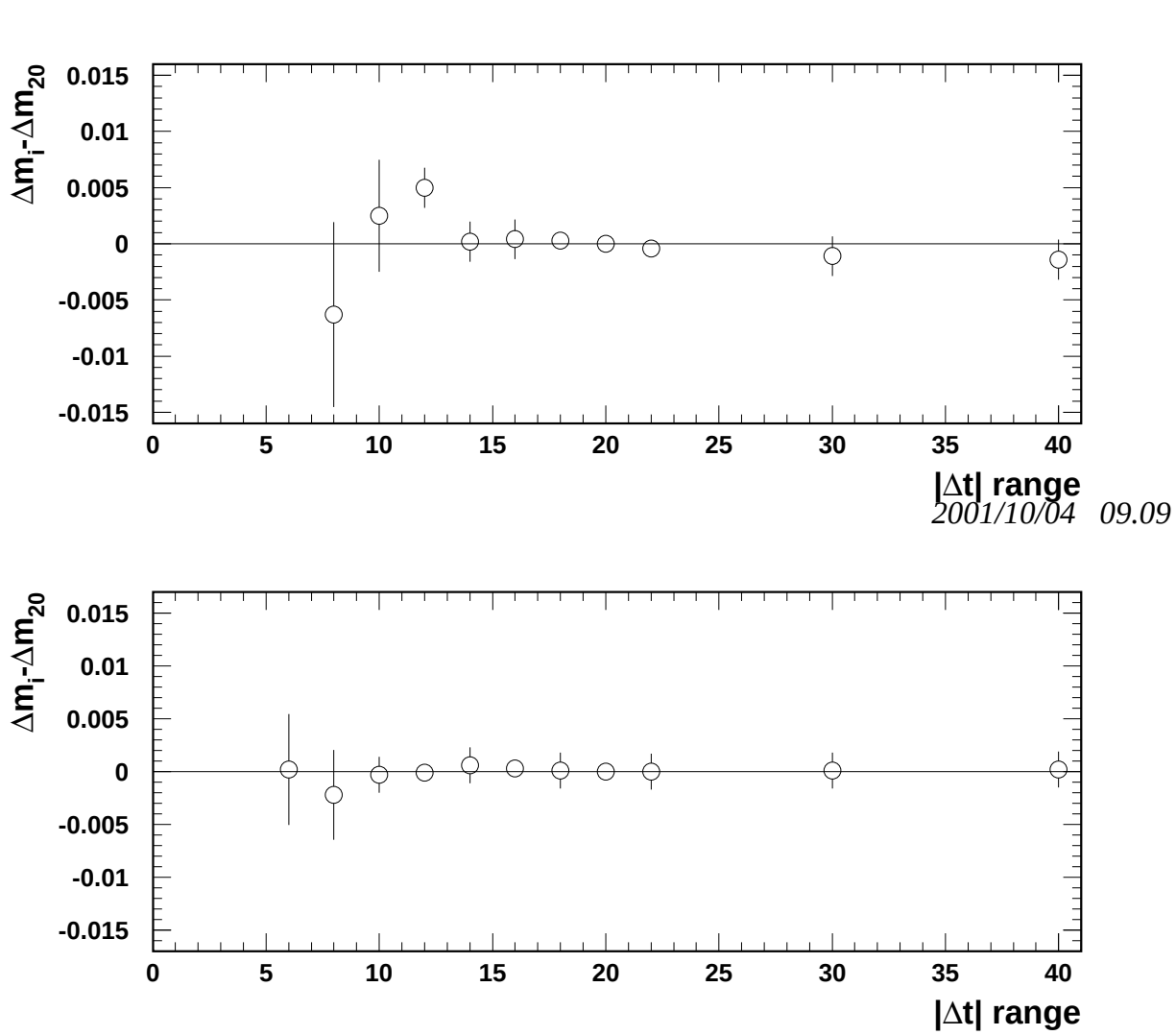


Figure 28: Fits with limits on the $\Delta t$ intervals used. The plot shows the *difference* (and the error on the difference) as a function of the imposed $\Delta t$ bound, with respect to the fit with $t_{bound}$ of 20 ps. In the fits shown on the top, all parameters are left free. In the fits on the bottom, only $\Delta m_d$ is left free.

**Restricted $\sigma_{\Delta t}$ ranges** To check whether $\Delta m_d$ measurement is independent of the $\sigma_{\Delta t}$ requirement we repeat the fit on both the data and MC, varying the requirement on $\sigma_{\Delta t}$ from 1 ps to 2 ps. The result is shown in Fig. 29. We assign a systematic uncertainty of $\pm$ 0.003 to this cut.

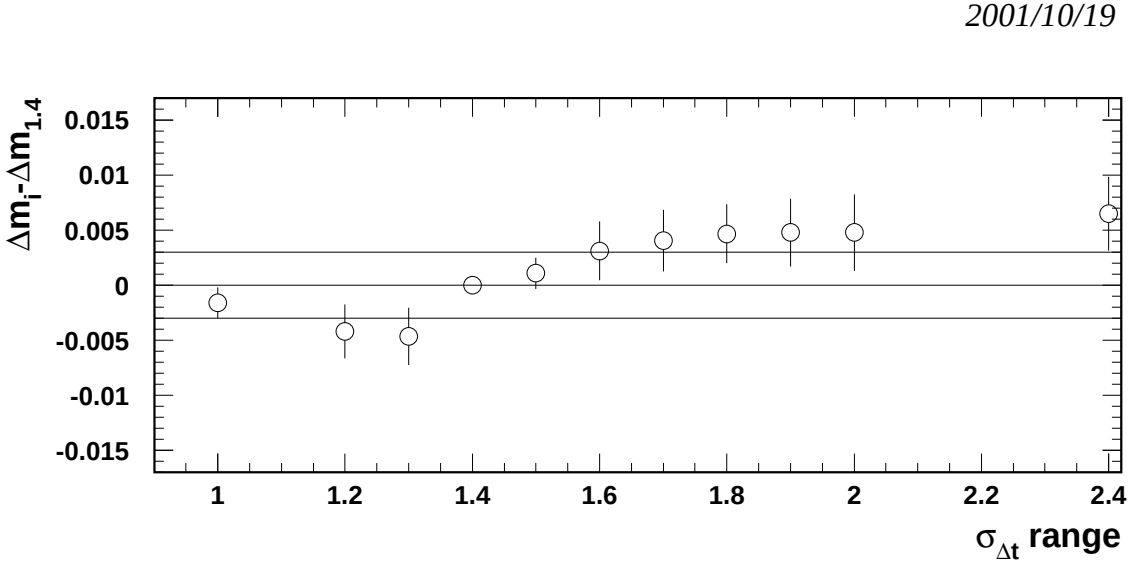


Figure 29: Fits on data, varying the requirement on $\sigma_{\Delta t}$. The figure shows the difference between the fit results as a function of the $\sigma_{\Delta t}$ bound and the nominal fit with a bound on $\sigma_{\Delta t}$ at 1.4 ps. In each fit, All parameters are left free.

**Tagging Separations** We extract the tagging dilutions for the selected $B$ candidates in simulated events from the reconstructed $B$ flavor tag and the MC truth information on the $B_{\rm tag}$ flavor by counting the number of correct tags for all event with $m_{\rm ES} > 5.27\,{\rm GeV}/c^2$. The results are listed in Table 6. The differences between the measured dilutions and the MC truth dilutions are interpreted as systematic biases and are applied as corrections to the measured tagging dilutions in data. The statistical uncertainties in those tagging dilutions are interpreted as systematic uncertainties. With the exception of the kaon tags, the corrections are small compared to the statistical uncertainties on the dilutions in the data sample.

As discussed in Section 6.13, there is a correlation between mistag fractions and $\Delta t$ determination. One additional check is to see whether wrong tag events are described by the *same* resolution function as right tag events. In order to do this, we use the same procedure as used in [11]: first determine the resolution function for right tag and wrong tag events seperately by fitting the MC $\Delta t$ residual; Then determine for each sample the value for

$\Delta m_d$ (taking the flavor tag from MC truth) seperately, and average. We then compare this average with the fit where both samples (i.e. right and wrong) are used, again taking the flavor tag from MC truth The difference (0.001) is assigned as a systematic error.

**Likelihood Fit** We perform the likelihood fit with candidates in simulated events selected with the same criteria as applied to data. The signal parameters fitted are the same as those used in the nominal fit to the data and any fixed resolution function parameter is given the same values as in the fit to the data. The $B^0$ lifetime is fixed to $\tau(B^0) = 1.548\,\mathrm{ps}$, as is used for event generation. A small combinatorial background in the selected events from the cocktail MC sample is rejected by requiring a positive MC truth association in addition to $m_{\mathrm{ES}} > 5.27\,\mathrm{GeV}/c^2$. In this case, no background parameters are required for the fit. The results of the fit, together with the generated value for $\Delta m_d$ in Monte Carlo, is shown in Table 2. We correct the value measured in data by the difference between the value determined with Monte Carlo and the generated value, i.e. subtract 0.0066. The statistical uncertainty on this difference is interpreted as a systematic uncertainty due to the limited Monte Carlo statistics used for the likelihood fit test.

**Variation of relative amounts of $D$ Species** The generic Monte Carlo generator we use to model the tag-side $B$ decays produces $D$ mesons using the known exclusive branching fractions for decays of $B$s to specific exclusive modes, and a model based on knowlege of the inclusive rates for $B \to DX$ for the rest. Our current knowlege of the relative rates for $B$ decays to charm is summarized in [10], page 636, and the inclusive rates for $B \to DX$ are listed in Table 27

Because of the uncertainty in this procedure, and the different rates for different $D$ species to decay to particles which provide tag information, it is possible that there is a bias introduced by inaccureate modeling of the relative rates for $B$ decays to different species of $D$s. To check this, we first classify events into one of five categories: One $D^+$, $D^0$, or $D_s$, two $D$s, or no $D$ mesons at all. We then vary the relative amounts of each $D$ species up and down by an extremely conservative 30%. The amount of this variation was chosen based on the numbers given in Table 27, and the observation that most of the relative exclusive branching fractions for $B^0$ and $B^+$ are similar within about 30%.

We then perform the full fit on each of these samples with enhanced/depleated amounts of each $D$ species. The results of these fits are summarized in Table 28 and Figure 30. We assign a very conservative systematic error of $\pm 0.001$ due to this effect.

Table 27: Inclusive rates for $B \to DX$ from the Particle Data Group

| | |
|---|---|
| $\Gamma(B \to D^{\pm}X)/\Gamma(\mathrm{total})$ | $0.241 \pm 0.019$ |
| $\Gamma(B \to D^{0}X)/\Gamma(\mathrm{total})$ | $0.635 \pm 0.029$ |
| $\Gamma(B \to D_s^{\pm}X)/\Gamma(\mathrm{total})$ | $0.100 \pm 0.025$ |

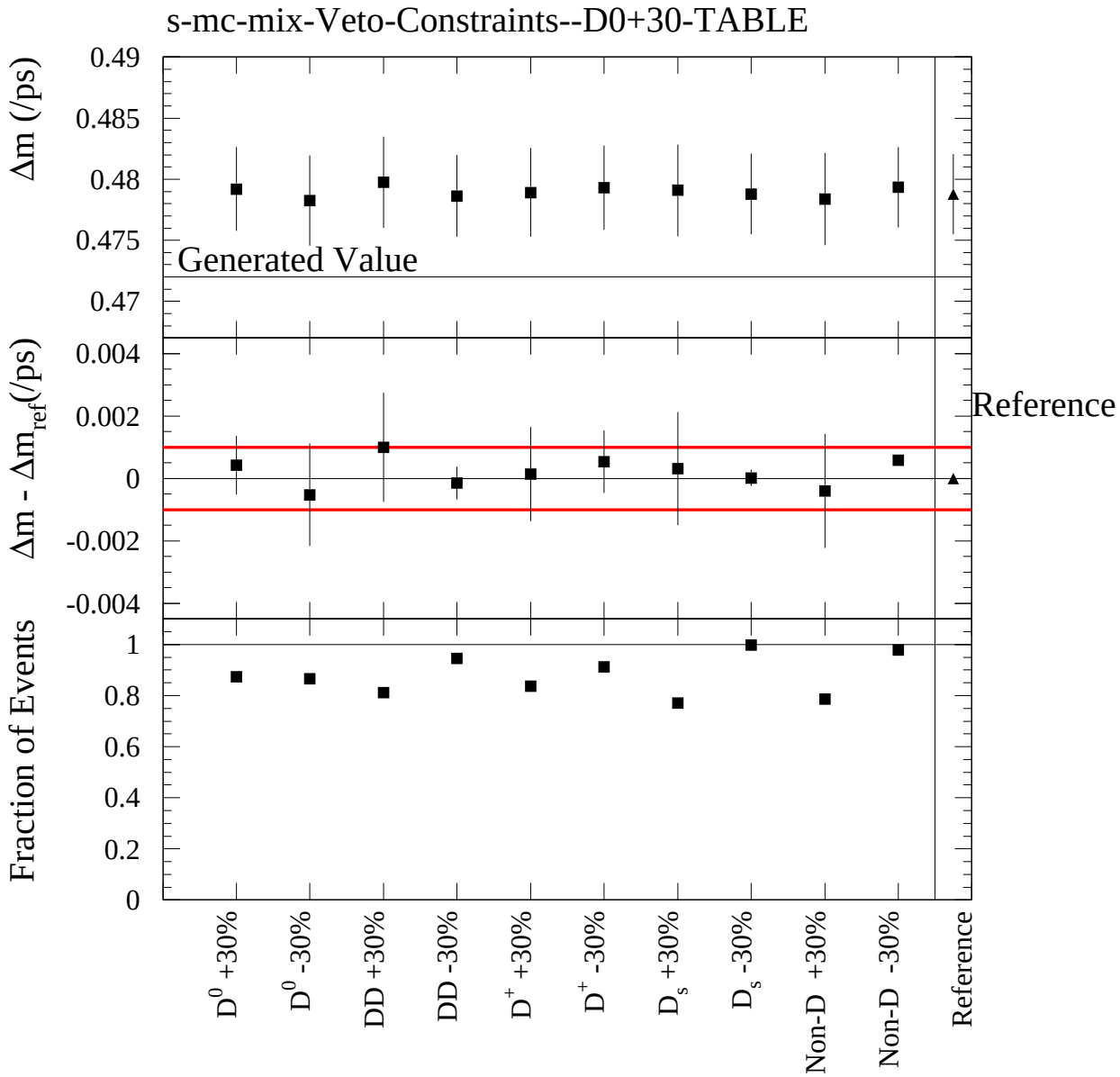


Figure 30: Fits to Monte Carlo samples with changes in the relative fractions of charm species on the tag side. The assigned systematic error is indicated by the horizontal red lines. The errors shown on the middle plot are computed as the difference in quadrature from the reference.

Table 28: Results from the likelihood fit to the $\Delta t$ distributions of the hadronic $\overline{B}^0$ decays in simulated signal events for different relative amounts of $D$ species. The sample of 2.8 million (no $B \to J/\psi K^*$) was reweighted with either 30% more or 30% less of the species under study.

| Parameter | -50.00-D0+30 | -50.00-D0-30 | -50.00-DD+30 | -50.00-DD-30 | -50.00-Dp+30 | -50.00-Dp-30 |
|---|---|---|---|---|---|---|
| $\mathcal{S}_{\text{core, sig}}$ | 1.142 ±.020 | 1.140 ±.021 | 1.142 ±.022 | 1.134 ±.020 | 1.149 ±.021 | 1.130 ±.022 |
| $\delta^L_{\text{core, sig}}$ | -.060 ±.023 | -.066 ±.024 | -.058 ±.025 | -.058 ±.022 | -.057 ±.024 | -.056 ±.024 |
| $\delta^K_{\text{core, sig}}$ | -.213 ±.015 | -.242 ±.015 | -.237 ±.016 | -.207 ±.014 | -.225 ±.015 | -.227 ±.015 |
| $\delta^{NT1}_{\text{core, sig}}$ | -.162 ±.029 | -.153 ±.030 | -.157 ±.031 | -.151 ±.028 | -.148 ±.030 | -.169 ±.029 |
| $\delta^{NT2}_{\text{core, sig}}$ | -.179 ±.022 | -.231 ±.022 | -.220 ±.023 | -.179 ±.021 | -.214 ±.022 | -.186 ±.022 |
| $\mathcal{S}_{\text{tail, sig}}$ | 3.858 ±.341 | 3.657 ±.278 | 3.671 ±.325 | 3.840 ±.316 | 3.845 ±.304 | 3.679 ±.372 |
| $\delta_{\text{tail, sig}}$ | -2.288 ±.518 | -2.164 ±.459 | -2.195 ±.483 | -2.169 ±.443 | -2.395 ±.529 | -1.979 ±.425 |
| $f_{\text{tail}}$ | .030 ±.007 | .038 ±.008 | .037 ±.009 | .033 ±.007 | .033 ±.007 | .036 ±.010 |
| $f_{\text{outlier}}$ | .004 ±.001 | .005 ±.001 | .004 ±.001 | .004 ±.001 | .004 ±.001 | .004 ±.001 |
| $D_{\text{L}}$ | .865 ±.006 | .837 ±.006 | .848 ±.007 | .859 ±.006 | .849 ±.006 | .861 ±.006 |
| $D_{\text{K}}$ | .728 ±.005 | .685 ±.005 | .698 ±.005 | .721 ±.005 | .706 ±.005 | .714 ±.005 |
| $D_{\text{NT1}}$ | .649 ±.009 | .586 ±.010 | .618 ±.010 | .627 ±.009 | .616 ±.010 | .632 ±.009 |
| $D_{\text{NT2}}$ | .338 ±.008 | .276 ±.009 | .311 ±.009 | .310 ±.008 | .295 ±.009 | .328 ±.008 |
| $\Delta D_{\text{L}}$ | .001 ±.010 | .000 ±.010 | -.003 ±.011 | .005 ±.009 | .002 ±.010 | -.002 ±.010 |
| $\Delta D_{\text{K}}$ | .040 ±.007 | .043 ±.008 | .044 ±.008 | .039 ±.007 | .043 ±.008 | .041 ±.007 |
| $\Delta D_{\text{NT1}}$ | -.046 ±.015 | -.044 ±.016 | -.055 ±.016 | -.039 ±.014 | -.040 ±.016 | -.053 ±.015 |
| $\Delta D_{\text{NT2}}$ | .067 ±.013 | .071 ±.013 | .069 ±.014 | .068 ±.013 | .072 ±.013 | .066 ±.013 |
| $\Delta m_d$ | .4792 ±.0034 | .4783 ±.0037 | .4798 ±.0037 | .4786 ±.0033 | .4789 ±.0036 | .4793 ±.0034 |
| Events | 101753 | 100900 | 94609 | 110230 | 97441 | 106455 |

| Parameter | -50.00-Ds+30 | -50.00-Ds-30 | -50.00-nonD+30 | -50.00-nonD-30 | all -50.0 |
|---|---|---|---|---|---|
| $\mathcal{S}_{\text{core, sig}}$ | 1.154 ±.021 | 1.129 ±.021 | 1.154 ±.021 | 1.126 ±.020 | 1.129 ±.020 |
| $\delta^L_{\text{core, sig}}$ | -.059 ±.025 | -.058 ±.023 | -.060 ±.025 | -.055 ±.022 | -.058 ±.022 |
| $\delta^K_{\text{core, sig}}$ | -.223 ±.016 | -.226 ±.014 | -.219 ±.015 | -.230 ±.014 | -.227 ±.014 |
| $\delta^{NT1}_{\text{core, sig}}$ | -.152 ±.031 | -.158 ±.028 | -.147 ±.031 | -.161 ±.028 | -.158 ±.027 |
| $\delta^{NT2}_{\text{core, sig}}$ | -.205 ±.023 | -.197 ±.021 | -.199 ±.023 | -.201 ±.021 | -.197 ±.021 |
| $\mathcal{S}_{\text{tail, sig}}$ | 3.795 ±.344 | 3.736 ±.319 | 3.754 ±.336 | 3.751 ±.287 | 3.717 ±.284 |
| $\delta_{\text{tail, sig}}$ | -2.486 ±.615 | -2.053 ±.394 | -2.457 ±.628 | -2.062 ±.385 | -2.060 ±.398 |
| $f_{\text{tail}}$ | .030 ±.008 | .037 ±.008 | .030 ±.008 | .038 ±.007 | .037 ±.008 |
| $f_{\text{outlier}}$ | .004 ±.001 | .004 ±.001 | .004 ±.001 | .004 ±.001 | .004 ±.001 |
| $D_{\text{L}}$ | .852 ±.007 | .854 ±.006 | .849 ±.007 | .857 ±.006 | .854 ±.006 |
| $D_{\text{K}}$ | .709 ±.005 | .710 ±.005 | .703 ±.005 | .716 ±.005 | .710 ±.005 |
| $D_{\text{NT1}}$ | .622 ±.010 | .624 ±.009 | .606 ±.010 | .641 ±.009 | .623 ±.009 |
| $D_{\text{NT2}}$ | .313 ±.009 | .308 ±.008 | .302 ±.009 | .319 ±.008 | .308 ±.008 |
| $\Delta D_{\text{L}}$ | -.001 ±.011 | .002 ±.009 | -.002 ±.011 | .003 ±.009 | .002 ±.009 |
| $\Delta D_{\text{K}}$ | .043 ±.008 | .041 ±.007 | .043 ±.008 | .040 ±.007 | .040 ±.007 |
| $\Delta D_{\text{NT1}}$ | -.046 ±.016 | -.048 ±.014 | -.043 ±.016 | -.052 ±.014 | -.049 ±.014 |
| $\Delta D_{\text{NT2}}$ | .067 ±.014 | .069 ±.012 | .064 ±.014 | .072 ±.012 | .069 ±.012 |
| $\Delta m_d$ | .4791 ±.0038 | .4788 ±.0033 | .4784 ±.0038 | .4794 ±.0033 | .4788 ±.0033 |
| Events | 89851 | 116327 | 91645 | 114010 | 116539 |

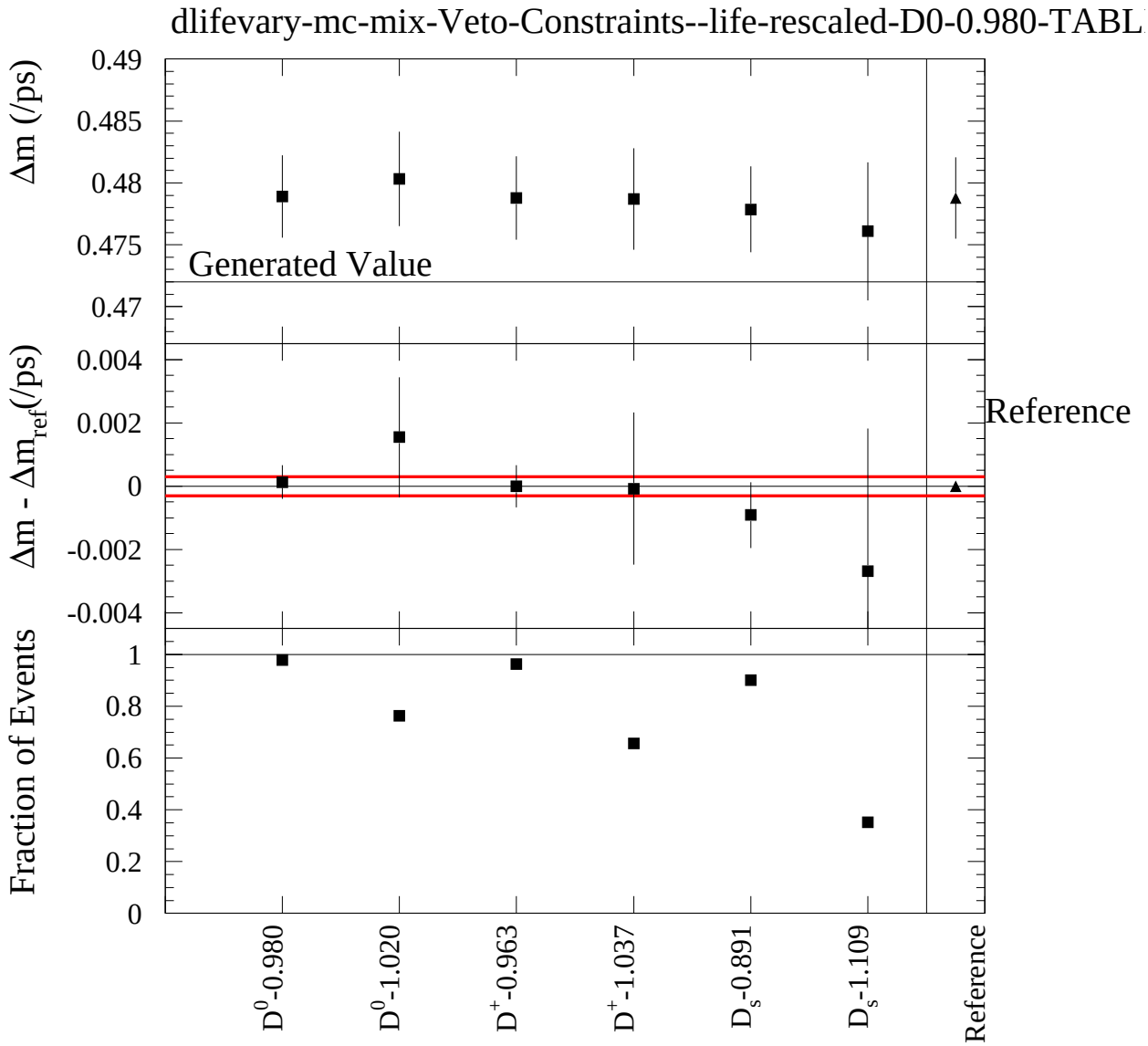


Figure 31: Fits to subsets of 2.8 million signal cocktail Monte Carlo events (no $B \to J/\psi K^*$) which have been reweighted with $3\sigma$ variations in lifetimes of the tag side D mesons. The systematic error for this effect is negligible.

**Variation of $D$ Lifetimes** The event generator uses PDG values for $D$ lifetimes. We check how sensitive $\Delta m_d$ is to the $D^+, D^0$ and $D_s$ lifetimes by varying them up and down by $3\sigma$ for tag-side $D$ mesons by reweighting the signal cocktail MC sample. The reweighting procedure is performed as follows: the sample is divided into two: events with a $D_i$, or without, where $D_i$ is the $D$ species under study. Events with a $D_i$ are removed, using truth, in such a way that the lifetime of the $D_i$ is modified. The algorithm maintains the relative abundances of other kinds of $B$ decays which don't contain a $D_i$ by removing the same fraction of those events as were removed to adjust the lifetime. The results of these fits are shown in Figure 31. We conclude that the systematic error due to this effect is negligible (less than 0.0005).

**Variation of wrong-sign Kaon amount** The event generator uses PDG values for the amount of $B$ decays which contain a final-state kaon which has a charge opposite what is expected from the (most common) $b \to c \to s$ transition. We vary the fraction of so-called wrong-sign kaons up and down by up to 100% in the MC by removing events using MC truth. Specifically for the removal, we call an event 'wrong-sign' if the sum of the charges of all true kaons in the event is opposite what is expected from the $B$ flavor. We then fit each subsample to determine the effect of differing amounts of wrong-sign kaon decays on $\Delta m_d$. The fits are shown in Figure 32 and Table 29. We assign a very conservative systematic error of $\pm 0.001$ due to this effect.

## 7.2 $\Delta t$ Resolution Function

To estimate the contribution to the statistical error on $\Delta m_d$ due to the resolution parameters, we perform two fits: one where only $\Delta m_d$ is allowed to float, and one where the signal resolution parameters are also free. The (quadratic) difference between the error on $\Delta m_d$ is taken as an estimate of the contribution to the statistical error on $\Delta m_d$ due to the uncertain resolution function (Table 30).

### 7.2.1 $\Delta t$ Outliers

A small fraction of the selected candidates (eg. $0.8\pm$ 0.4 % for run 1 and less than 0.01% for run 2) have very large $|\Delta t|$ values ($\Delta t$ *outliers*). These candidates are accounted for in the likelihood function of the $\Delta t$ distributions by an *outlier Gaussian* with fixed rms of 8 ps and zero bias. The fraction of outliers is a free fit parameter. Therefore, the actual fraction of outliers should not bias the fit result. To study the systematic uncertainty due to these outliers, we vary the width of the outlier fraction from 4 to 18 ps. In addition we replace the outlier gaussian with a flat pdf centered around zero with a varying width. The variations are summarized in table 31 and shown in Fig. 33. We estimate the systematic uncertainty due to $\Delta t$ outliers and their description to be $\pm 0.001\,\hbar\,\mathrm{ps}^{-1}$ for $\Delta m_d$.

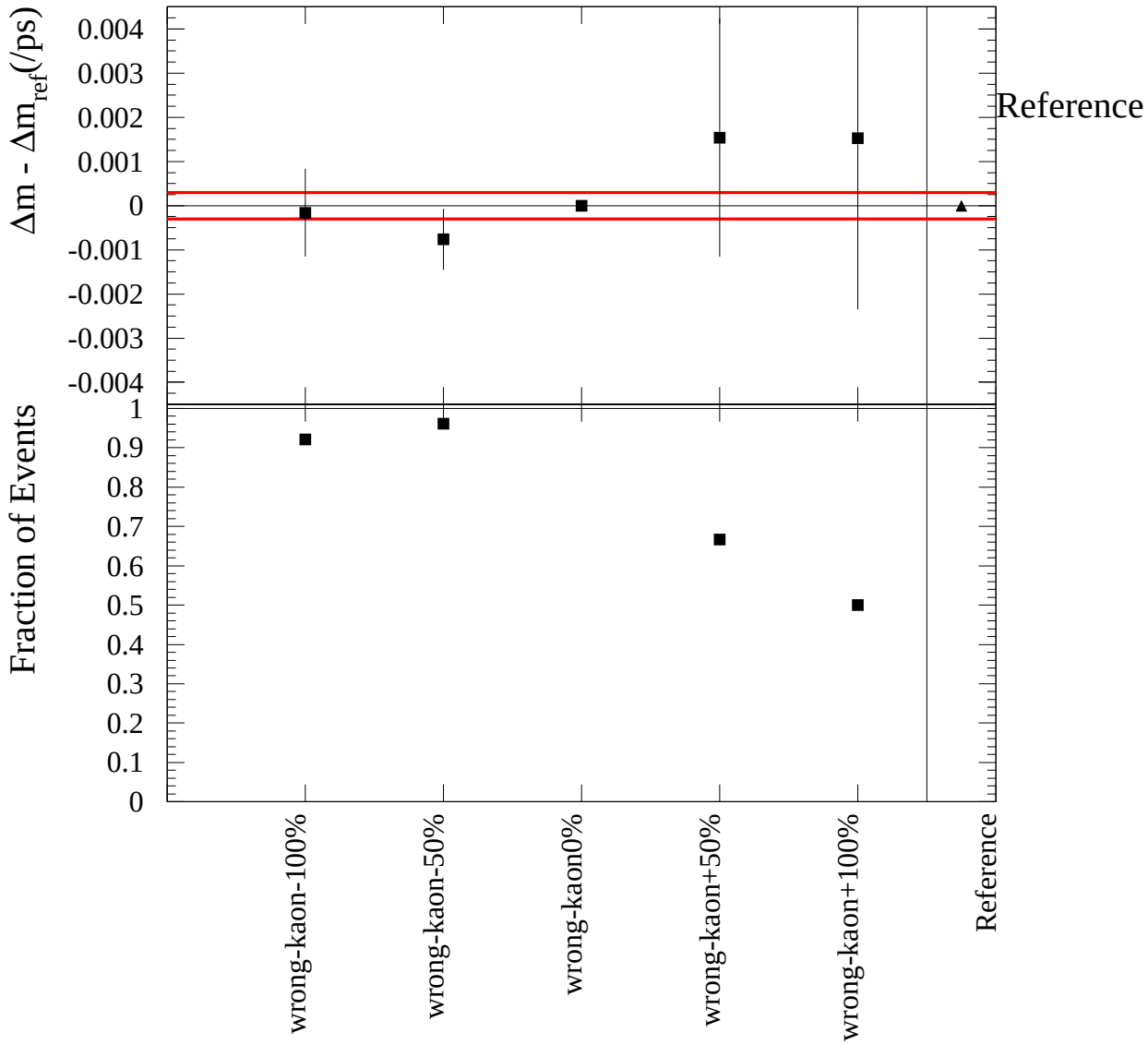


Figure 32: Fits to Monte Carlo samples (no $B \to J/\psi K^*$) with $3\sigma$ variations in amount of $B$ decays with wrong-sign kaons. The assigned systematic error is indicated by the horizontal red lines.

Table 29: Results from the likelihood fit to the $\Delta t$ distributions of the hadronic $\overline{B}^0$ decays in simulated signal events for different amounts of wrong-sign kaon events. The sample of 2.8 million (no $B \to J/\psi K^*$) was reweighted to have up to $\pm$ 100% wrong-sign kaon fraction.

| Parameter | wrong-kaon –100% | wrong-kaon –50% | wrong-kaon 0% | wrong-kaon +50% | wrong-kaon +100% | all 50.0 |
|---|---|---|---|---|---|---|
| $\mathcal{S}_{\text{core, sig}}$ | 1.133 ±.020 | 1.125 ±.020 | 1.129 ±.020 | 1.135 ±.025 | 1.102 ±.047 | 1.129 ±.020 |
| $\delta^L_{\text{core, sig}}$ | -.052 ±.023 | -.056 ±.022 | -.058 ±.022 | -.053 ±.028 | -.021 ±.038 | -.058 ±.022 |
| $\delta^K_{\text{core, sig}}$ | -.238 ±.014 | -.232 ±.014 | -.227 ±.014 | -.208 ±.018 | -.208 ±.026 | -.227 ±.014 |
| $\delta^{NT1}_{\text{core, sig}}$ | -.162 ±.028 | -.160 ±.028 | -.158 ±.027 | -.157 ±.034 | -.115 ±.044 | -.158 ±.027 |
| $\delta^{NT2}_{\text{core, sig}}$ | -.210 ±.021 | -.204 ±.021 | -.197 ±.021 | -.176 ±.026 | -.166 ±.035 | -.197 ±.021 |
| $\mathcal{S}_{\text{tail, sig}}$ | 3.867 ±.352 | 3.753 ±.279 | 3.717 ±.284 | 3.621 ±.363 | 3.160 ±.509 | 3.717 ±.284 |
| $\delta_{\text{tail, sig}}$ | -1.865 ±.358 | -1.936 ±.363 | -2.060 ±.398 | -2.314 ±.592 | -1.645 ±.548 | -2.060 ±.398 |
| $f_{\text{tail}}$ | .035 ±.008 | .038 ±.008 | .037 ±.008 | .036 ±.010 | .059 ±.028 | .037 ±.008 |
| $f_{\text{outlier}}$ | .004 ±.001 | .004 ±.001 | .004 ±.001 | .004 ±.001 | .005 ±.001 | .004 ±.001 |
| $D_{\text{L}}$ | .860 ±.006 | .855 ±.006 | .854 ±.006 | .853 ±.007 | .856 ±.008 | .854 ±.006 |
| $D_{\text{K}}$ | .839 ±.004 | .769 ±.004 | .710 ±.005 | .643 ±.006 | .584 ±.007 | .710 ±.005 |
| $D_{\text{NT1}}$ | .637 ±.009 | .631 ±.009 | .623 ±.009 | .614 ±.011 | .611 ±.013 | .623 ±.009 |
| $D_{\text{NT2}}$ | .314 ±.008 | .312 ±.008 | .308 ±.008 | .307 ±.010 | .290 ±.011 | .308 ±.008 |
| $\Delta D_{\text{L}}$ | .001 ±.010 | .001 ±.010 | .002 ±.009 | .001 ±.012 | .004 ±.013 | .002 ±.009 |
| $\Delta D_{\text{K}}$ | .038 ±.006 | .041 ±.007 | .040 ±.007 | .041 ±.009 | .034 ±.011 | .040 ±.007 |
| $\Delta D_{\text{NT1}}$ | -.045 ±.015 | -.043 ±.014 | -.049 ±.014 | -.038 ±.017 | -.059 ±.020 | -.049 ±.014 |
| $\Delta D_{\text{NT2}}$ | .064 ±.013 | .069 ±.012 | .069 ±.012 | .073 ±.015 | .090 ±.017 | .069 ±.012 |
| $\Delta m_d$ | .4786 ±.0031 | .4780 ±.0032 | .4788 ±.0033 | .4803 ±.0043 | .4803 ±.0051 | .4788 ±.0033 |
| Events | 107300 | 111922 | 116539 | 77682 | 58327 | 116539 |

Table 30: Contribution to the statistical error due to the uncertainty in the signal resolution parameters.

| floating parameters | $\sigma(\Delta m_d)$ |
|---|---|
| $\Delta m_d$ | 0.0139 |
| $\Delta m_d$, signal resolution parameters | 0.0148 |
| difference: | 0.0050 |

Figure 33: Systematic uncertainties in $\Delta m_d$ and in the mistag fractions due to fixed width of the $\Delta t$ outliers estimated from data by varying the width and replacing the Gaussian outlier model with a flat PDF model. $\delta\Delta m_d$ is the difference of the blind $\Delta m_d$ for the specified fit and the reference fit with a Gaussian outlier with a width of 8 ps. The errors are computed as the difference in quadrature of the statistical errors of the fit under consideration and the reference fit.

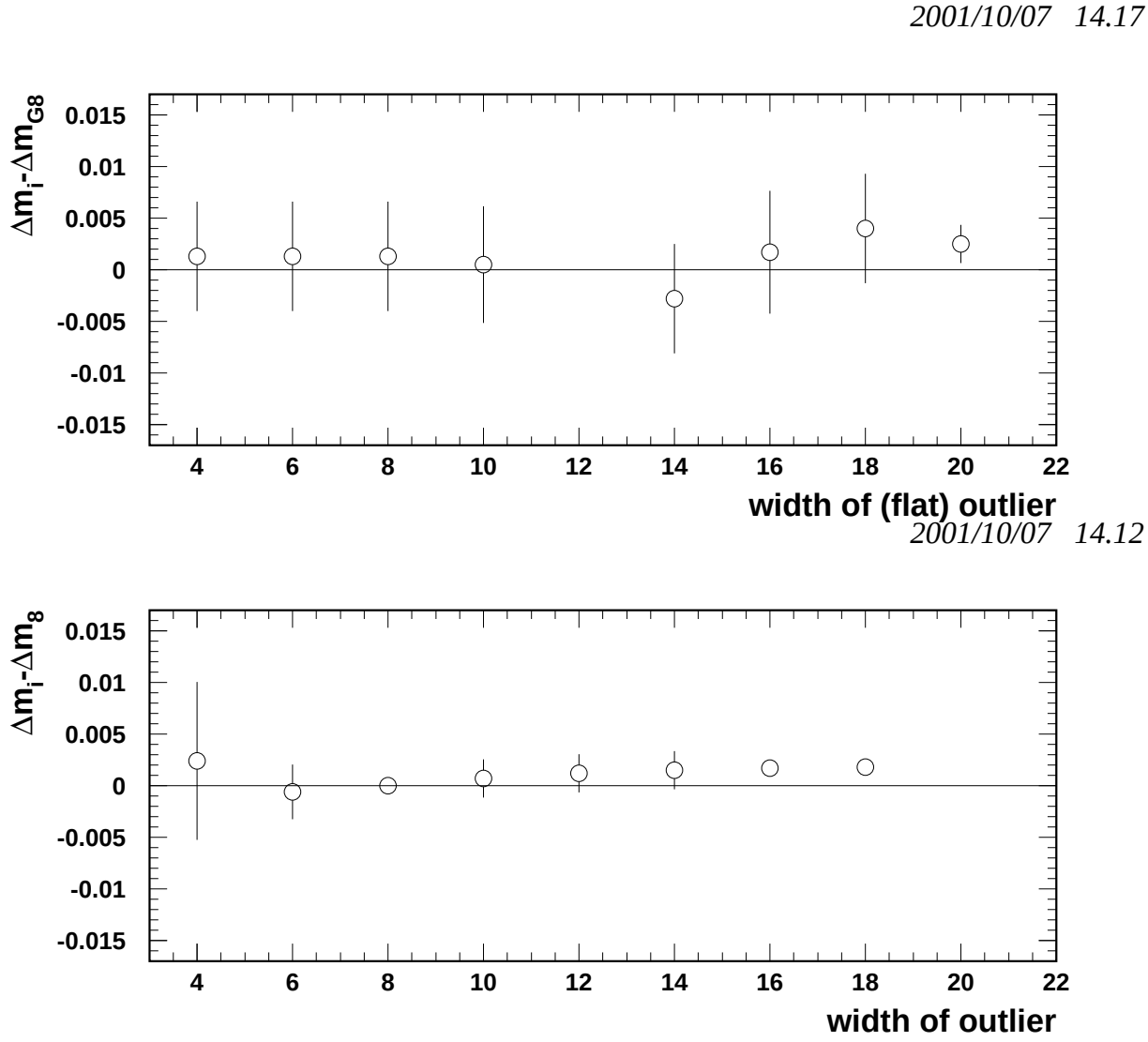

Table 31: Systematic uncertainties in $\Delta m_d$ due to fixed width of the $\Delta t$ outliers estimated from data by varying the width and replacing the Gaussian outlier model with a flat PDF model. $\delta\Delta m_d$ is the difference of the blind $\Delta m_d$ for the specified fit and the reference fit with a Gaussian outlier with a width of 8 ps.

| Outlier width | $\delta\Delta m_d$ | Outlier width | $\delta\Delta m_d$ |
|---|---|---|---|
| Gaussian model | | Flat model | |
| 4 | 0.002 ±0.008 | 4 | 0.001 ±0.005 |
| 6 | -0.001 ±0.003 | 6 | 0.001 ±0.005 |
| 8 | 0.000 ±0.000 | 8 | 0.001 ±0.005 |
| 10 | 0.001 ±0.002 | 10 | 0.001 ±0.006 |
| 12 | 0.001 ±0.002 | 14 | -0.003 ±0.005 |
| 14 | 0.002 ±0.002 | 16 | 0.002 ±0.006 |
| 16 | 0.002 ±0.000 | 18 | 0.004 ±0.005 |
| 18 | 0.002 ±0.000 | 20 | 0.003 ±0.002 |
| 20 | 0.002 ±0.002 | 40 | 0.003 ±0.002 |
| Syst. Error | ± 0.001 | | |

## 7.3 $B^0$ Lifetime

We fix the $B^0$ lifetime for the nominal fit to the world average of $\tau_{B^0} = 1.548 \pm 0.032$ ps [10] and estimate the systematic bias due to the corresponding uncertainty by repeating the likelihood fit with $\tau_{B^0}$ varied by $\pm 0.032$ ps. The measured values for $\Delta m_d$ and the tagging dilutions are listed in Table 32 and shown in Figure 34. The 'break' shown in the figure coincides with a change in the resolution function parameters for run1. We take the slope of the dependence at the PDG $B^0$ lifetime, and multiply it with the PDG uncertainty as a systematic uncertainty, leading to a systematic of 0.0056 on $\Delta m_d$.

Table 32: Systematic uncertainties in $\Delta m_d$ due to the uncertainty in the $B^0$ lifetime. $\delta\Delta m_d$ is the difference in the blinded value of $\Delta m_d$ for the specified fit and the reference fit where $\tau_{B^0}$ is fixed to the PDG value of 1.548 ps.

| $\tau_{B^0}$ [ ps ] | $\Delta m_d$ [$\hbar$ ps$^{-1}$] |
|---|---|
| 1.612 ($+2\sigma$) | XX- 0.0086 ±0.0157 |
| 1.580 ($+1\sigma$) | XX- 0.0035 ±0.0158 |
| 1.548 (PDG 2000) | XX ±0.0161 |
| 1.516 ($-1\sigma$) | XX+ 0.0056 ±0.0163 |
| 1.484 ($-2\sigma$) | XX+ 0.0117 ±0.0165 |
| $\sigma_{\rm syst}$ | ± 0.006 |

Figure 34: Systematic uncertainty in $\Delta m_d$ due to the uncertainty in the $B^0$ lifetime. The 'break' at 1.57 ps coincides with a change in the run1 resolution function parameters.

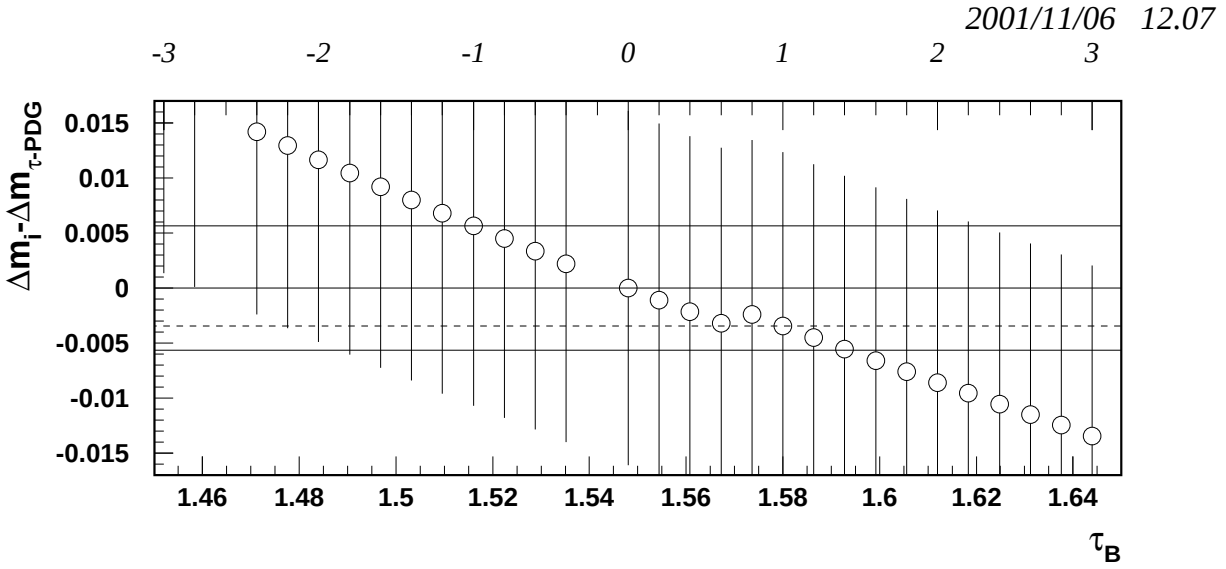


## 7.4 $z$ Scale

The difference between the $z$ positions of the two $B$ decay vertices, $\Delta z$, is used to calculate the decay-time difference in the $\Upsilon(4S)$ rest frame. A potential bias in the $z$ scale will directly translate into a systematic bias of the $B^0$ lifetime and $\Delta m_d$. The uncertainty in the scale of the $\Delta z$ measurement is less than $\pm 0.4\%$ [12]. Note that the measurements in [12] pertain to the beampipe, and the uncertainty has been conservatively increased by a factor of 2 to allow for scenarios where the measurements at the beampipe radius are correct, but measurements at the beamspot are not. The corresponding systematic error in $\Delta m_d$ is smaller than $\pm 0.002\,\hbar\,\mathrm{ps}^{-1}$.

## 7.5 $z$ Boost

The $\Upsilon(4S)$ boost in the $z$ direction is used to calculate the decay-time difference using the "average $\tau_B$" approximation [7]. A potential systematic bias in the boost translates directly into a systematic bias of $\Delta m_d$. The boost is known to a relative uncertainty of $\pm 0.1\%$ [17]. We estimate the systematic error due to the boost in $\Delta m_d$ to be $\pm 0.0005\,\hbar\,\mathrm{ps}^{-1}$, but no systematic error is assigned to the tagging dilutions due to this source.

Another source of uncertainty is the one intrinsic to the method used to convert $\Delta z$ into $\Delta t$. We compare the "average $\tau_B$" approximation with the "average boost" approximation

on MC and data in Table 33. We interpret the observed difference in data (after applying the corresponding MC corrections) of 0.0014 $\hbar\,\mathrm{ps}^{-1}$as a systematic error due to the $\Delta z$ to $\Delta t$ conversion *method*. Note that in case of the "average boost" approximation it can be shown that the resolution depends on the value of $\Delta z$ due to the non-zero boost of the $B$ mesons in the $\Upsilon(4S)$ frame (see [15] and for more details).

Table 33: Comparison between different boost approximations on data on MC. The data values have been *not* been corrected by the deviation of the MC difference.

| | MC | data | difference |
|---|---|---|---|
| average $\tau_B$ | 0.4786 $\pm$0.0032 | X $\pm$0.017 | |
| average boost | 0.4751 $\pm$0.0032 | X-0.0049 $\pm$0.017 | |
| difference | -0.0035 | -0.0049 | -0.0014 |

## 7.6 Beamspot position

The beamspot position is used in the computation of the tag vertex [7]. We investigate (using signal cocktail MC) the dependence of $\Delta m_d$ on the assumed position of the beamspot. The assumed position of the beamspot is either systematically shifted for all events or moved (event-by-event) by a random amount, drawn from a gaussian with a given spread (Table 34). Note that we *do* re-evaluate the resolution function in all cases. In addition, for data, we use instead of the default beamspot determined from twoprong events the beamspot as determined from hadronic events; The difference in $\Delta m_d$ is -0.002 $\pm$0.002 where the error is the difference in quadrature of the errors of the two values.

## 7.7 Background $\Delta t$ Distribution

We study the robustness of the treatment of the combinatorial background in the hadronic $B$ sample. To this end, we add a third component to the zero lifetime and non-zero lifetime components used in the nominal fit. The additional term describes an oscillatory $\Delta t$ distribution to account for a contribution of (mis-reconstructed) $B^0\overline{B}^0$ background. The additional mixing component requires seven more fit parameters than the nominal fit. As a result of using more fit parameters, the errors on the background parameters increase. However, the signal parameters ($\Delta m_d$ and the signal dilutions) remain unaffected because of the small correlation between background and signal parameters already observed in the nominal fit. The results of this study are listed in Table 35 and the projections of the various fits for the $m_{\mathrm{ES}}$ sideband are shown in Fig. 35. We conclude that the systematic error due to the description of the decay time structure of the combinatorial background is less than $\pm 0.001\,\hbar\,\mathrm{ps}^{-1}$.

Table 34: Variation of $\Delta m_d$ when shifting or smearing the y position of the beamspot position. The reported error is the difference in quadrature between the fit under consideration and the nominal fit.

| Size of Variation [$\mu$m] | $\delta\Delta m_d$ [$\hbar\,\mathrm{ps}^{-1}$] |
|---|---|
| shift | |
| 5 | -0.0004±0.0008 |
| 10 | -0.0001±0.0008 |
| 20 | 0.0000±0.0008 |
| 40 | -0.0004±0.0008 |
| 80 | 0.0002±0.0012 |
| smear | |
| 10 | -0.0003±0.0008 |
| 20 | -0.0003±0.0008 |
| 40 | -0.0001±0.0008 |
| 80 | -0.0010±0.0013 |

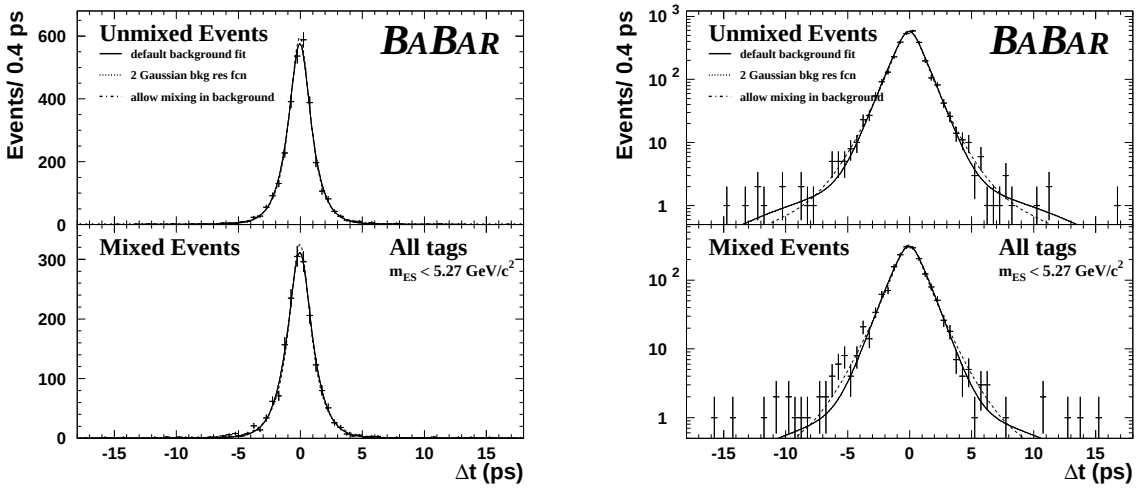


Figure 35: Comparison of the fits with different treatment of the background description for the $m_{\mathrm{ES}}$ sideband events

Table 35: Result of likelihood fit results for hadronic $B$ decays using the nominal $\Delta t$ description of the combinatorial background and using an additional oscillatory term.

| $\Delta m_d$ | XX+0.0006 ±0.015 |
|---|---|
| Scale core Sig Run 1 | 1.397 ±0.072 |
| Scale core Sig Run 2 | 1.166 ±0.108 |
| Bias core Sig Kaon Run 1 | -0.245 ±0.071 |
| Bias core Sig Kaon Run 2 | -0.240 ±0.090 |
| Bias core Sig Lep Run 1 | -0.035 ±0.124 |
| Bias core Sig Lep Run 2 | -0.037 ±0.164 |
| Bias core Sig NT1 Run 1 | -0.055 ±0.153 |
| Bias core Sig NT1 Run 2 | -0.502 ±0.216 |
| Bias core Sig NT2 Run 1 | -0.544 ±0.121 |
| Bias core Sig NT2 Run 2 | -0.254 ±0.162 |
| Bias tail Sig Run 1 | -6.885 ±2.507 |
| Bias tail Sig Run 2 | -7.541 ±1.576 |
| Frac tail Sig Run 1 | 0.007 ±0.005 |
| Frac tail Sig Run 2 | 0.016 ±0.006 |
| Frac outl Sig Run 1 | 0.009 ±0.004 |
| Frac outl Sig Run 2 | 0.000 ±0.013 |
| aveD Sig Kaon | 0.665 ±0.023 |
| aveD Sig Lep | 0.829 ±0.029 |
| aveD Sig NT1 | 0.573 ±0.045 |
| aveD Sig NT2 | 0.318 ±0.043 |
| DeltaD Sig, Kaon | 0.019 ±0.035 |
| DeltaD Sig, Lep | -0.011 ±0.048 |
| DeltaD Sig, NT1 | -0.093 ±0.071 |
| DeltaD Sig, NT2 | 0.106 ±0.063 |
| Scale core Bkg Run 1 | 1.333 ±0.028 |
| Scale core Bkg Run 2 | 1.205 ±0.034 |
| Bias core Bkg Run 1 | -0.123 ±0.030 |
| Bias core Bkg Run 2 | -0.018 ±0.038 |
| Frac outl Bkg Run 1 | 0.013 ±0.003 |
| Frac outl Bkg Run 2 | 0.024 ±0.005 |
| DeltaM Mix Bkg | 1.011 ±0.062 |
| Tau mix Bkg | 1.160 ±0.072 |
| Tau nonprompt Bkg | 1.236 ±0.050 |
| aveD Bkg 1, Kaon | 0.446 ±0.024 |
| aveD Bkg 1, Lep | -1.700 ±0.221 |
| aveD Bkg 1, NT1 | 0.649 ±0.073 |
| aveD Bkg 1, NT2 | 0.157 ±0.041 |
| aveD Bkg 2, Kaon | 0.222 ±0.044 |
| aveD Bkg 2, Lep | 1.886 ±0.305 |
| aveD Bkg 2, NT1 | -0.647 ±0.239 |
| aveD Bkg 2, NT2 | 0.104 ±0.077 |
| aveD Bkg 3, Kaon | 0.741 ±2.692 |
| aveD Bkg 3, Lep | 2.000 ±2.777 |
| aveD Bkg 3, NT1 | -1.064 ±0.257 |
| aveD Bkg 3, NT2 | -0.084 ±0.140 |
| f(mix of tau>0) mix Bkg Ka | 0.000 ±0.679 |
| f(mix of tau>0) mix Bkg Le | 0.713 ±0.058 |
| f(mix of tau>0) mix Bkg NT1 | 0.630 ±0.037 |
| f(mix of tau>0) mix Bkg NT2 | 1.000 ±0.758 |
| f(tau=0) mix Bkg Kaon | 0.656 ±0.022 |
| f(tau=0) mix Bkg Lep | 0.281 ±0.022 |
| f(tau=0) mix Bkg NT1 | 0.556 ±0.031 |
| f(tau=0) mix Bkg NT2 | 0.504 ±0.053 |

## 7.8 Background Resolution Function

We estimate the error due to the unknown background $\Delta t$ resolution function by varying the functional form of the $\Delta t$ resolution function. Instead of a single Gaussian plus outlier Gaussian, we allow for an additional tail Gaussian in the resolution function. The differences for $\Delta m_d$ and the mistag rates are listed in Table 36. The observed differences are interpreted as systematic errors due to the uncertainty on the functional form of the background resolution function. We conclude that the systematic uncertainty due to the background $\Delta t$ resolution function is less than $\pm 0.001\,\hbar\,\mathrm{ps}^{-1}$.

Table 36: Result of a likelihood fit using an additional second Gaussian (seperate for run 1 and run 2) for the background resolution function. Note that first the background parameters are determined from the sideband region ($m_{\mathrm{ES}} < 5.27$ GeV), and fixed during the mixing fit.

| $\Delta m_d$ | XX-0.0006 ±0.017 | Scale core Bkg Run 1 | 1.225 ±0.031 |
|---|---|---|---|
| Bias core Sig Kaon Run 1 | -0.249 ±0.080 | Scale core Bkg Run 2 | 1.217 ±0.037 |
| Bias core Sig Kaon Run 2 | -0.246 ±0.094 | Bias core Bkg Run 1 | -0.104 ±0.034 |
| Bias core Sig Lep Run 1 | -0.039 ±0.127 | Bias core Bkg Run 2 | 0.023 ±0.040 |
| Bias core Sig Lep Run 2 | -0.047 ±0.166 | Scale tail Bkg Run 1 | 3.241 ±0.170 |
| Bias core Sig NT1 Run 1 | -0.052 ±0.155 | Scale tail Bkg Run 2 | 4.813 ±0.335 |
| Bias core Sig NT1 Run 2 | -0.513 ±0.218 | Bias tail Bkg Run 1 | -0.364 ±0.202 |
| Bias core Sig NT2 Run 1 | -0.541 ±0.124 | Bias tail Bkg Run 2 | -1.106 ±0.418 |
| Bias core Sig NT2 Run 2 | -0.261 ±0.164 | Frac tail Bkg Run 1 | 0.164 ±0.016 |
| Bias tail Sig Run 1 | -7.879 ±0.638 | Frac tail Bkg Run 2 | 0.117 ±0.013 |
| Bias tail Sig Run 2 | -8.179 ±2.735 | Frac outl Bkg Run 1 | 0.017 ±0.004 |
| DeltaD Sig, Kaon | 0.018 ±0.035 | Frac outl Bkg Run 2 | 0.010 ±0.004 |
| DeltaD Sig, Lep | -0.009 ±0.048 | Tau nonprompt Bkg | 0.552 ±0.030 |
| DeltaD Sig, NT1 | -0.093 ±0.071 | aveD Bkg 1, Kaon | 0.479 ±0.031 |
| DeltaD Sig, NT2 | 0.107 ±0.063 | aveD Bkg 1, Lep | -0.888 ±0.967 |
| Frac outl Sig Run 1 | 0.008 ±0.004 | aveD Bkg 1, NT1 | 1.116 ±0.110 |
| Frac outl Sig Run 2 | 0.002 ±0.003 | aveD Bkg 1, NT2 | -0.132 ±0.132 |
| Frac tail Sig Run 1 | 0.006 ±0.010 | aveD Bkg 2, Kaon | 0.207 ±0.040 |
| Frac tail Sig Run 2 | 0.012 ±0.009 | aveD Bkg 2, Lep | 0.308 ±0.075 |
| Scale core Sig Run 1 | 1.394 ±0.092 | aveD Bkg 2, NT1 | -0.579 ±0.076 |
| Scale core Sig Run 2 | 1.163 ±0.115 | aveD Bkg 2, NT2 | 0.135 ±0.030 |
| aveD Sig Kaon | 0.667 ±0.024 | f(tau=0) mix Bkg Kaon | 0.561 ±0.045 |
| aveD Sig Lep | 0.832 ±0.030 | f(tau=0) mix Bkg Lep | 0.000 ±0.120 |
| aveD Sig NT1 | 0.576 ±0.046 | f(tau=0) mix Bkg NT1 | 0.405 ±0.027 |
| aveD Sig NT2 | 0.320 ±0.043 | f(tau=0) mix Bkg NT2 | 0.327 ±0.105 |

## 7.9 Background in the Signal Region

We split the backgrounds in two categories: peaking and combinatorial. The properties of the combinatorial background are determined from the $m_{\mathrm{ES}}$ sideband ($5.20 < m_{\mathrm{ES}} <$

5.27 GeV/$c^2$).

### 7.9.1 Combinatorial Background

Table 37: Variation in $\Delta m_d$ when the parameters of the $m_{\rm ES}$ fit are varied by their statistical uncertainty.

| parameter | 1 $\sigma$ up | 1$\sigma$ down |
|---|---|---|
| $\xi$ | -0.0014 | 0.0013 |
| $m_B$ | 0.0004 | -0.0001 |
| $N_{Bgd}$ | 0.0008 | -0.0009 |
| $N_{Sig}$ | -0.0008 | 0.0006 |
| $\sigma_{m_B}$ | -0.0004 | 0.0003 |
| sum in quadrature | $\pm$0.0016 | |

Since the $m_{\rm ES}$ fit is independent of the likelihood fit to the $\Delta t$ distributions, we account for the statistical uncertainties on the signal probabilities as systematic uncertainties in the $\Delta t$ fit. We vary the parameters of the $m_{\rm ES}$ fit up and down by one sigma, and add the resulting variations in $\Delta m_d$ in quadrature. The individual contributions are shown in Tab. 37. The total systematic error on $\Delta m_d$ thus obtained is 0.0016. As an alternative, we divide the full $m_{\rm ES}$ range into two parts, $m_{\rm ES} < 5.27$ and $m_{\rm ES} > 5.27\,{\rm GeV}/c^2$. The events below $5.27\,{\rm GeV}/c^2$ are assigned a signal probability of zero, while the events above $5.27\,{\rm GeV}/c^2$ are assigned a signal probability corresponding to the purity of the sample listed in table 1. This fit yields a $\Delta m_d$ of 'X'+0.0009 $\pm$0.016, where 'X' is the blind value of the nominal fit. This fit is then repeated, varying the signal probabilities by $\pm 1\sigma$; the resulting variations are $\pm$0.0021.

An additional uncertainty originates from the assumption that the $\Delta t$ structure of the sideband band region is a good description of the $\Delta t$ structure of the background underneath the signal. To test this assumption, we vary the *lower edge* of the $m_{\rm ES}$ distribution from 5.20 to $5.27\,{\rm GeV}/c^2$. The result is shown in Fig. 36.

In addition, we split the sideband in seven equal slices each 10 MeV/$c^2$ wide, and use each of these ranges (seperately) in the mixing fit. The resulting values (relative to the nominal fit) are shown in Fig. 37 and Tab. 38. Extrapoling the values obtained for $\Delta m_d$ to the $B$ mass, we find a correction of $-0.024\pm0.020$. We correct $\Delta m_d$ by this amount, and quote the statistical error of this correction of $\pm$0.020 as a systematic error.

### 7.9.2 Peaking Background

There is MC evidence for a small fraction of background that peaks in $m_{\rm ES}$ and therefore is not accounted for with the phase-space ARGUS model for extrapolating the $m_{\rm ES}$ sideband. Studies using MC ([13]) indicate that this background arises from misreconstructed $B$'s. In the case of misreconstructed $B^0$'s, this is irrelevant, since their time structure is identical

Table 38: Values of $\Delta m_d$ when using restricted, mutually exclusive slices of the $m_{\rm ES}$ sideband.

| $m_{\rm ES}$ sideband range | $\Delta m_d$ |
|---|---|
| 5.20— 5.21 | +0.0010 ±0.0164 |
| 5.21— 5.22 | +0.0012 ±0.0162 |
| 5.22— 5.23 | -0.0017 ±0.0161 |
| 5.23— 5.24 | +0.0014 ±0.0162 |
| 5.24— 5.25 | -0.0022 ±0.0161 |
| 5.25— 5.26 | -0.0011 ±0.0162 |
| 5.26— 5.27 | -0.0013 ±0.0163 |
| weighted average | -0.000379277 ±0.00612777 |
| extrapolation to 5.28 | -0.0024 ±0.0020 |

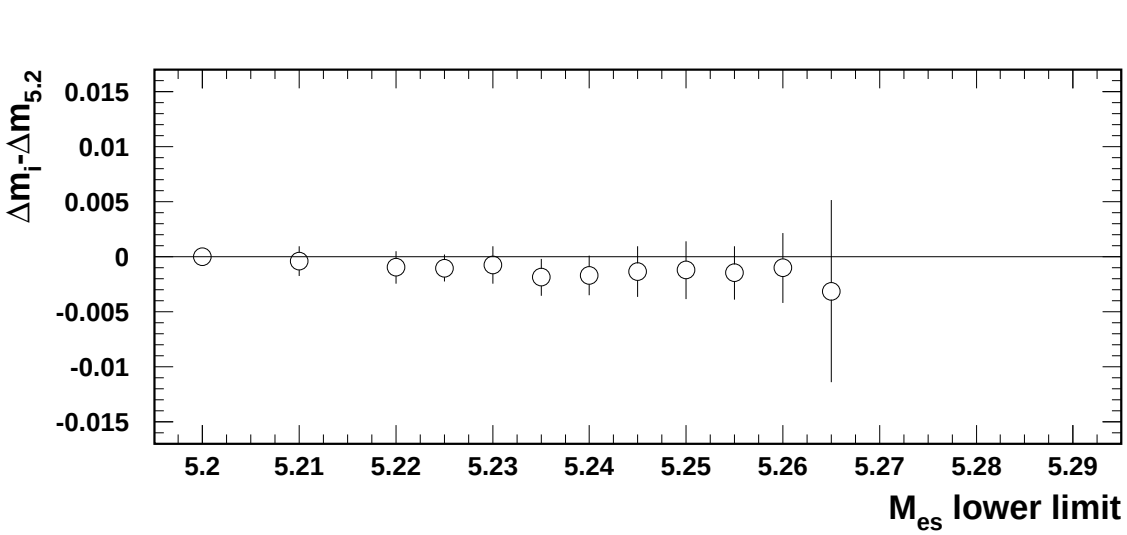


Figure 36: Value of $\Delta m_d$ when changing the lower bound on $m_{\rm ES}$. The plot shows the variation of $\Delta m_d$ relative to the reference fit with a cut at $m_{\rm ES} = 5.2$ GeV. The errors are the difference in quadrature between the plot under consideration and the reference fit.

*2001/10/27 22.34*

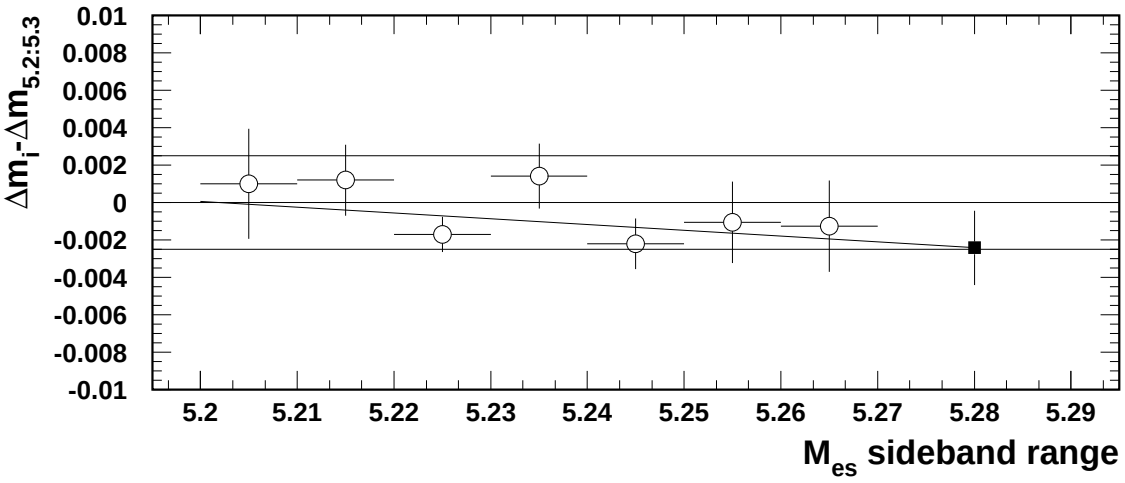


Figure 37: Variation of $\Delta m_d$ when using restricted, mutually exclusive slices of the $m_{\rm ES}$ sideband, shown as open circles. The errors on these points is given by the difference in quadrature between the fit under consideration and the nominal fit. A fit is performed on these points, and then extrapolated to 5.28. The resulting value, -0.0024 $\pm$0.0020, is indicated by the solid square.

Table 39: Variation of $\Delta m_d$ due to adding $B^+$ events to the $B^0$ signal MC.

| $B^+$ fraction added (%) | $\delta\Delta m_d$ (%) | slope |
|---|---|---|
| 1.7 | -0.4 | -0.24 |
| 3.4 | -2.0 | -0.59 |
| 5.1 | -4.0 | -0.78 |
| 6.8 | -5.2 | -0.76 |
| 17 | -10.6 | -0.62 |

Table 40: Variation of $\Delta m_d$ due to changing the assumed fraction of $B^+$ events in the fit to data (relative to the asumption of no $B^+$ events).

| $B^+$ fraction assumed (%) | $\delta\Delta m_d$ (%) | slope |
|---|---|---|
| 0 | 0.0 | — |
| 3 | +1.8 | 0.62 |
| 5 | +3.1 | 0.62 |
| 8 | +4.9 | 0.62 |
| 10 | +6.1 | 0.61 |
| 15 | +9.2 | 0.61 |

to the signal. Only charged $B$s, which are reconstructed as a neutral $B$, require special attention, since these do not mix.

We use a Monte Carlo sample of charged $B$ events generated in the modes indicated to be the main source of the peaking background by the generic Monte Carlo to characterize these backgrounds. As a check, we verify that those which are mis-reconstructed as $B^0$s have a time structure consistent with the charged $B$ lifetime (Fig. 38). We fit for the lifetime of the peaking component of this background, using the resolution function parameters as determined from the fit to the full $B^0$ sample and dilutions from the charged $B$ sample. We find the lifetime of the peaking background to be $1.42 \pm 0.17$ps.

To estimate the effect on $\Delta m_d$ from charged $B$ peaking background, we take $B^0$ signal MC and add different levels of charged $B$ MC to it. The variation of $\Delta m_d$ with this fraction is shown in Table 39. Another test is done varying the assumed fraction of charged $B$ peaking background in the fit to data. Those results are listed in Table 40.

We estimate the amount of charged $B$ peaking background by using generic and cocktail Monte Carlo events generated in the charged $B$ modes which are indicated to be the main source of the background in the generic Monte Carlo. We estimate the $B^-$ contamination to be $1.3 \pm 0.3^{+0.2}_{-0.5}\%$, and thus, given the dependence shown in Table 40, we assign a systematic error of $\pm 0.002$ to $\Delta m_d$ due to this effect.

As a cross-check, we leave the fraction of peaking background as a free parameter in the likelihood fit, which yields a value of 0.8% $\pm$5.6%, and a value of $\Delta m_d$ which is 0.0016 lower than the nominal fit, in good agreement with the above estimates. The statistical error of the fit increases from 0.016 to 0.023 when floating this fraction.

## 7.10 Dilution

The signal dilutions (and the difference between $B^0$ and $\overline{B}^0$ dilutions) are allowed to float during the fit. In order to determine the contribution to the statistical error due to the uncertainty in the estimation of the dilutions, we do two fits: one where only $\Delta m_d$ is allowed to float while all other parameters are fixed to their nominal fit values and one where, in addition, the signal dilutions and their differences are allowed to float. The contribution to

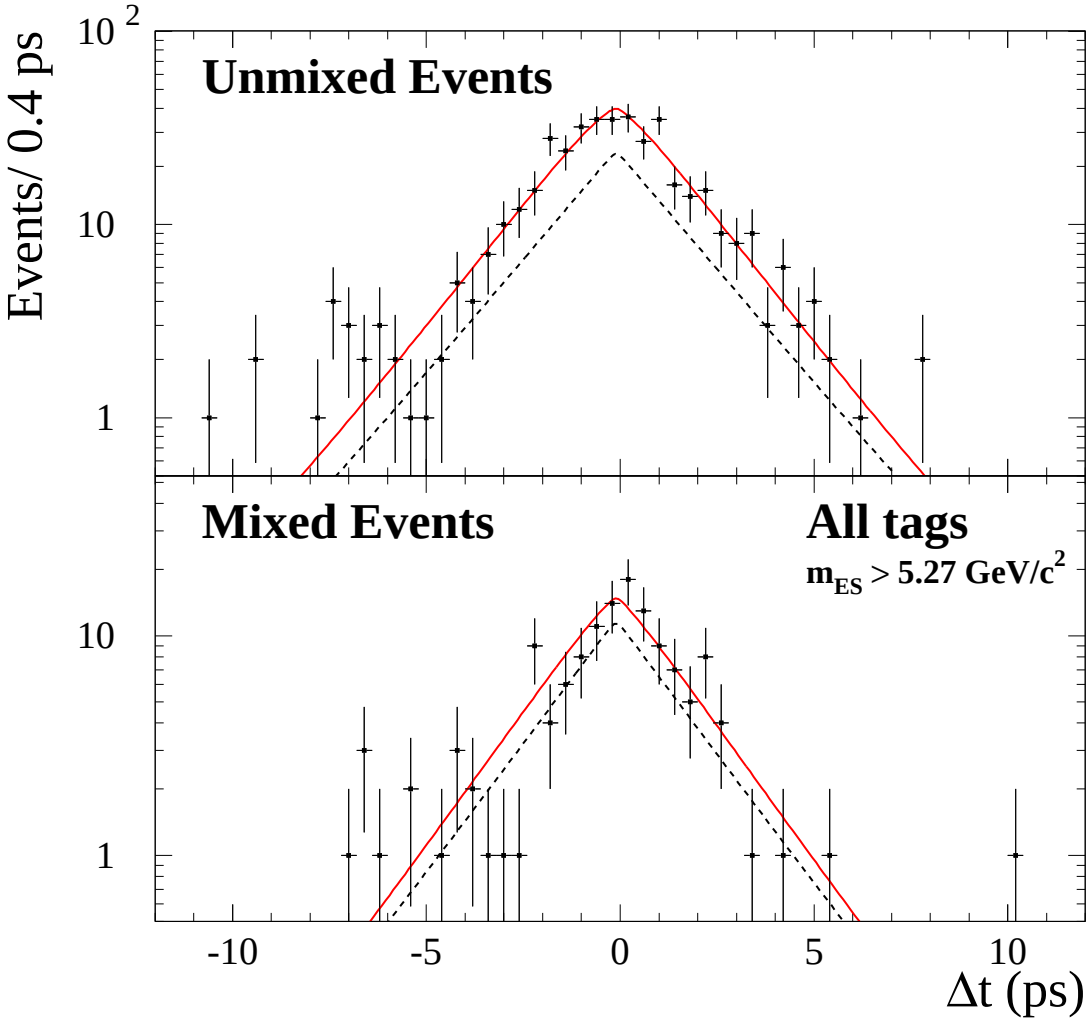


Figure 38: $\Delta t$ distributions for Monte Carlo charged $B$s reconstructed as $B^0$s. Projections of the lifetime fit are overlaid.

Table 41: Contribution to the statistical error due to the uncertainty in the dilutions.

| Floating parameters | $\sigma(\Delta m_d)$ |
|---|---|
| $\Delta m_d$ only | 0.0139 |
| $\Delta m_d$, dilutions | 0.0148 |
| difference: | 0.0051 |

the statistical error is then computed by taking the difference in quadrature of the two errors as summarized in Table 41.

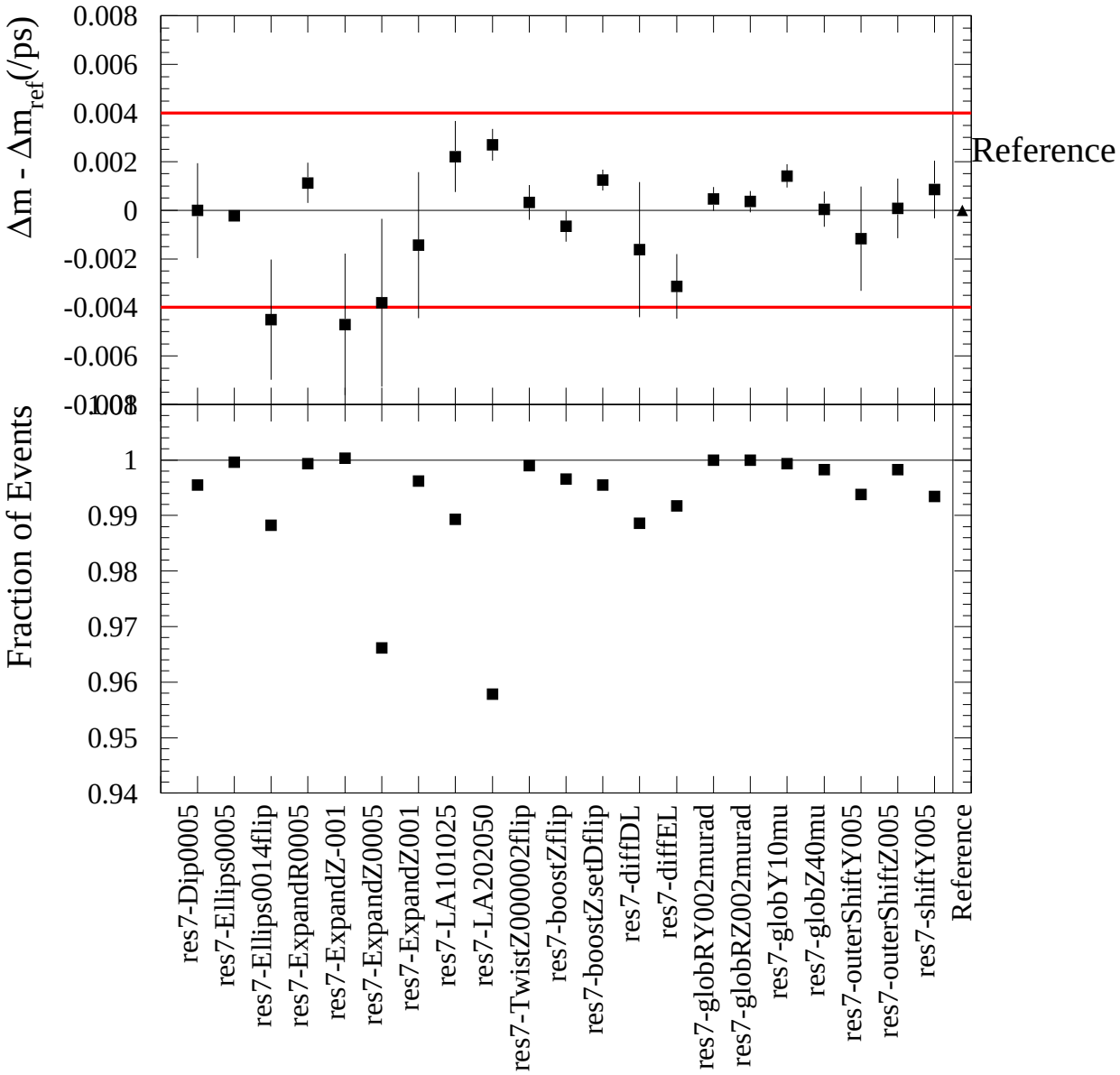


Figure 39: Effect of several possible SVT misalignment scenarios on $\Delta m_d$. The error quoted is the difference in quadrature between the zero misalignment set and the fit under investigation. In these fits (the results of which are shown in Table 42), the tag side flavor is determined from MC truth, and the dilutions fixed accordingly. The assigned systematic error is indicated by the horizontal red lines.

### 7.11 SVT Alignment

In order to estimate the systematics due to possible misalignments of the SVT, the same sample of MC events is reconstructed with a set of possible distortions. Note that due to the fact that this couldn't be done in MC production, only a very limited sample is available; more information on this sample can be found in [7]. The results are shown in Table 42, Figure 39 and Table 43. In the first case, all parameters are floated as in the nominal MC fit. In the second case, in order to improve the statistical power from the limited sample, the tag side flavor is taken from MC truth and the dilutions are fixed at 1 and the dilution differences at 0. The various scenarios are described in Ref. [7]. Note that some scenarios (rotateY0005, rotateZ0005, and TwistZ005) are unrealistically exaggerated. We assign a systematic error of 0.004 $\hbar\,\mathrm{ps}^{-1}$ on $\Delta m_d$ due to the uncertainty in the SVT alignment, based on the diffDL and diffEL scenarios, using the result from Table 43.

### 7.12 Summary of Systematic Uncertainties

We add the systematic uncertainties due to the individual sources in quadrature to calculate the total systematic uncertainty in $\Delta m_d$ and the mistag rates. The results are listed in Table 45. The statistical errors for $\Delta m_d$ and the mistag rates is the uncertainty from the nominal fit result, where the resolution function and the parameters of the combinatorial background are also fitted.

## 8 Summary

In $30\,\mathrm{fb}^{-1}$, we measure the $B^0\overline{B}^0$ oscillation frequency and the flavor mis-tag rates for Elba tagger using the hadronic $B$ sample and find:

$$\Delta m_d \;=\; 0.516 \pm 0.016\ (\mathrm{stat.}) \pm 0.010\ (\mathrm{syst.})\ \hbar\,\mathrm{ps}^{-1}$$

## 9 Acknowledgments

It is a pleasure to thank Patrick Robbe and Jan Stark for their help in $B$ reconstruction and selection. It is always a pleasure to thank Bob Cahn for stimulating discussions on many issues related with $\Delta t$ fits.

## References

[1] M. Kobayashi and T. Maskawa, Prog. Theo. Phys**49**, (1973)

[2] B tagging in BaBar, B.A.D. 119

Table 42: Effect of several possible SVT misalignment scenarios on $\Delta m_d$. The error quoted is the difference in quadrature between the zero misalignment set and the fit under investigation. The number in parenthesis is the deviation of the difference divided by the error on the difference. In these fits, all parameters are fit as part of the mixing fit

| scenario | fit result | difference wrt Zero |
|---|---|---|
| ExpandZ0005 | 0.466 ±0.020 | -0.007 ±0.002 ( -4.3 ) |
| globRZ20murad | 0.080 ±0.217 | -0.393 ±0.216 ( -1.8 ) |
| globRY20murad | 0.325 ±0.110 | -0.148 ±0.109 ( -1.4 ) |
| outerShiftY005 | 0.469 ±0.020 | -0.005 ±0.003 ( -1.4 ) |
| ExpandR0005 | 0.470 ±0.020 | -0.003 ±0.003 ( -1.2 ) |
| TwistZ0005 | 0.452 ±0.030 | -0.022 ±0.022 ( -1.0 ) |
| rotateZ005 | 0.452 ±0.033 | -0.021 ±0.026 ( -0.8 ) |
| TwistZ000002flip | 0.471 ±0.020 | -0.002 ±0.003 ( -0.8 ) |
| Ellips0005 | 0.471 ±0.020 | -0.003 ±0.004 ( -0.7 ) |
| ExpandZ-001 | 0.472 ±0.020 | -0.002 ±0.004 ( -0.5 ) |
| boostZflip | 0.473 ±0.020 | -0.000 ±0.001 ( -0.1 ) |
| Zero | 0.474 ±0.020 | 0.000 ±0.000 ( 0.0 ) |
| Ellips0014flip | 0.473 ±0.021 | -0.000 ±0.006 ( -0.0 ) |
| globY10mu | 0.474 ±0.020 | 0.001 ±0.002 ( 0.2 ) |
| outerShiftZ005 | 0.474 ±0.021 | 0.001 ±0.004 ( 0.2 ) |
| ExpandZ001 | 0.475 ±0.021 | 0.001 ±0.005 ( 0.3 ) |
| globZ40mu | 0.474 ±0.020 | 0.001 ±0.001 ( 0.6 ) |
| shiftY005 | 0.478 ±0.021 | 0.004 ±0.006 ( 0.8 ) |
| globRZ002murad | 0.475 ±0.020 | 0.002 ±0.002 ( 0.9 ) |
| boostZsetDflip | 0.477 ±0.021 | 0.004 ±0.004 ( 1.0 ) |
| LA101025 | 0.481 ±0.021 | 0.008 ±0.006 ( 1.4 ) |
| diffDL | 0.483 ±0.021 | 0.009 ±0.006 ( 1.5 ) |
| diffEL | 0.480 ±0.021 | 0.006 ±0.004 ( 1.5 ) |
| globRY002murad | 0.476 ±0.020 | 0.002 ±0.002 ( 1.5 ) |
| LA202050 | 0.492 ±0.022 | 0.018 ±0.009 ( 2.0 ) |
| rotateY005 | 0.513 ±0.026 | 0.040 ±0.016 ( 2.5 ) |

Table 43: Effect of several possible SVT misalignment scenarios on $\Delta m_d$. The error quoted is the difference in quadrature between the zero misalignment set and the fit under investigation. The number in parenthesis is the deviation of the difference divided by the error on the difference.In these fits, the tag side flavor is determined from MC truth, and the dilutions fixed accordingly in order to increase the statistical power of the samples available.

| scenario | fit result | difference with Zero alignment |
|---|---|---|
| Ellips0005 | 0.4765 ±0.0115 | -0.0002 ±0.0001 ( -4.4 ) |
| diffEL | 0.4736 ±0.0115 | -0.0031 ±0.0013 ( -2.4 ) |
| Ellips0014flip | 0.4722 ±0.0118 | -0.0045 ±0.0025 ( -1.8 ) |
| ExpandZ-001 | 0.4720 ±0.0112 | -0.0047 ±0.0029 ( -1.6 ) |
| boostZflip | 0.4761 ±0.0116 | -0.0007 ±0.0006 ( -1.1 ) |
| ExpandZ0005 | 0.4729 ±0.0121 | -0.0038 ±0.0035 ( -1.1 ) |
| diffDL | 0.4751 ±0.0119 | -0.0016 ±0.0028 ( -0.6 ) |
| ExpandZ001 | 0.4753 ±0.0119 | -0.0014 ±0.0030 ( -0.5 ) |
| outerShiftY005 | 0.4756 ±0.0117 | -0.0012 ±0.0021 ( -0.5 ) |
| rotateZ005 | 0.4716 ±0.0227 | -0.0051 ±0.0196 ( -0.3 ) |
| Zero | 0.4767 ±0.0115 | 0.0000 ±0.0000 ( 0.0 ) |
| Dip0005 | 0.4767 ±0.0114 | -0.0000 ±0.0020 ( -0.0 ) |
| globZ40mu | 0.4768 ±0.0116 | 0.0000 ±0.0007 ( 0.1 ) |
| outerShiftZ005 | 0.4768 ±0.0116 | 0.0001 ±0.0012 ( 0.1 ) |
| TwistZ000002flip | 0.4771 ±0.0116 | 0.0003 ±0.0007 ( 0.5 ) |
| shiftY005 | 0.4776 ±0.0116 | 0.0009 ±0.0012 ( 0.7 ) |
| globRZ002murad | 0.4771 ±0.0115 | 0.0004 ±0.0004 ( 0.8 ) |
| TwistZ0005 | 0.4878 ±0.0166 | 0.0111 ±0.0119 ( 0.9 ) |
| globRY002murad | 0.4772 ±0.0116 | 0.0005 ±0.0005 ( 0.9 ) |
| rotateY005 | 0.4861 ±0.0143 | 0.0094 ±0.0085 ( 1.1 ) |
| globRZ20murad | 0.5133 ±0.0356 | 0.0365 ±0.0337 ( 1.1 ) |
| ExpandR0005 | 0.4779 ±0.0115 | 0.0011 ±0.0008 ( 1.4 ) |
| LA101025 | 0.4789 ±0.0116 | 0.0022 ±0.0015 ( 1.5 ) |
| globRY20murad | 0.5251 ±0.0271 | 0.0484 ±0.0246 ( 2.0 ) |
| boostZsetDflip | 0.4780 ±0.0116 | 0.0012 ±0.0004 ( 2.8 ) |
| globY10mu | 0.4781 ±0.0115 | 0.0014 ±0.0005 ( 2.9 ) |
| LA202050 | 0.4794 ±0.0116 | 0.0027 ±0.0007 ( 4.1 ) |

Table 44: Final results on $\Delta m_d$.

| Source | $\Delta m_d$ $[\hbar\,\mathrm{ps}^{-1}]$ |
|---|---|
| Fitted value | 0.525±0.016 |
| MC Correction | -0.0066 |
| sideband extrapolation | -0.0024 |
| $\Delta m_d$ | 0.516±0.016 |

Table 45: Systematic uncertainties in $\Delta m_d$ and in the mistag rates measured with hadronic $B$ decays.

| Source | $\Delta m_d$ $[\hbar\,\mathrm{ps}^{-1}]$ |
|---|---|
| Signal MC Statistics | 0.0032 |
| $\Delta t$ Outliers | 0.002 |
| $\sigma_{\Delta t}$ cut | 0.003 |
| SVT Alignment | 0.004 |
| Background Probability | 0.0016 |
| Sideband Extrapolation | 0.0020 |
| Background $\Delta t$ structure | 0.001 |
| Background $\Delta t$ resolution | 0.001 |
| Peaking $B^+$ Background | 0.002 |
| $B^0$ lifetime | $^{+0.0056}_{-0.0056}$ |
| $z$ scale | <0.002 |
| $z$ boost (param) | 0.0005 |
| $z$ boost (method) | 0.0014 |
| Beamspot position/size | 0.0010 |
| tag-side $D$ composition | 0.001 |
| resolution dependence on right/wrong tag | 0.001 |
| Total Syst. | 0.0096 |
| Statistical Error | 0.0161 |
| Total Error | 0.019 |

[3] `Treating current directory as a test release based on analysis-11`
`AbsBTagging GR-010724 (Release uses V00-01-09)`
`BRecoUser rf-091301 (Release uses V00-08-41)`
`BTaggingSequences V00-00-08 (Release uses V00-00-08)`
`BTaggingTools GR-010724 (Release uses V00-01-30)`
`BTaggingUser GR-010724 (Release uses V00-00-03)`
`BetaBuildPidEnv V00-00-01 (Release uses V00-00-00)`
`BetaCoreTools GR-010713 (Release uses V00-00-19)`
`BetaMicro V00-01-14 (Release uses V00-01-14)`
`BetaMicroTruth GR-010713 (Release uses V00-00-05)`
`BetaPid GR-010724 (Release uses V00-01-31)`
`BetaSequences V00-10-07 (Release uses V00-10-07)`
`BlindTools sp-21august2001 (Release uses V00-00-05)`
`BtaDataP V00-02-08-01 (Release uses V00-02-08-01)`
`BtaMicroSequences V00-01-02-01 (Release uses V00-01-02)`
`CERNLIB V98-00-02 (Release uses V98-00-02)`
`CharmUser rf-061901 (Release uses V00-03-26)`
`CompositionFactory GR-010630 (Release uses V00-00-09)`
`CompositionTools V00-09-12 (Release uses V00-09-12)`
`PDT V00-03-17-01 (Release uses V00-03-17-01)`
`PhysProdTools V00-09-30 (Release uses V00-09-30)`
`StdHepDataP V00-00-22 (Release uses V00-00-22)`
`TruthTools GR-010713 (Release uses V00-10-11)`
`UpsilonTools GR-010724 (Release uses V00-00-02)`
`VtxFitter GR-010724 (Release uses V00-08-56)`
`tFit shr-21aug01 (not in Release)`

[4] `ASCII` files used as input for the fitting are available in `/nfs/farm/babar/AWG5/Breco/production/Dlight/ascii/a11d/summary/`

[5] Exclusive B reconstruction to open charm final states, B.A.D. 150
Supporting document for the Run 1 sin2beta analysis, B.A.D. 115 (for $J/\psi\ K^*$)

[6] Measurements of the charged and neutral B meson lifetimes using fully reconstructed B decays , B.A.D. 144

[7] Babar Vertexing, B.A.D. 102 Babar Vertexing, B.A.D. 130 Babar Vertexing, B.A.D. 254

[8] $f(x) \propto x\sqrt{1-x^2}\exp(\xi(1-x^2))$ where $x \equiv M(B)/E_{\rm beam}$ and $\xi$ is determined by the fit. ARGUS Collaboration, H. Albrecht *et al.*, Phys. Lett. **B 241** (1990) 278

[9] `tFit` — a program to fit decay time (difference) distributions to study $B^0/B^{\pm}$ lifetimes, $B^0\bar{B}^0$ Oscillations and CP asymmetry parameters, B.A.D. 101

[10] Particle Data Group, D.E. Groom *et al.*, Eur. Phys. J. C **15**, (2000)

[11] Supporting document for summer 2001 sin2beta analysis, B.A.D. 205

[12] P. Robbe, C.Hast and W.Dunwoodie,
`http://babar-hn.slac.stanford.edu:5090/HyperNews/get/recoTracking/334.html`
`http://www.slac.stanford.edu/~wmd/beampipe/dec00.talk`
Private Communication

[13] Presentations of B. Brau and P. Robbe,
`http://babar-hn.slac.stanford.edu:5090/HyperNews/get/EHBDOC/241/1.html`,
`http://babar-hn.slac.stanford.edu:5090/HyperNews/get/EHBDOC/262/4.htm`

[14] Presentation of G. Raven, March 29th Mixing and Lifetimes AWG meeting
`http://www.slac.stanford.edu/BFROOT/www/Physics/Analysis/AWG/BBMixingHadr/Meetings/`

[15] Presentations of Chih-Hsiang Cheng and G. Raven, July 5th Mixing and Lifetimes AWG meeting
`http://www.slac.stanford.edu/BFROOT/www/Physics/Analysis/AWG/BBMixingHadr/Meetings/`

[16] Presentations of M. Sullivan and S. Prell at the forum meeting on May 16th, 2000.

[17] The *BABAR* detector; SLAC-PUB-8569, hep-ex/0105044, to appear in NIM Abi Soffer, private communication

[18] Presentations of B. Cahn:
http://babar-hn.slac.stanford.edu:5090/HyperNews/get/sin2beta/159.html
http://babar-hn.slac.stanford.edu:5090/HyperNews/get/sin2beta/183.html

[19] Presentations of D. Lange:
http://babar-hn.slac.stanford.edu:5090/HyperNews/get/Bmixing/258/1/1.html